AD-A040 010 TEXAS UNIV AT AUSTIN APPLIED RESEARCH LABS F/G 14/5
DEVELOPMENT AND USE OF A SCHLIEREN SYSTEM FOR SOUND PULSE STUDI--ETC(U)
AUG 76 D R KLEEMAN F44620-76-C-0040
UNCLASSIFIED ARL-TR-76-43 AFOSR-TR-77-0679 NL

1 OF 2
AD A040010

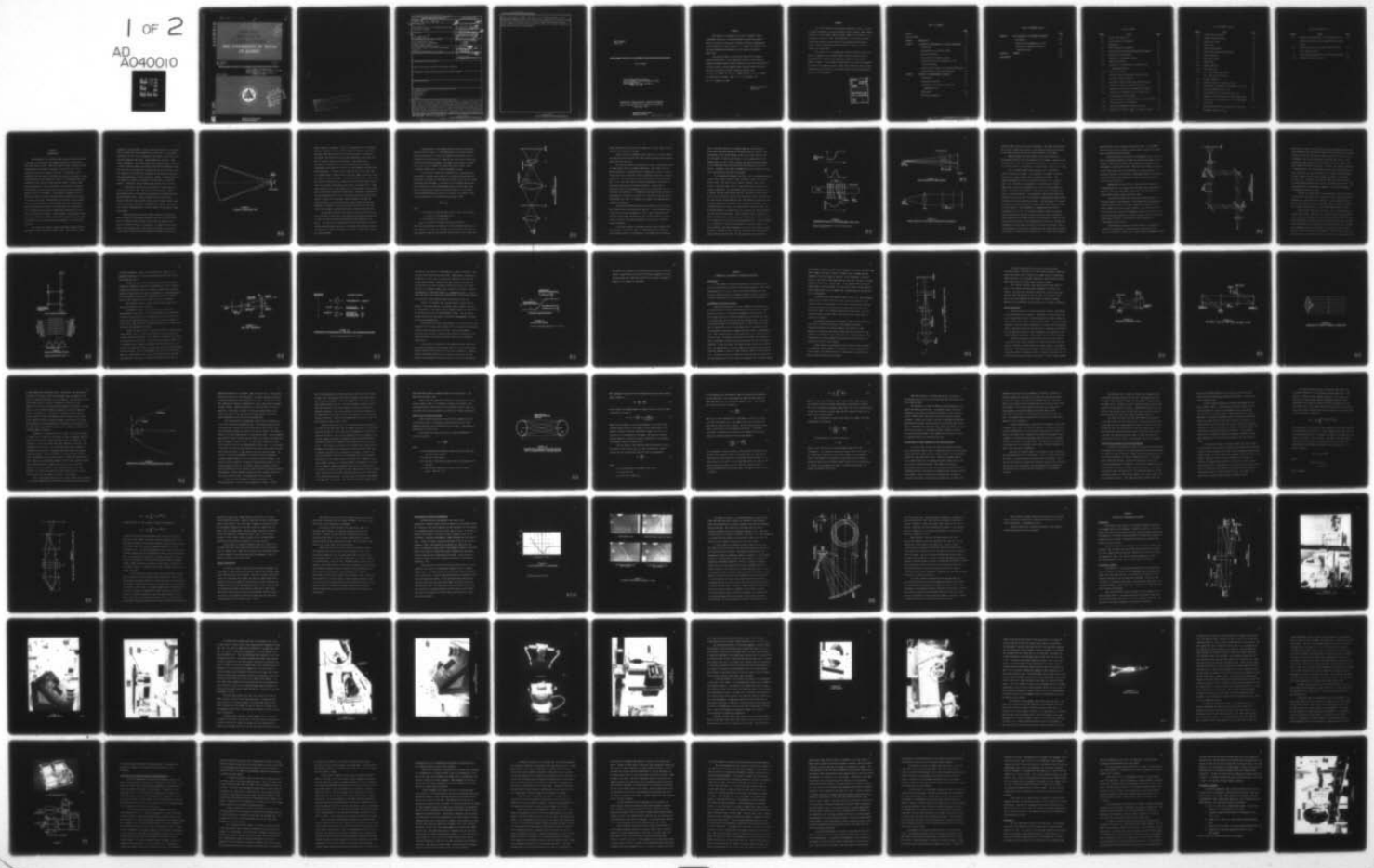

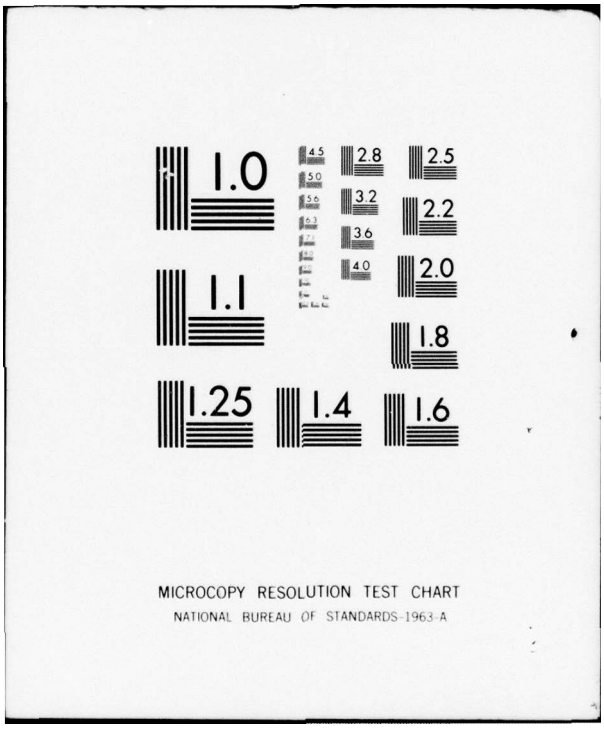
1.0
1.1
1.25
1.4
1.6
1.8
2.0
2.2
2.5
2.8
3.2
3.6
4.0
4.5
5.0
5.6
6.3
MICROCOPY RESOLUTION TEST CHART
NATIONAL BUREAU OF STANDARDS-1963-A

APPLIED RESEARCH LABORATORIES
THE UNIVERSITY OF TEXAS AT AUSTIN

ARL-TR-76-43
August 1976

Copy No.

DEVELOPMENT AND USE OF A SCHLIEREN SYSTEM FOR SOUND PULSE STUDIES

Air Force Office of Scientific Research
Contracts F44620-71-C-0015 and F44620-76-C-0040
Office of Naval Research
Contracts N00014-70-A-0166, Task 0021 and
N00014-75-C-0867

David R. Kleeman

UNCLASSIFIED

SECURITY CLASSIFICATION OF THIS PAGE (When Data Entered)

REPORT DOCUMENTATION PAGE

READ INSTRUCTIONS BEFORE COMPLETING FORM

1. REPORT NUMBER: AFOSR-TR-77-0679	2. GOVT ACCESSION NO.
3. RECIPIENT'S CATALOG NUMBER	
4. TITLE (and Subtitle): DEVELOPMENT AND USE OF A SCHLIEREN SYSTEM FOR SOUND PULSE STUDIES,	5. TYPE OF REPORT & PERIOD COVERED: INTERIM rept.
	6. PERFORMING ORG. REPORT NUMBER: ARL-TR-76-43
7. AUTHOR(s): DAVID R. KLEEMAN	8. CONTRACT OR GRANT NUMBER(s): F44620-71-C-0015, F44620-76-C-0040
9. PERFORMING ORGANIZATION NAME AND ADDRESS: THE UNIVERSITY OF TEXAS, APPLIED RESEARCH LABORATORIES, AUSTIN, TEXAS 78712	10. PROGRAM ELEMENT, PROJECT, TASK AREA & WORK UNIT NUMBERS: 2307A1, 61102F
11. CONTROLLING OFFICE NAME AND ADDRESS: AIR FORCE OFFICE OF SCIENTIFIC RESEARCH/NA, BLDG 410, BOLLING AIR FORCE BASE, D C 20332	12. REPORT DATE: Aug 76
	13. NUMBER OF PAGES: 132 (136 p.)
14. MONITORING AGENCY NAME & ADDRESS (if different from Controlling Office)	15. SECURITY CLASS. (of this report): UNCLASSIFIED
	15a. DECLASSIFICATION/DOWNGRADING SCHEDULE

16. DISTRIBUTION STATEMENT (of this Report)

Approved for public release; distribution unlimited.

17. DISTRIBUTION STATEMENT (of the abstract entered in Block 20, if different from Report)

18. SUPPLEMENTARY NOTES

19. KEY WORDS (Continue on reverse side if necessary and identify by block number)

SCHLIEREN SYSTEM
SOUND PULSES
DIFFRACTION
N WAVES
FOCUSING

20. ABSTRACT (Continue on reverse side if necessary and identify by block number)

Herein is described the schlieren photographic method, in which a density disturbance, such as an acoustic N wave, refracts light passing through it in such a manner that an optical image of the disturbance can be formed on a piece of film. The presentation of the method includes a theoretical description which relies on both geometrical and physical optics. Design considerations and the details of putting a system into operation are also given. The results of two investigation using the schlieren method are presented. Propagation of an acoustic pulse in a duct is modeled, and the photographs are compared with a geometrical prediction

DD FORM 1 JAN 73 1473 EDITION OF 1 NOV 65 IS OBSOLETE

404 434

UNCLASSIFIED

SECURITY CLASSIFICATION OF THIS PAGE (When Data Entered)

based on the method of images. The focusing of a spherical N wave is also photographed. The results are compared to both a linear prediction that includes diffraction and to the results of a previous investigation (E.P. Cornet, "Focusing of an N Wave by a Spherical Mirror," Technical Report ARL-TR-72-40, Applied Research Laboratories, University of Texas at Austin, AD 757 035), in which the measurement was done with a microphone.

ARL-TR-76-43
August 1976

DEVELOPMENT AND USE OF A SCHLIEREN SYSTEM FOR SOUND PULSE STUDIES

David R. Kleeman

Air Force Office of Scientific Research
Contracts F44620-71-C-0015 and F44620-76-C-0040
Office of Naval Research
Contracts N00014-70-A-0166, Task 0021 and
N00014-75-C-0867

APPLIED RESEARCH LABORATORIES
THE UNIVERSITY OF TEXAS AT AUSTIN
AUSTIN, TEXAS 78712

FOREWORD

This report is an adaptation of David R. Kleeman's thesis "Development and Use of a Schlieren System for Sound Pulse Studies," which was written for the degree of Master of Science in Engineering at The University of Texas at Austin. Mr. Kleeman was enrolled in the Electrical Engineering Department, and his degree was granted in August 1976.

The research began in 1974 and was carried out at Applied Research Laboratories. It was supported by the Air Force Office of Scientific Research under Contracts F44620-71-C-0015 and F44620-76-C-0040 and by the Office of Naval Research under Contracts N00014-70-A-0166, Task 0021 and N00014-75-C-0867. Technical monitors were Lt. Col. G. S. Lewis, Lt. Col. R. C. Smith, and Lt. Col. L. W. Ormand for AFOSR and Mr. George L. Boyer, Dr. W. M. Madigosky, and Dr. L. E. Hargrove for ONR.

David T. Blackstock
Supervisor

ABSTRACT

This report describes the schlieren photographic method, in which a pressure disturbance, such as an acoustic N wave, refracts light passing through it in such a manner that an optical image of the disturbance can be formed on a piece of film. The presentation of the method includes a theoretical description which relies on both geometrical and physical optics. Design considerations and the details of putting a system into operation are also given.

The results of two investigations using the schlieren method are given. Propagation of an acoustic pulse in a duct is modeled and the photographs are compared with a geometrical prediction that uses the method of images. The focusing of a spherical N wave is also photographed. The results are compared to both a linear theory prediction that includes diffraction and the results of a previous thesis in which the measurement was done with a microphone.

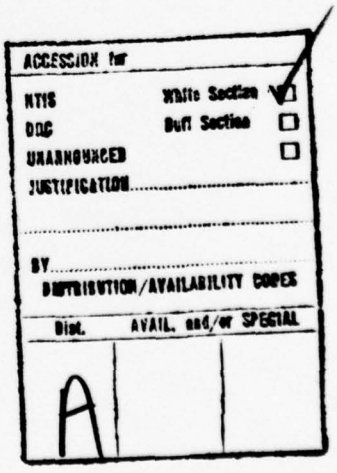

TABLE OF CONTENTS

TABLE OF CONTENTS (Cont'd)

LIST OF FIGURES

LIST OF FIGURES (Cont'd)

LIST OF FIGURES (Cont'd)

CHAPTER 1

INTRODUCTION

The measurement of an acoustic signal usually involves the use of a microphone, which measures the temporal variation of the field at a particular region in space. There are, however, many situations in which a measurement of the spatial variation of the acoustic field is as desirable as that of the temporal variation. A particularly vivid example of this need arises in the study of sound pulse focusing. If only a microphone and a level indicator is used, it is necessary to move the microphone to many positions about the focal region in order to have enough information to deduce the behavior of the pulse as it focuses. The microphone, being of finite size, perturbs the field, causing the measured values to be weighted. If the spatial information is to be gained at a specific instant, many microphones placed about the region of interest can be used. Unfortunately, when the wave is not incident on all of the microphones at about the same time, some of the microphones will measure the acoustic field resulting from a superposition of the original sound pulse and a delayed pulse diffracted off one or more of the earlier microphones. Other phenomena, the physical behavior of which is difficult to deduce from microphone measurements alone, are the diffraction of a sound pulse and the propagation of a sound pulse in a duct.

Kock (1971) has devised a spatial measurement method in which a microphone is swept through the acoustic field. The electrical signal

generated by the microphone is used to alter the intensity of a neon lamp which is placed near the microphone and is swept with it. The spatial distribution of sound thus corresponds to the spatial distribution of the amplitude modulated neon light. The information is stored on a time exposed photograph. This simple method gives a smeared image of the beam; in order to see the beam as a wavetrain, Kock sums the microphone output with the output of the generator supplying the drive for the sound source. The intensity of the light then corresponds to the amplitude resulting from the interference of the two electrical signals. Although quite good for steady state signals, the method is not applicable to transient signals. Furthermore, the microphone again disturbs the sound field.

An alternative approach is thus required to capture the wave in space at a particular time. The solution of the problem of spatial measurement actually occurred before the problem of microphone measurements manifested itself. Toepler (1866) found that the sensitive Foucault knife edge test (described below), used to detect surface imperfections in mirrors and material imperfections in lenses, could also be used to detect inhomogeneities in the air adjacent to the optical element being tested.

The Foucault knife edge test (1859) as applied to a spherical mirror consists of illuminating the mirror (see Fig. 1.1) with a point source of light displaced slightly from the axis of symmetry of the mirror at the mirror center of curvature, R. An image of the source is formed on the opposite side of the center of curvature by the mirror. If one looks at the mirror from just behind the image, the mirror will

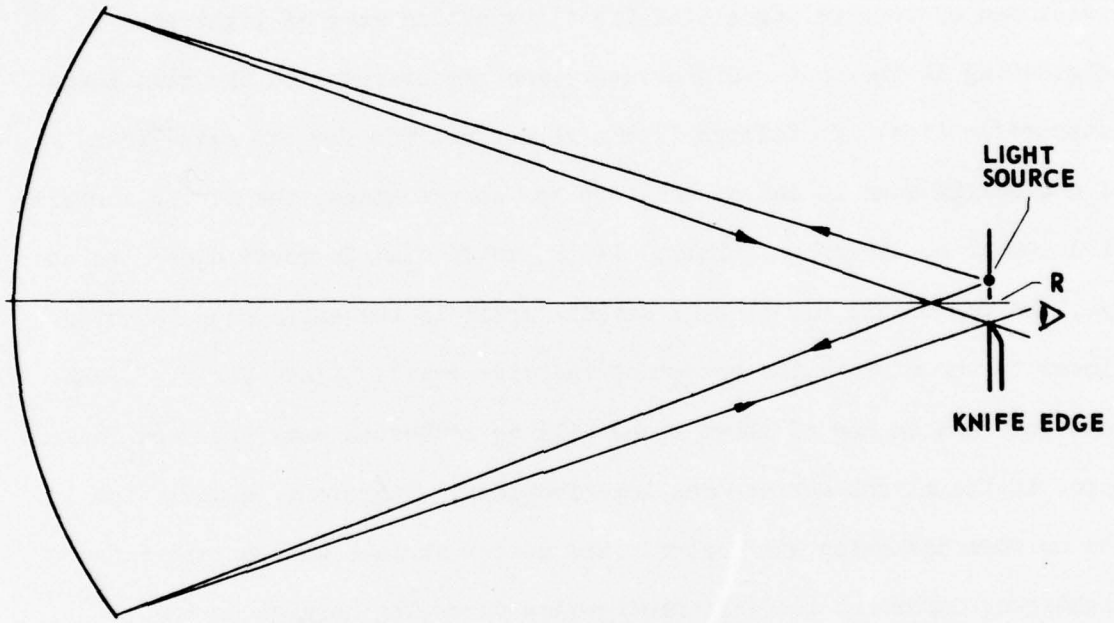

FIGURE 1.1
FOUCAULT KNIFE EDGE TEST

appear uniformly illuminated. This is not surprising if it is recalled that the curvature of the incident wavefront will coincide with that of the mirror only when the point source is at the center of curvature of the mirror. The reflected wave will then reconverge to the source position by specular reflection at the mirror. This process can be envisioned by considering all of the illuminating rays of light as originating at the center of curvature and reconverging to the same point after reflection. It follows (for a source not too far off axis) that if a blocking edge is introduced into the source image, the mirror surface will appear to darken uniformly. If the knife edge is moved closer to the eye, the top of the mirror will darken first; if the knife edge is moved closer to the mirror, the bottom of the mirror will darken first. Light rays incident on one of these areas will be reflected away from the image point if the mirror surface has imperfections. Therefore, a deviation in the uniform darkening will occur. The mirror surface will appear either lighter or darker at the disturbed region depending on whether the deviated rays go over the blocking edge or move farther into the edge. Gradation of darkening occurs because of the finite size of the light source and its image. See Hardy and Perrin (1932) and Linfoot (1955).

In applying Foucault's knife edge test, Toepler noticed not only that he was able to see flaws in the surface of the mirror but also that he could see convection waves disturbing the medium adjacent to the mirror. As a result of his experience with the knife edge test, Toepler devised optical systems specifically for viewing disturbances in the air. The technique of viewing disturbances in the air is called the striation or schlieren method.

A representation of the system used by Toepler and other early workers is shown in Fig. 1.2. The modifications to the basic Foucault test are the addition of a lens L_3 to image the disturbance onto the screen and the substitution of a spark as the light source to facilitate the study of transient phenomena. The light from the spark is focused onto a slit by L_1 to present the system with a well-defined, evenly illuminated light source. A cursory explanation follows.

If the optical elements are considered free of aberrations and diffraction is ignored, the screen will be uniformly darkened when the knife edge is inserted into the image of the light source just far enough to totally block the image. If a pocket of air of higher density than the surrounding air is now placed between lens L_2 and the edge, those rays of light passing through the disturbed region will be refracted. The relationship between the density of a gas and its refractive index is given empirically by the Gladstone-Dale equation (1863)

$$\frac{n-1}{\rho} = K_{GD} \quad ,$$

where

n is the ratio of the free space speed of light c to the speed of light v in the gas being used,

ρ is the density of the gas, and

K_{GD} is a constant for a particular gas and frequency.

Those rays going through the upper part of the disturbed region will be bent downward, will pass over the edge, will be focused by L_3, and will thus produce an image of the disturbed region on the screen. Those rays

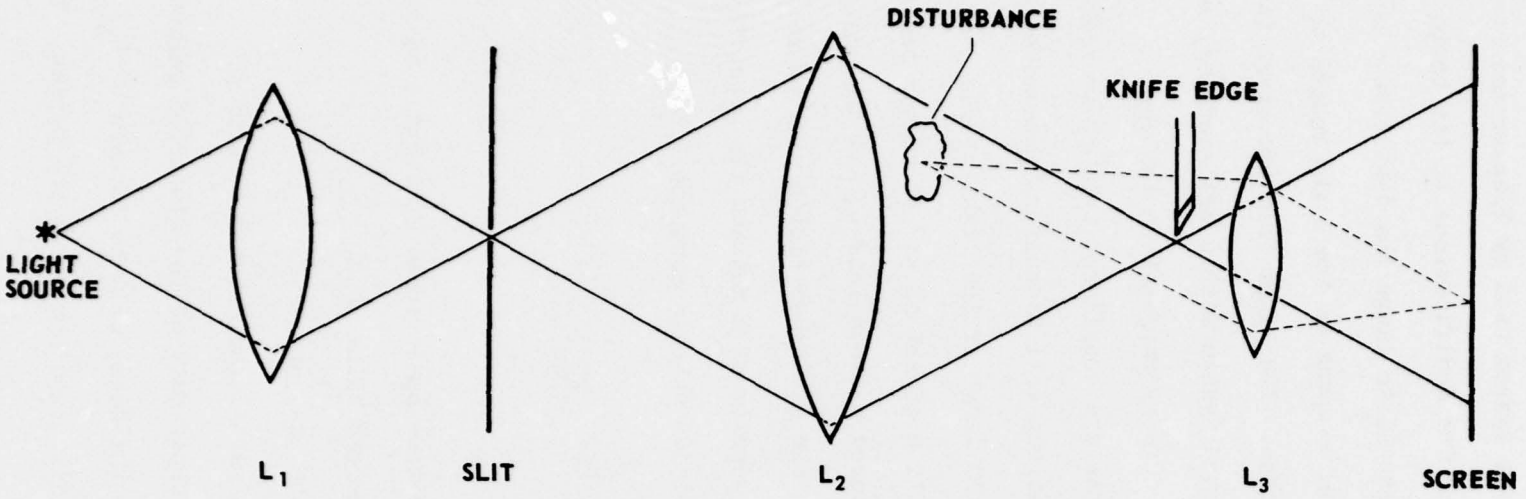

FIGURE 1.2
TOEPLER SCHLIEREN ARRANGEMENT

passing through the lower part of the region will be bent upward and will continue to be blocked by the edge.

Using the above arrangement, Toepler was able to visually observe the spherical sound waves sent off from a second spark gap fired slightly before the first spark gap.

The schlieren method was explored by a number of scientists before it became widely used by aerospace researchers. Mach (1876) used the method extensively to photograph the air compressions caused by bullets. He was particularly interested in the disturbances produced by supersonic projectiles. He also studied the sound waves given off by arcing spark gaps. R. W. Wood (1899) applied schlieren photography to the study of sound waves interacting with various boundaries. He was able to demonstrate some of the fundamental principles of wave motion, such as reflection and diffraction. In Bergman's (1949) application of schlieren photography to ultrasonics, the sound to be visualized diffracts rather than refracts the light. He obtained, for example, the beam patterns of ultrasonic transducers.

Schlieren photography has been used extensively in wind tunnels where flows around various bodies are studied. It has also been applied to heat flow and shock propagation in tubes. Before continuing with schlieren photography, the subject of the next two chapters, it will be useful to consider alternative approaches to the study of refractive index disturbances.

A technique similar to schlieren was developed by Dvorak (1880). The technique is called the shadow or shadowgraph method and has been quite popular because of its simplicity. The shadow effect occurs when

rays of initially parallel or diverging light are intercepted by a screen after they pass through the disturbed region of interest. The illumination of the screen depends on the flux of light rays incident per unit area. As can be seen in Fig. 1.3, the illumination will be highest where the rays of light converge, the rays from areas adjacent to the bright area having been shifted by the refraction in the test section. Similarly, the lowest illumination will be on that part of the screen from which the rays have been shifted.

In its simplest arrangement (see Fig. 1.4), the shadowgraph method requires only a point source of light, typically a spark, and a photographic plate. The spark source is placed a distance from the test section so that the plate, which is placed beyond the test section, is properly illuminated. The photographic plate is usually placed at such a distance that the rays bent the most will just meet the unbent rays. If the film is placed too far from the disturbance, many of the bent rays will have already crossed adjacent rays. The difference between the dark and light regions will be greater, but a blurring of the image of the refracting region will occur. If, alternatively, the film is too close to the disturbance, the sensitivity will be low and the film may possibly interfere with the disturbance. Often a parallel beam of light will be passed through the test section (Fig. 1.5) so that all of the test region can be imaged onto the film with uniform magnification. In many instances it is undesirable to have the film adjacent to the test section; a 2-mirror parallel light beam arrangement (as is also used in many schlieren systems) is employed so that a lens may be placed in the confined beam coming from the second mirror. The lens images the plane where the

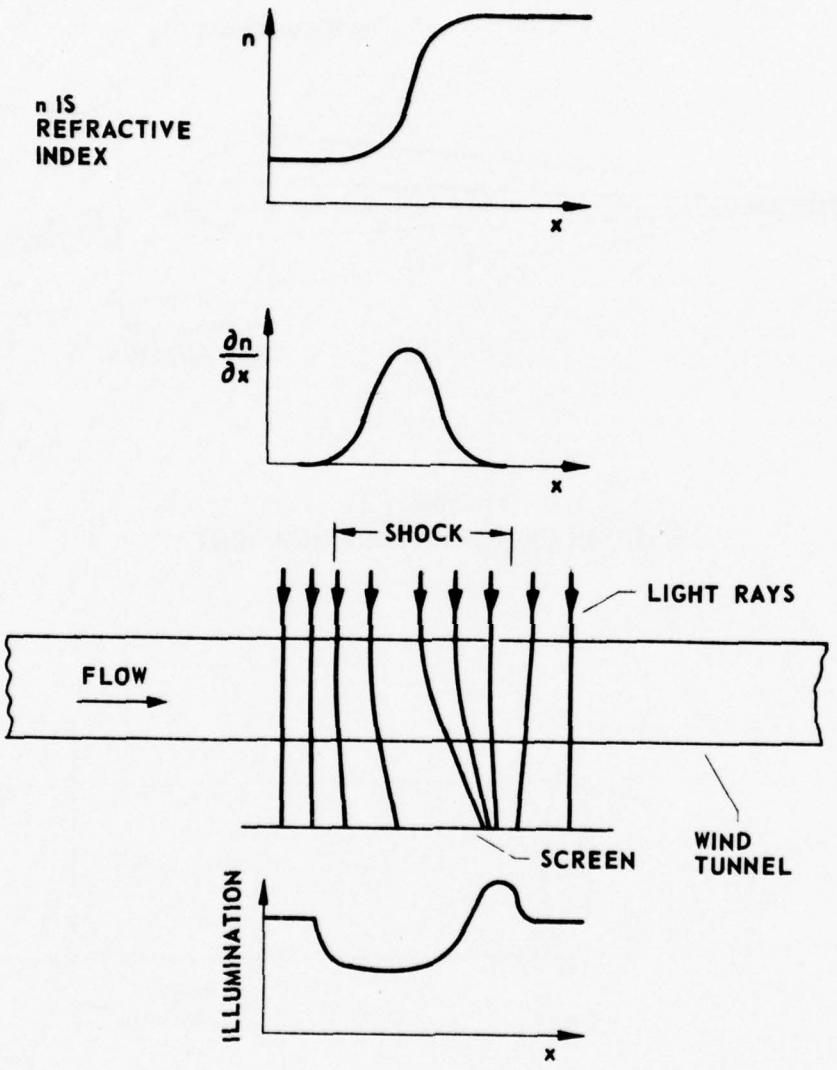

FIGURE 1.3
SHADOWGRAPH IMAGE OF A TWO-DIMENSIONAL SHOCK WAVE

Reproduced from Modern Developments in Fluid Dynamics; High Speed Flow, Edited by L. Howarth (1953)

ARL - UT
AS-76-755
DRK - DR
7 - 1 - 76

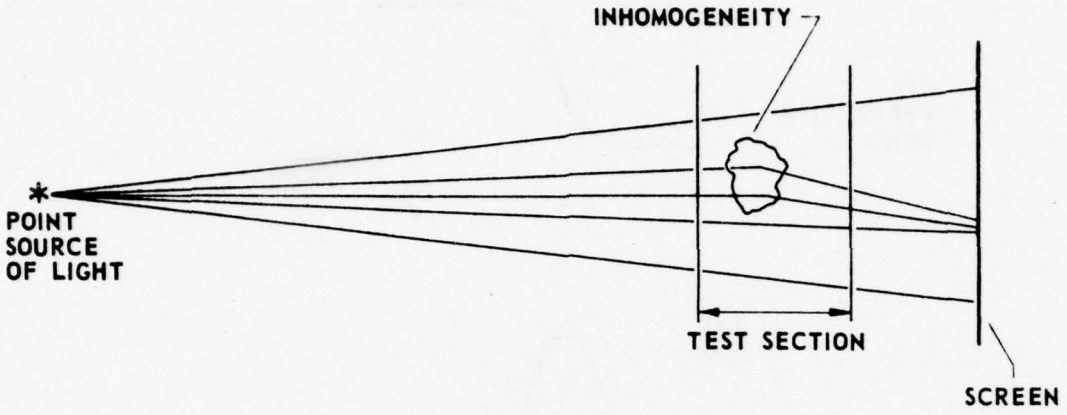

FIGURE 1.4
BASIC SHADOWGRAPH ARRANGEMENT

ARL - UT
AS-76-756
DRK - DR
7 - 1 - 76

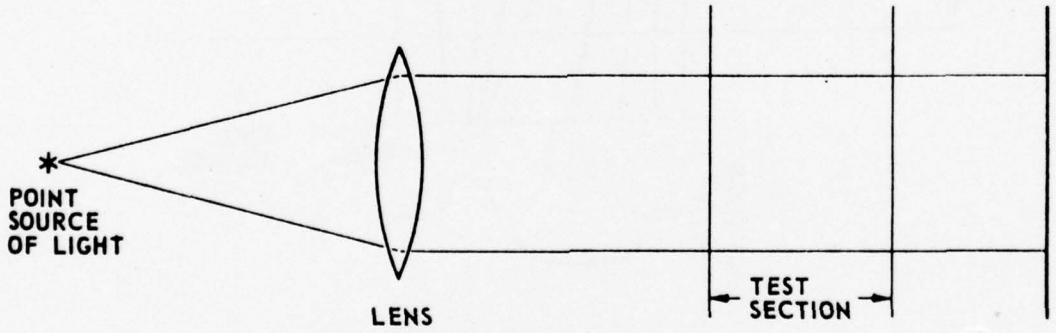

FIGURE 1.5
SIMPLE PARALLEL LIGHT BEAM SHADOWGRAPH ARRANGEMENT

ARL - UT
AS-76-757
DRK - DR
7 - 1 - 76

film would have been put onto the new film plane. The image actually will not be quite as sharp when a lens is used, since the region on both sides of the object plane of the lens will also contribute to the image.

Shadow phenomena are quite common in the everyday experience. The apparent heat flow from a hot automobile is an example. Another is the projection onto a wall in a darkened room of the flow of water over a window when the window is illuminated by a single distant light source at night.

Use of a simple shadow system can assist one in observing relatively weak fluid changes. It is possible, for example, to observe the flow of a stream of water within a larger body of water. This simple experiment can be done in a bathtub with about 4 in. or more of water in it. The water is illuminated by a single source of distant light, which the typical incandescent bulb built into the bathroom will supply. The bottom of the bathtub is the screen (white is probably the best color for the bathtub). The experimenter places a hand beneath the surface of the water so that the forefinger is approximately midway between the bottom of the tub and the water surface. The disturbance of the water created by inserting the hand will generate surface waves that are visible on the tub bottom. (This experiment is probably best done with the experimenter in the tub.) If no further movement is made, the surface waves should damp out and the tub bottom should be evenly illuminated. With a simple and quick single motion of the forefinger, in which the only movement should be that of the forefinger about its joint at the hand, the experimenter sets the water in motion in the center of the body of water. The disturbance will show up at a distance from the finger within a second or two and will appear to be a turbulent eddy. Of course, more fingers or

some other object like a popsicle stick can be used. It is necessary only to be able to move a section of water within a larger body without unduly disturbing the water surface.

Using the simple point source-film arrangement, Foley (1905) was able to photograph diffraction fringes from electric discharges and fluid streams. Later Foley and Souder (1912) applied the technique to the photography of spark excited waves. They also took a number of pictures in which the sound pulses were constrained by various boundaries. Of particular interest is the sequence of photographs showing the progressive reflections within a two-dimensional ellipse in which the spark was placed at one of the foci.

Shadowgraphs have been used in studies of wave reflections in building models (see, for example, Davis and Kaye, 1927), and have been applied to shock tube experiments (Sturtevant, 1974) and projectile flight studies (Sanai, Toong, and Pierce, 1976).

A third method based upon the refractive index variation in a disturbed region is interferometry. This method yields measurements of extreme sensitivity and is used when a quantitative analysis of the density change in the test region is desired. The extreme sensitivity gives rise to many problems of implementation that can be resolved only with an appreciable expenditure of time and money. For this reason, this method was not employed. Nevertheless, a basic explanation of interferometry will be given.

Interferometry as applied to density studies is probably best understood by examination of the Mach-Zehnder (1892) system (see Fig. 1.6). The beam of light from a single narrowband (quasimonochromatic)

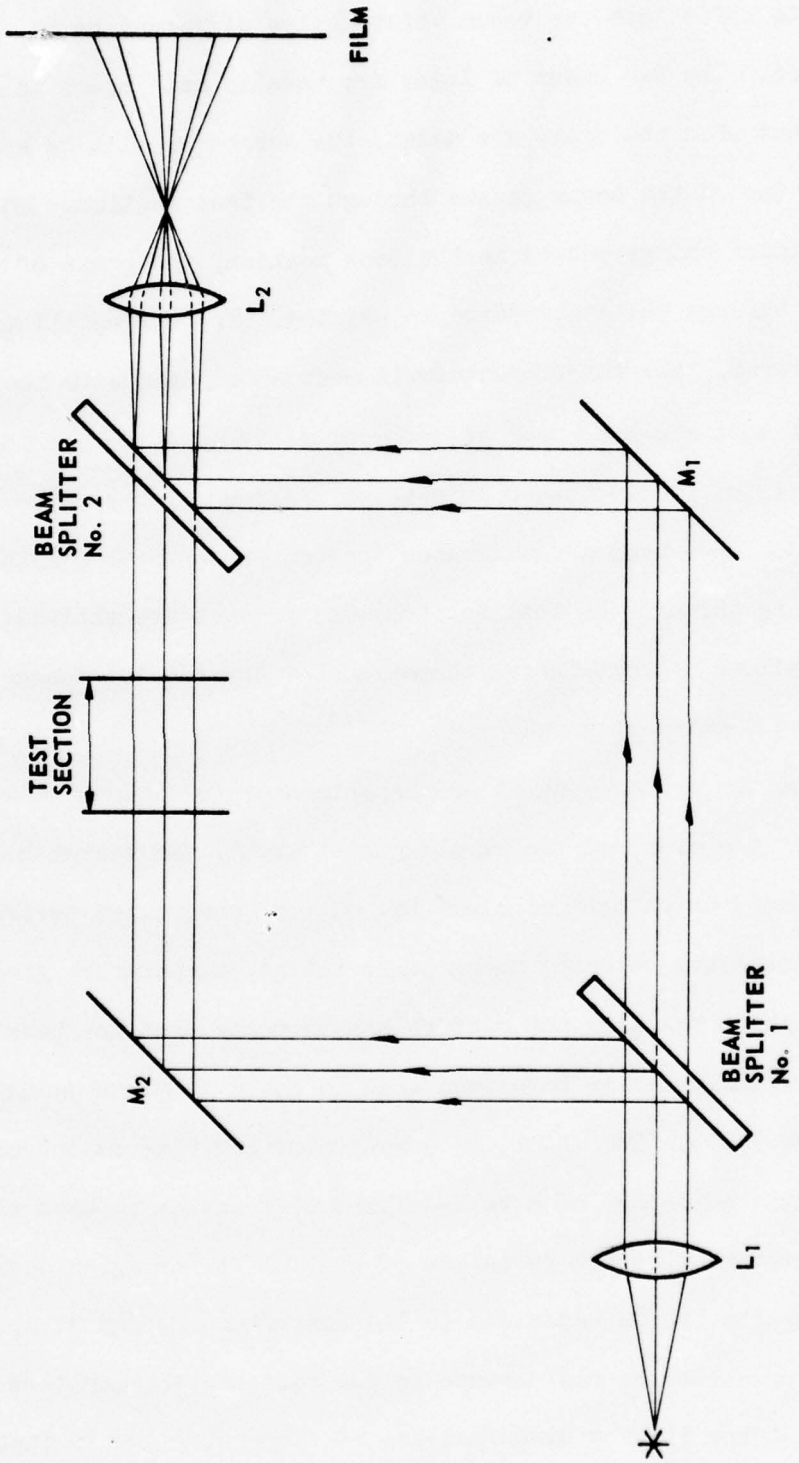

FIGURE 1.6
MACH-ZEHNDER INTERFEROMETER

ARL - UT
AS-76-758
DRK - DR
7 - 1 - 76

light source is split into two beams which follow different paths and are then recombined. The two beams of light are usually made equal in optical distance so that when the beams are added, the screen or film is evenly illuminated. One of the beams passes through the test section. When a refractive index change occurs in the test section, the phase of the light passing through the disturbance is shifted. The screen illumination is thereby altered. The interferometer is most often used with the two beams incident on the second beam splitter at slightly different angles so that a number of evenly spaced fringes will appear on the screen (see Fig. 1.7). Thus when a disturbance changes the optical length of the beam passing through the test section, the fringes are shifted. This fringe shift allows a quantitative comparison of the density change if the undisturbed density is known.

Because the system enables the experimenter to detect a change of optical path of the order of the wavelength of light, the system requires extremely well-corrected optical elements. A very controlled environment is also necessary so that, among other things, temperature gradients and building vibrations will not disturb measurements that are taken.

More recently lasers have been used in basic 2-mirror schlieren systems (Clark, 1975). The laser, as a source of coherent monochromatic light, offers the advantage of a well-defined diffraction pattern at the knife edge region so that the technique of spatial filtering as developed from Fourier optics (to be explained in the next chapter) can be applied. More information about the disturbance in the test section may thus be derived. One of the biggest disadvantages of coherent light is that each particle of dust on an optical surface or in the optical path gives rise to

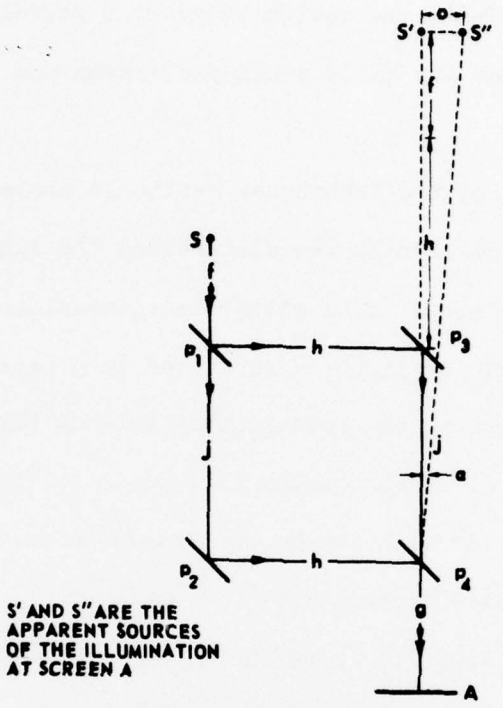

THE MACH-ZEHNDER INTERFEROMETER

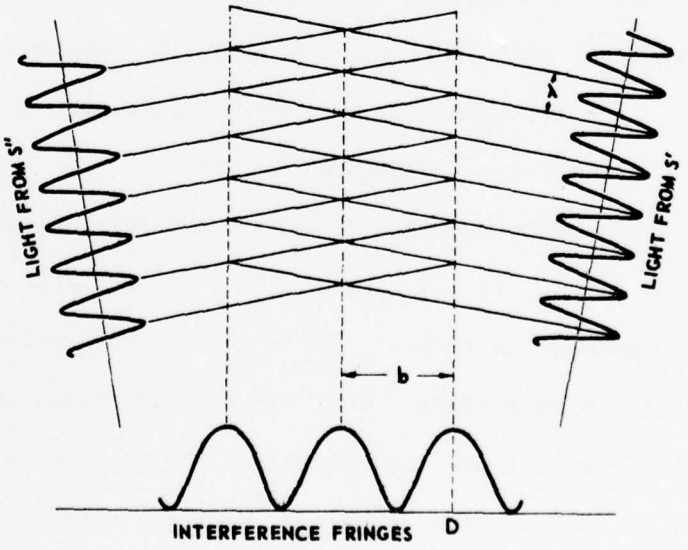

FIGURE 1.7
FORMATION OF INTERFERENCE FRINGES

Reproduced From Modern Developments in Fluid Dynamics: High Speed Flow, Edited by L. Howarth (1953)

a diffraction pattern. Thus, the system requires a degree of care somewhere between that for the basic schlieren system and that for the interferometric system.

In order for any of the techniques mentioned above to provide unambiguous information concerning the disturbance the light is passing through, the disturbance needs to be either two-dimensional or axially symmetric so that each ray of light is refracted in a predictable manner. Further discussion concerning the relationship between the schlieren image and its conjugate disturbed region will occur in Chapter 2.

Some graphical aids will now be used to indicate what can be measured by the three basic techniques.

As indicated in Fig. 1.8, a refracted ray of light can be characterized in three ways: 1) by the time change (Δt) of the arrival of the ray at the screen, 2) by the angular shift ($\Delta\theta$) of the ray with respect to its undeviated position, and 3) by its position change (Δh) on the screen. The variables are measured respectively by interferometry, schlieren, and shadowgraph techniques.

Figure 1.9 shows how Δt, $\Delta\theta$, and Δh are related to various simple shapes (Hilton, 1951). If the rays of light are in vacuo except when incident upon the objects made of, for example, crown glass, the behavior of the rays will be as follows. When the rays are normally incident on a rectangular piece of glass, no bending of the rays takes place. The rays are only delayed in time; thus their time of arrival at some distant screen is altered. Only an interferometer can detect this deviation of the rays. Rays incident upon a glass prism experience both time delay and refraction. The prism or a similarly shaped object can thus be

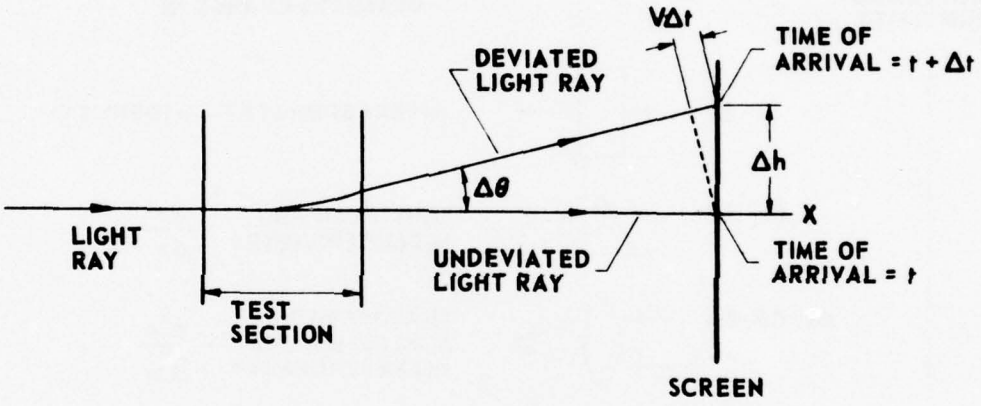

FIGURE 1.8
LIGHT RAY PARAMETERS

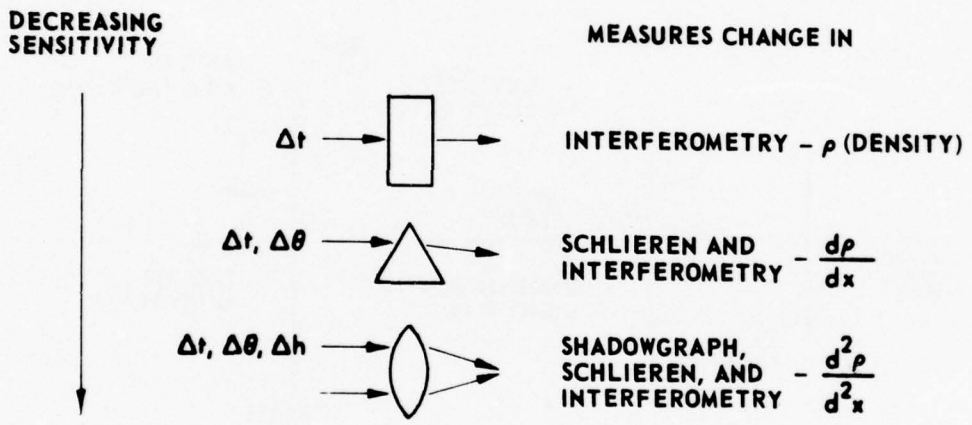

FIGURE 1.9
COMPARISON OF INTERFEROMETRIC, SCHLIEREN, AND SHADOWGRAPH METHODS

Adapted from High Speed Aerodynamics by W. F. Hilton (1951)

detected by using either an interferometer or a schlieren system. The lens also delays the rays and bends them. Additionally, the amount of refraction of a given ray is a function of what part of the lens the ray has passed through. Therefore the rays converge or diverge, as the case may be, and the illumination beyond the lens is not uniform. The lens or a similarly shaped object can thus be detected by using an interferometer, a schlieren system, or a shadowgraph system. It can be shown that each of the three basic methods given is functionally related to the density of the disturbed region as indicated in Fig. 1.9.

Figure 1.10 indicates how a typical shock at a given time is detected by the three methods. The spatial density change is detected by interferometry. The spatial rate of change of density is detected by the schlieren as well as the interferometric method. And the second spatial derivative of the density is detected by shadowgraph, schlieren, and interferometric methods.

As mentioned previously, interferometry is the most sensitive and quantitative of the three basic methods, but it is also the most expensive in terms of both equipment and setup time. Since interferometric facilities were not readily available and an existing schlieren system became available, the schlieren method was used in the investigation reported here.

A more detailed explanation of the schlieren method, which will include the limitations of the equipment that can be used and the consequential general design criteria, will be given in Chapter 2. Chapter 3 contains information pertaining to the specific system used for this research and experimental procedures relevant to the use of the system.

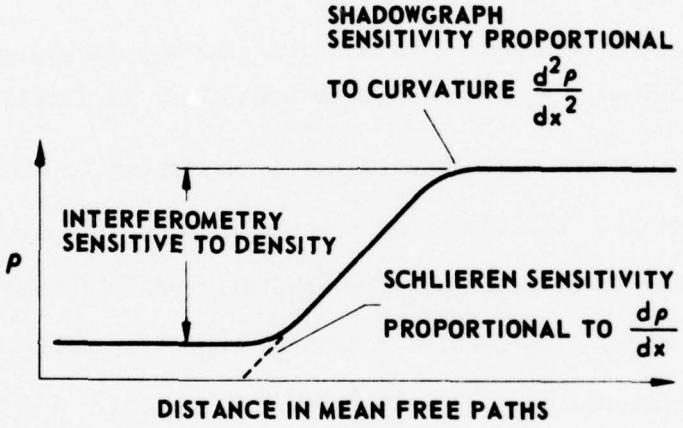

FIGURE 1.10
TYPICAL SHOCK FRONT

Reproduced from High Speed Aerodynamics by W. F. Hilton (1951)

The reader not interested in procedural detail may wish to skip this chapter. Applications to the study of N waves propagating in a duct and reflecting off a spherical reflector are discussed in Chapter 4. Chapter 5 is a summary of the report.

CHAPTER 2

A THEORETICAL DEVELOPMENT OF SCHLIEREN PHOTOGRAPHY

Introduction

In this chapter the schlieren process will be examined in more detail by considering the behavior of the system components. Some system configurations will be given. After the optical phenomena have been discussed, design criteria for a general schlieren system, in which use is made of both geometrical and physical optics, will be delineated.

Arrangements of a Schlieren System

Before the characteristics of the components are discussed, an overview of some of the basic configurations used to realize a schlieren system will be given. The simplest arrangement is shown in Fig. 1.2. This system consists of a narrow rectangular source of light, the field or schlieren lens, the knife edge, and the viewing system. For all but the simplest systems the rectangular source of light consists of light that is focused onto a slit by a condensing lens or lens system. The viewing system is typically an imaging lens and a screen or photographic film. This schlieren system is both simple and not too costly for small fields of view. The greatest deficiency of the single lens schlieren is that a disturbance extended along the optical axis will not be uniformly magnified. If the test region is between the light source and the field lens, the rays deviated at the knife edge will be bent most when a given refractive gradient is near the light source as opposed to being near the lens. If the test section is between the knife edge and the field lens, the ray deviation at the knife edge will be greatest when the given refrac-

tive gradient is near the field lens as opposed to being near the knife edge. When a single field lens is used, its diameter must be larger than the dimension of the disturbance so that all of the disturbance of interest will be in the cone of light associated with the lens. The cost of a large diameter corrected lens is quite high. If the desired field of view is large enough, it may be cheaper to use two field lenses to form a parallel beam of light than to use one larger lens to ensure that the test section will be illuminated.

A parallel light lens system is shown in Fig. 2.1. The rectangular light source is placed at the focal plane of the first field lens, and a parallel beam of light emerges from the lens. The beam passes through the test section and is then incident on the second field lens, which focuses the light to the conjugate image of the light source. As in all schlieren systems the knife edge is introduced at this image plane, as explained in Chapter 1.

The greatest advantage of the parallel light schlieren system is that there is uniform magnification of the imaged disturbance. Furthermore observation of axially symmetric disturbances is less ambiguous with parallel light because those rays that contribute to the image will be refracted by only a small section of the disturbance. The interpretation of axially symmetric disturbance schlieren pictures is presented at the end of this chapter.

Concave mirrors can replace the field lenses in either a parallel or nonparallel beam arrangement. The mirrors are usually spherical and front surfaced. The relative merits of using lenses or mirrors will be taken up when aberrations are discussed.

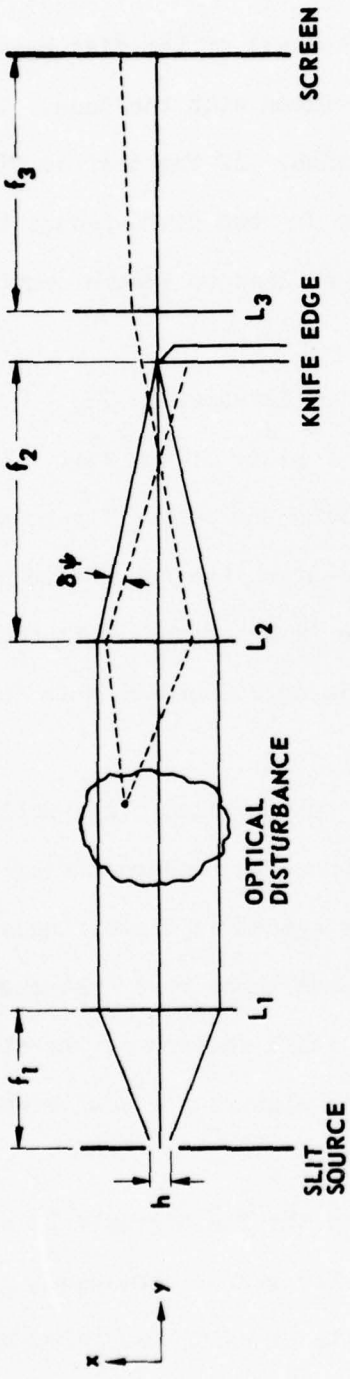

FIGURE 2.1
TWO LENS, PARALLEL LIGHT BEAM SCHLIEREN SYSTEM

ARL - UT
AS-76-763
DRK - DR
7 - 1 - 76

A single concave mirror can be used in a multiple pass, coincident system. (See Fig. 2.2.) The coincident system is used only where a high sensitivity is required and image quality, in particular image resolution, is of secondary importance. Holder and North (1963) give further details on single mirror schlieren systems.

The 2-mirror, parallel light beam schlieren system shown in Fig. 2.3 is probably the most common arrangement for serious flow studies. The significant difference between the 2-mirror and 2-lens parallel light beam systems is that the light is introduced on the axis of the lens system and off of the axis of the mirror system. Because of this difference, the two systems must be analyzed separately.

Optical Aberrations

Further discussion of lenses and mirrors requires consideration of the aberrations of the elements. Aberrations are usually dealt with by use of geometrical optics. Useful references are those by Hardy and Perrin (1932), Brown (1965), and Born and Wolf (1970). For more extensive treatment of optical element aberrations, see Conrady (1943) and Southall (1936). Aberrations that are observable and of consequence in schlieren work are spherical aberration, coma, astigmatism, and longitudinal and lateral chromatic aberration. Each of these will be briefly discussed.

Spherical aberration occurs when the rays from a point source on the axis of the optical element do not form a point image after the rays are refracted or reflected from the optical element. The image is spread out. This smearing of the image is easily seen when the focusing of parallel light by a spherical mirror is observed. (See Fig. 2.4.) It should be noted that the spread of the image on the axis becomes greater

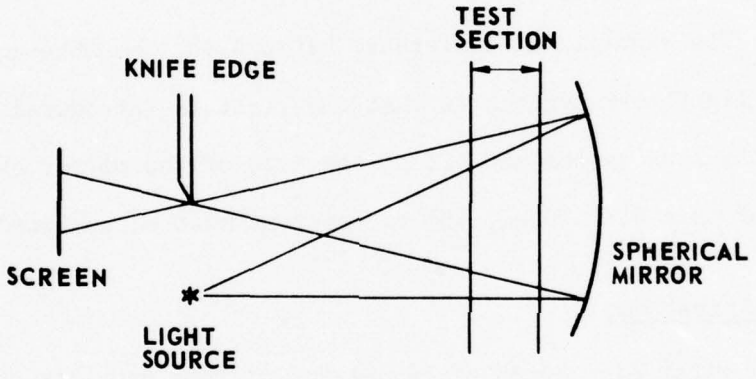

FIGURE 2.2
COINCIDENT SCHLIEREN SYSTEM

ARL - UT
AS-76-764
DRK - DR
7 - 1 - 76

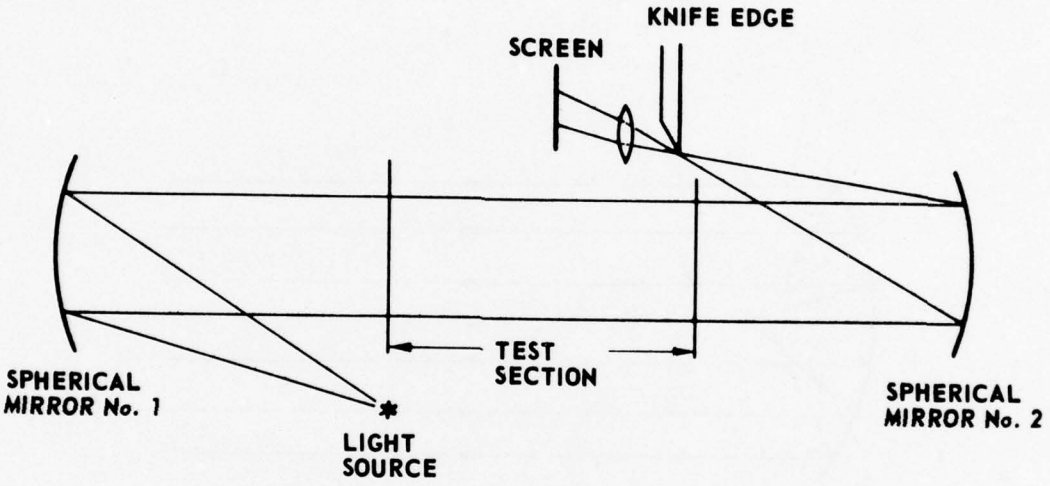

FIGURE 2.3
TWO MIRROR, PARALLEL LIGHT BEAM SCHLIEREN SYSTEM

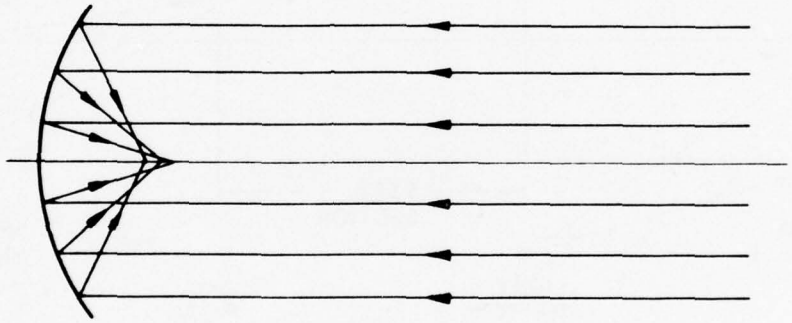

FIGURE 2.4
SPREADING OF FOCUS BY SPHERICAL ABERRATION

as rays farther from the axis are used. This implies that the radius of curvature of the mirror should be much greater than the diameter of the mirror if spherical aberration is to be minimized. When the ratio of the focal length, which is one half the radius of curvature, to the diameter of the mirror (the ratio being designated the f/number) is large, there is little difference between a parabolic mirror and a spherical mirror. (See Fig. 2.5.) In reality, if a parallel beam of light is desired, parabolic rather than spherical mirrors should be used, since only a parabolic mirror will perfectly image a point source at infinity or alternatively (as a manifestation of the principle of reversibility of the light path) a point source at the focus of a parabolic mirror will be perfectly imaged at infinity.

Similarly if a large lens were to be used, it would be necessary to figure, that is, shape the lens surface so that the marginal rays far from the lens axis would undergo the proper amount of refraction. The figuring of a lens to any shape other than spherical is difficult, time consuming, and thus costly. In a system with many lenses, spherical aberration can be reduced by choosing lenses with similar but opposite signed aberrations. Positive aberration is associated with a positive lens, the paraxial focus, that is, the focus of those rays near the optic axis, being the ray intersection farthest from the lens. Negative aberration is associated with a negative lens, that is, one in which the paraxial focus is the nearest of the intersecting rays to the lens. Because of the expense associated with large corrected lenses, lenses are used only where the region of interest is rather small.

When a comet-shaped image of a point source results from a variation of the lateral magnification for different regions of the lens, the second

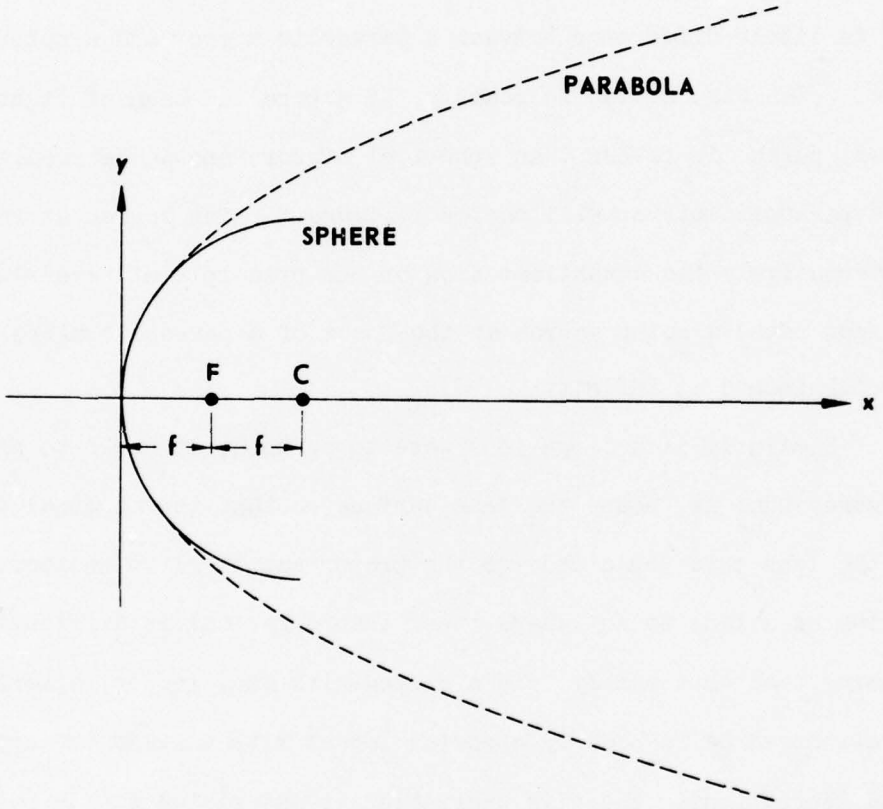

FIGURE 2.5
COMPARISON OF SPHERICAL AND PARABOLOIDAL SURFACES

ARL - UT
AS-76-812
DRK - DR
7 - 8 - 76

aberration considered in this paper, coma, is said to exist. Coma affects objects near but not on the optical axis. In lenses coma may be corrected by properly shaping the curved surfaces of the lens. In fact, for a thin lens, coma may be completely eliminated for a given object-source distance by proper shaping. Spherical aberration, on the other hand, can only be minimized. Fortunately the shape of a lens for minimum coma is quite close to the shape of the same lens for minimum spherical aberration. Coma as manifested in mirrors will be discussed later.

The third aberration, astigmatism, results from the difference in the foci for meridional and sagittal rays. The meridional rays are rays in the plane that contains the optical axis and the ray from the object point that passes through the center of the optical element. The sagittal rays are in a plane perpendicular to the meridional plane. When the sagittal rays cross in a plane different from the plane of crossing of the meridional rays, astigmatism is said to exist. In other words, instead of a point focus, there are two line foci perpendicular to each other. It is necessary to introduce the light into the system off the optical axis when mirrors are used so that the source of light does not block the reflected light. The existence of coma and astigmatism for off-axis sources is perhaps the strongest argument against the use of mirrors in schlieren systems. The solution of this problem for the parallel beam schlieren system is to use off-axis parabolic mirrors. The off-axis figuring eliminates coma and reduces astigmatism, and the parabolic shape eliminates spherical aberration. Unfortunately, off-axis parabolic mirrors are quite expensive because, as with large corrected lenses, the figuring must be done by hand.

Up to now we have assumed no frequency dependence of the refracting material. This is a poor assumption for lenses. In fact

each of the monochromatic aberrations actually varies with the frequency of light used. Additionally there are two chromatic aberrations which result from the dependence of the focal length of a lens on the color of light passing through the lens. The first chromatic aberration results from axial variation of the focal length and is called longitudinal chromatic aberration. The second aberration results from dependence of the magnification of the image on the focal length and is called lateral chromatic aberration. Higher order aberrations can occur but these will arise mainly for large fields of view.

From the discussion above, it is seen that lenses and mirrors do not suffer to the same degree from the primary aberrations. As previously mentioned, mirrors can suffer from coma and astigmatism in addition to spherical aberration. When off-axis paraboloids are not available for a 2-mirror system, the system is arranged so that the off-axis error of one mirror is effectively negated by the off-axis error of the second mirror. Additionally any elongation of the light source image because of astigmatic and higher order aberrations is placed along the knife edge so that the sensitivity of the system is not reduced. If most of the refractive gradient components in a disturbance are vertical, maximum sensitivity will be obtained using a horizontal slit. Therefore, if the source image is going to be elongated because of astigmatism, it is best that the image be elongated along the edge so that the sensitivity is not altered. To achieve horizontal source image elongation and to minimize coma, one places the knife edge, spherical mirrors, and the light source in the same horizontal plane. The knife edge is placed at the astigmatic line image that is horizontal. The light source and knife edge should

make equal small angles on opposite sides of the optical axis. (See Barnes and Bellinger, 1945.)

Mirrors have the additional advantage of requiring only a single properly shaped surface to be metalized, usually with aluminum. This requirement greatly reduces the cost of and concern over the quality of the glass used and also eliminates any concern for chromatic aberrations.

Sensitivity of a Schlieren System

Other properties which can be dealt with by geometrical optics and which are useful in evaluating a schlieren system are the light gathering capability and the sensitivity of the system. Some background material will be given first.

The luminous flux (dF) of a source of light intercepted by a receiver is given by

$$dF = B \frac{dSdA}{r^2} \quad ,$$

where

B is the luminance (the luminous flux per unit solid angle per unit area from a source),

dS is the area of the source,

dA is the area of the receiver (whose normal is perpendicular to dS), and

r is the distance between the source and receiver along a normal. (See Fig. 2.6.)

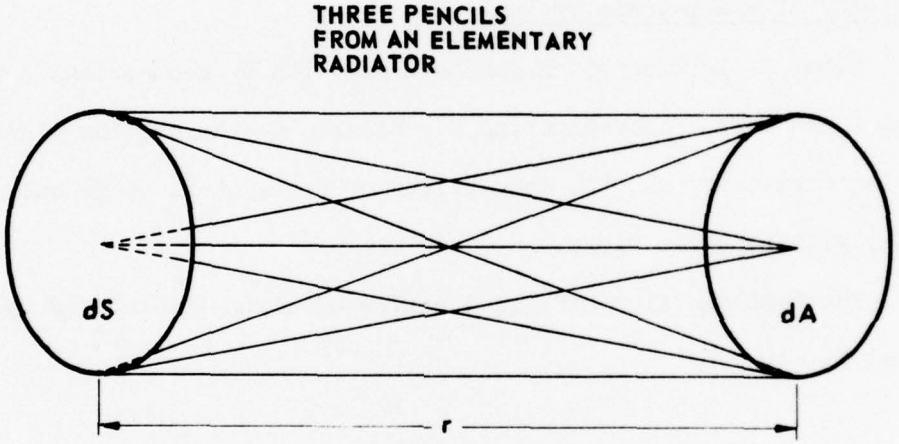

FIGURE 2.6
LUMINOUS FLUX TRANSMITTED BY ONE SURFACE
THAT IS INTERCEPTED BY A SECOND SURFACE

ARL - UT
AS-76-814
DRK - DR
7 - 12 - 76

The illuminance (dE), which is the luminous flux per unit area incident upon a surface, is

$$dE = \frac{dF}{dA} = B \frac{dS}{r^2} \quad . \tag{1}$$

For the case of an imaging system or element such as a lens, the image illumination is given by

$$E = B\omega' = B \frac{\pi d^2}{f^2} = B \frac{\text{const}}{(\text{f/number})^2} \quad , \tag{2}$$

where the solid angle ω' is given approximately by the area of the imaging element divided by the element's focal length squared. The rapidity or speed with which a photographic image is built up is a function of the illumination of the image. The speed of a lens or optical system is, therefore, inversely proportional to the square of its f/number (Jenkins and White, 1950).

For the parallel light beam schlieren system shown in Fig. 2.1, the luminous flux incident on L_1 (L_1 and L_2 being either lenses or mirrors for this consideration) per unit time is approximately

$$F = \frac{BhAw}{f_1^2} \quad , \tag{3}$$

where

w is the width and h the height of the source,

A is the area, and

f_1 is the focal length of L_1.

If the absorption and scattering of light in the system are negligible and the knife edge is not intercepting the light, the same amount of light that fell on L_1 will fall on the screen or film . The illumination of the screen will therefore be

$$E_o = \frac{Bhw}{m^2 f_1^2} \quad , \tag{4}$$

where m, the linear magnification of the image, is given by f_1/f_2 and f_2 is the focal length of L_2. The magnification will determine over what area the luminous flux is spread. At the knife edge position the image of the source will have dimensions mh and mw. If the edge is parallel to dimension w and blocks all but height a of the source image, the uniform illumination on the screen becomes

$$E = \frac{a}{\left(\frac{f_2}{f_1}\right)h} E_o = \frac{Baw}{m^2 f_1 f_2} \quad . \tag{5}$$

If a disturbance occurring between L_1 and L_2 causes a refractive index gradient with a component normal to the knife edge, the light passing through the disturbed region will be deflected through an angle $\delta\psi$ in a plane normal to the cutoff. The corresponding part of the image of the source in the focal plane of L_2 will shift by a distance $f_2\delta\psi$ in a direction perpendicular to the knife edge. The angle $\delta\psi$ shown in Fig. 2.1 is given by

$$\delta\psi = \frac{1}{n_o} \int_{y_1}^{y_2} \frac{\partial n}{\partial x}\, dy \quad , \tag{6}$$

where n is the local refractive index in the disturbed region and n_o is the refractive index of the same region when no disturbance is present. The y axis is along the undisturbed light beam, the x axis is perpendicular to both the y axis and the knife edge, and the integral is taken over the depth of the disturbed region.

For a displacement of $f_2\delta\psi$ of the light source image, the screen illumination will change by

$$\delta E = \frac{f_2\delta\psi}{\left(\frac{f_2}{f_1}\right)h} E_o = \frac{B\delta\psi w}{m^2 f_1} \quad . \tag{7}$$

The sensitivity S is usually defined as

$$S = \frac{dc}{dp} \tag{8}$$

where c is the contrast and p is any parameter that affects the illumination. The contrast is defined by $c=\delta E/E$, where in this case, E is the background illumination, and δE is the change in the illumination. Since in the geometric ray approach the rays detected by a schlieren system are those that are deviated enough to pass over the blocking edge, it follows that the smaller the angle of detected deviated rays, the greater the system's sensitivity.

From the definition of contrast and Eq. (8), $c=f_2\delta\psi/a$ and $S=dc/d\psi=f_2/a$, where dp in Eq. (8) is (for this case) the angular shift of the rays of light.

The implication is that the larger f_2 and the smaller a, the greater the system's sensitivity. In practice, a has a lower limit determined by the minimum illumination necessary to expose film when a short duration flash light source is used for studying transient phenomena. A large focal length is now seen to decrease the spherical aberration and increase the sensitivity but to lower the speed of the system. Furthermore the larger the focal length, the greater the space needed for the system. A compromise f/number is chosen to satisfy the conflicting requirements. The f/number for the system's mirrors is typically chosen to be between f/6 and f/12.

Considerations of Other Components in the Schlieren System

It is rare that the source of light will present the system with a well-defined beam of light. As has been pointed out in discussing typical schlieren systems, there is usually a lens or lens system which focuses the light source onto a slit. The slit is smaller than the source image so that only the brightest and most uniform parts of the source will illuminate the system. The reason for requiring a well-defined light source, as well as for requiring that the source be rectangular and the blocking edge be straight and well aligned with the source image, is that the sensitivity increases with a decrease in effective source image. The greater the sensitivity, the smaller the

deviation a given ray has to go through to be detected. Therefore, a sensitive system will have most of its light rays near the knife edge so that even slightly bent rays will illuminate the film. The knife edge is quite popular because accurate edges in the form of razor blades are available. An accurate edge and an accurate source image-knife edge alignment are desirable because an accurate image of some disturbance necessitates a uniform sensitivity for each ray near the edge. The straight edge is also useful if the direction of the density gradient is to be determined.

A system configuration in which the source geometry is other than rectangular can be used. In fact, one approach in setting up a system is to place a photographic plate in the knife edge plane and to obtain the image of the light source. Depending upon whether the developed film is a negative or a positive, the developed plate will then be a conjugate obstacle or aperture of the light source. The system and the rays near the boundary have to be deviated little to make the rays illuminate the film, either positively or negatively.

There may be occasions when it is desirable to detect refractive gradients equally well in all directions. If so, a circular light source and either a circular aperture or an opaque stop are employed. Use of the circular light source enables any refractive gradient directed across the test section to be detected, but the omnidirectional character of the detection also prevents accurate determination of the gradient direction.

The condenser lens is chosen by considering the magnification desired and the space available for the lens. The magnification m is the ratio of the lens-slit distances to the distance T from the lens to the light source. A geometrical optics calculation shows that the focal length of the lens should be $f=mT/m+1$. Although the condenser does not have to be of the same quality as the field lens, it should be free of material defects and should have minimal chromatic aberration.

The convex lens behind the knife edge images the disturbance in the test section onto the screen or film. This lens should be large enough that all of the light passing over the knife edge will also pass through the lens. The lens should of course be of high quality. Its focal length will determine how far from the knife edge the film should be and will also determine the solid angle of light which the film intercepts and thus the portion of the system's field of view recorded.

Physical Optics Analysis of Schlieren Photography

As effective as geometrical optics is in dealing with aberrations and imaging, it is limited in its usefulness because of the fact that the wave nature of light is ignored. Foremost among the phenomena that occur but cannot be explained by classical geometrical optics is diffraction. Keller (1962) has developed a higher order geometrical theory which includes the phenomenon of diffraction. The so-called geometrical theory of diffraction is enjoying increasing popularity because it provides an alternate and many times analytically less complicated means of solving engineering problems in which the wavelengths used are small relative to the system being studied. (See IEEE Proceedings, November 1974.) As

useful as this method appears to be, it does not provide the most intuitive way of understanding diffraction; therefore, it will not be further mentioned here.

A fairly complete analysis of schlieren photography has been done by Shafer (1949). In his analysis, based upon physical optics, he used contrast and density as the parameters which characterize the qualities of a schlieren system. These parameters are of prime importance in detailed photography because the difference between the darker and lighter regions on the film is what the eye detects. For that difference to be pronounced there has to be sufficient background illumination so that the extremes of lightness and darkness appear with their density relationships relatively unaltered. It was thought superfluous to recapitulate Shafer's development; therefore, only his basic approach will be described after which his conclusions will be given.

If the optical system is considered linear, any object imaged by the system may be considered to consist of an infinite set of discrete points of varying intensity, each point being independently imaged by the optical system. The final image is the summation of the individual point images. From this point of view it is possible, in principle, to determine the imaging characteristics of an optical system by using a single point source. Furthermore, it can be shown that the point source acts as a spatial forcing function for the optical system analogous to an impulse applied to a linear electric network. For example, see Brown (1965), Goodman (1968), and Hayt and Kemmerly (1971).

The linear systems approach is essentially what Shafer used. The system considered is a 2-field lens, parallel beam system. (See Fig. 2.7.) After deriving a general equation for the complex field amplitude in a plane distant from an illuminated aperture, Shafer characterizes the schlieren system by deriving an expression for the light amplitude G in the focal plane of the second field lens resulting from a point source displaced from the optic axis and in the focal plane of the first lens; G is given by

$$G(\Gamma) = \text{const} \int_{-A}^{A} e^{ik[\Phi(x)+\varphi(x)]}dx \quad . \tag{7}$$

The integration is done across the test section in a plane that intersects the optical axis at a distance x. In his integration the limits were set by wind tunnel window size. In general, the limits are determined by the extent of the light in the test region. The phase of the differential radiators across the section is accounted for by the term $\Phi(x)$, and the refractive index change is accounted for by the term $\varphi(x)$. If we define a function

$$f(x) = |f(x)|e^{ik\varphi(x)} \quad ,$$

where

$$\begin{aligned} |f(x)| &= 0, \quad |x| > A \\ &= 1, \quad |x| < A \quad , \end{aligned}$$

Eq. (7) becomes

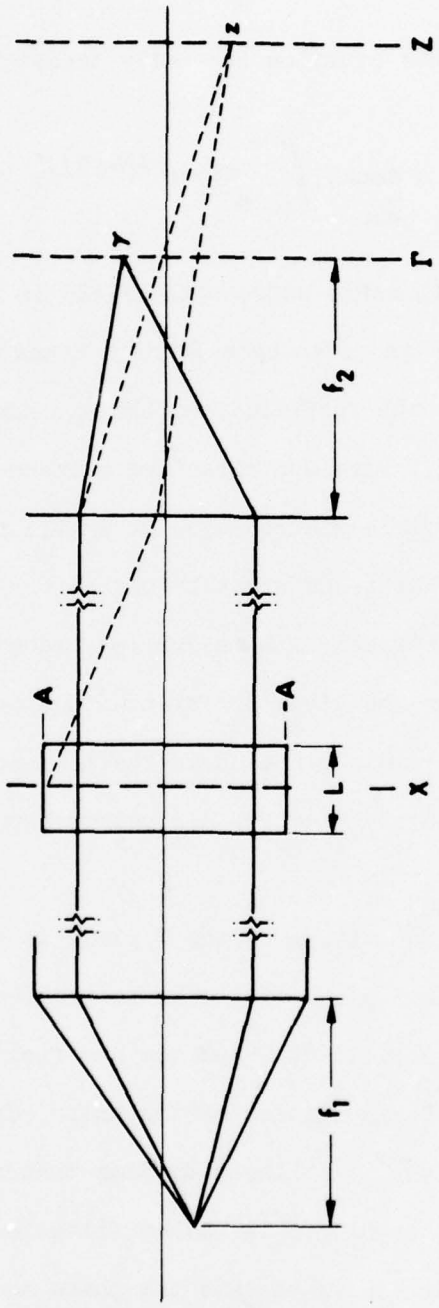

FIGURE 2.7
TWO LENS SCHLIEREN SYSTEM FOR PHYSICAL OPTICS ANALYSIS

ARL - UT
AS-76-811
DRK - DR
7 - 1 - 76

$$G(\gamma) = \text{const} \int_{-\infty}^{\infty} f(x) e^{ik\Phi(x)} dx \quad . \tag{8}$$

As Shafer points out, this equation is easily transformed into

$$f(x) = \text{const} \int_{-\infty}^{\infty} G(\gamma) e^{-ik\Phi(\gamma)} d\gamma \quad . \tag{9}$$

In other words the relationship between the field in the X plane and the field in the Γ plane is given by a Fourier transform pair. The third plane Z located in the farfield from the Γ plane will have a field distribution that is the farfield diffraction pattern of the field distribution at Γ. The field distribution at Z will thus, by definition, represent a spatial Fourier transformation of the Γ plane field distribution. Since the Fourier transform of a Fourier transform of a given function is equivalent to the given function with a negative argument (Goodman, 1968), the field distribution in the Z plane is the field in the X plane inverted. In practice the Z plane is brought closer to the Γ plane by a lens.

If the diffraction pattern in the Γ plane is modified, then the field distribution in the Z plane will also be modified. The relationship between the modified field at Γ and the new field at Z results from the spatially transformed convolution of the knife edge with the diffraction pattern in the Γ plane. In linear systems theory, modification of a function by altering its transform is called filtering. The desired result for a schlieren system is to have the phase modulated field at plane Γ give rise to an intensity modulated field at Z. The positive and negative frequencies associated with Fourier transforms are manifested

spatially by higher order fringes about the zero order or dc fringe in the diffraction pattern. (Spatial frequencies are more traditionally known as wave numbers.) The knife edge is normally introduced to block all the spatial frequencies on one side of the slit image as well as some of the slit image itself. The slit image is partially blocked to control the background illumination at the Z plane. The intensity variation in the Z plane is thus a function of the unblocked spatial frequencies arising from the refraction in the test section.

Relying mostly on numerical methods, Shafer got results for an extended light source and a generalized disturbance of which the shock wave is a special case. Shafer also considered the relationship between the focal length of a mirror and the mirror's astigmatism. Some of Shafer's conclusions will now be given.

Design Considerations

As the focal length of the second field element increases, the displacement of the disturbance diffraction pattern (the refracted light rays) from the optical axis increases. Thus for a desired system sensitivity, the larger the focal length, the wider the light source can be. Moreover as the focal length of the second field element increases, the astigmatic errors and the light gathering ability of the system decrease. The astigmatism increases as the parallel light beam is made larger because the light source and knife edge displacement from the system's axis have to be increased to prevent the light source and knife edge from blocking any of the parallel beam of light.

The light flux density at the film plane increases as the light source size is increased but the contrast decreases. The actual light source size is best determined by experiment.

As the knife edge blocking of the light source image and refracted rays increases, the contrast increases and the density decreases. It should be noted that the relationship between the contrast and the density is not inversely proportional over all the range of the knife edge blocking of the light. The optimum knife edge position is, in most cases, at the optical axis.

Shafer also states that f/10 is the best compromise f/number the system can have with the light sources available in 1949. This conclusion is generally still true when spark light sources are used. The necessary density of light at the film plane is ultimately dictated by the sensitivity of the film used. Therefore, when a system is to be designed, the considerations of light source illuminance and the system's light gathering capability should be based upon the anticipated use of the system and the sensitivity of the available film. Shafer's conclusions concerning focal length do not necessarily apply to the first field element of a 2-element system. When a 2-mirror schlieren system is used, it is best that both mirrors have the same focal length so that when the mirrors are arranged to minimize the off-axis aberrations, complete cancellation of coma will occur (See the above discussion of aberrations.)

Interpretation of Schlieren Photography

Although schlieren photographs do not easily yield quantitative information about the fluid density in the disturbed region, the direction of the density gradient of the disturbance can be discerned if a rectangular light source and a knife edge are used. In the case of acoustic wave studies it is useful to have a temporal picture of the disturbance. For this investigation a spark discharge was the source of sound. Figure 2.8 shows a typical oscilloscopic trace of the waveform (Anderson, 1974). The pressure has an abrupt rise, called the fore shock, an essentially linear decay to below ambient pressure, and another abrupt rise, called the after shock, which terminates the disturbance. The after shock is not as sharp as the fore shock. (For a review of nonlinear acoustics and a more complete description of the N wave see Blackstock, 1972.)

Some schlieren pictures of N waves are shown in Fig. 2.9. The wavefront can be seen to be essentially spherical; see, for example, Wright (1971). In these pictures the fore and after shocks are seen to be thin white lines. The knife edge was horizontal and introduced from above the light source image. If the horizontal knife edge had been introduced from below the light source image, the shock fronts would have been dark lines. The after shock is not as distinct as the fore shock because, as already mentioned, the after shock is more diffuse. The effect of the sphericity of the N wave on the light will now be more fully explained.

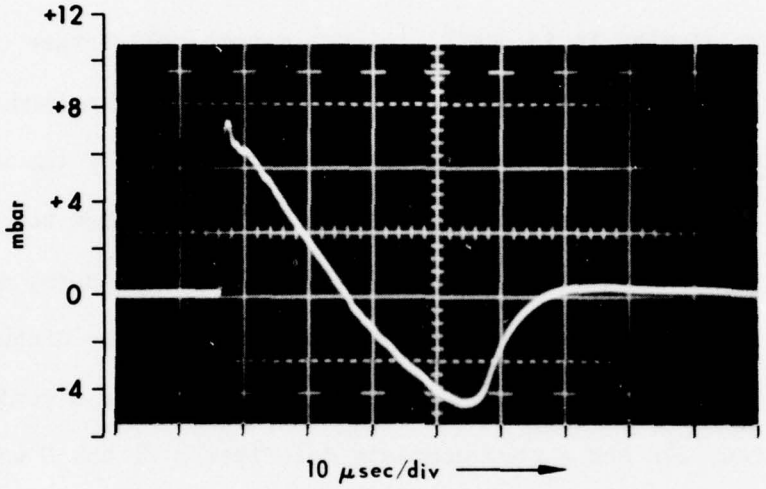

FIGURE 2.8
N WAVE RECEIVED BY A MICROPHONE

(Reproduced from Anderson, 1974)

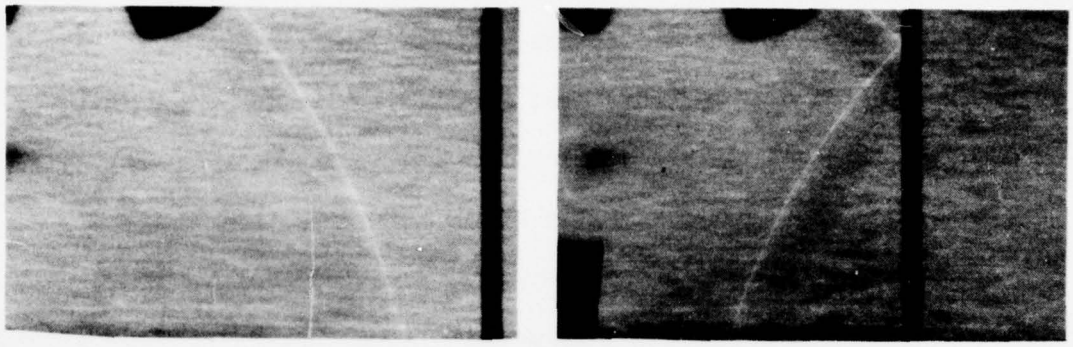

a. SHOWS INCIDENT WAVE

b. REFLECTION FROM A RIGID FLAT SURFACE

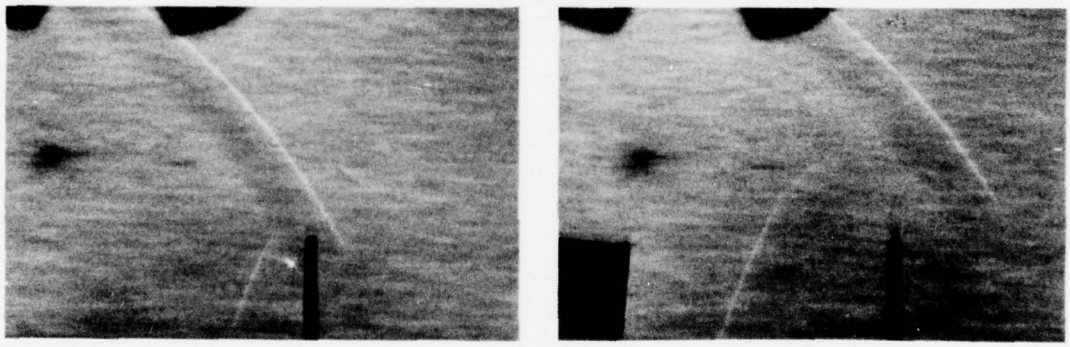

c. DIFFRACTION AND REFLECTION FROM A BARRIER

d. DIFFRACTION AND REFLECTION FROM A BARRIER

FIGURE 2.9
SCHLIEREN PHOTOGRAPHS OF SPHERICAL N WAVES

As stated in Chapter 1, the schlieren method is used to detect light rays which have been deviated by a refractive index gradient. Those rays propagating in a direction normal to the refractive gradient are bent the most. Rays traveling in the same direction as the refractive gradient will not be angularly deviated at all. There will be time delay but no change in direction. (See Fig. 1.9.) Rays propagating at an angle with the gradient of the refractive index are bent by the gradient vector component perpendicular to the ray's path.

A cross section of a spherical N wave is shown in Fig. 2.10. The paths of a few of the light rays which pass through the wave and on to the knife edge are indicated. The angular deviations have been exaggerated to make the phenomenon easier to visualize. A ray of light passing at a grazing angle through the shock region of the wave will experience the greatest deviation. Ray No. 1 in Fig. 2.10 passing through the top of the spherical wave is bent downward because the density gradient of the shock front is toward the shock source. Inside the spherical N wave the density gradient and thus the refractive index gradient are directed outward from the shock source, but the gradient is so much smaller than at the shock front that the ray effectively propagates through the inside of the N wave in the direction from which it leaves the shock front. The ray is further refracted downward upon leaving the N wave because the component of the inwardly directed refractive gradient normal to the ray is downward. The downward bent ray continues downward after reflecting from the spherical and the plane mirrors. The ray is blocked by the knife edge introduced from

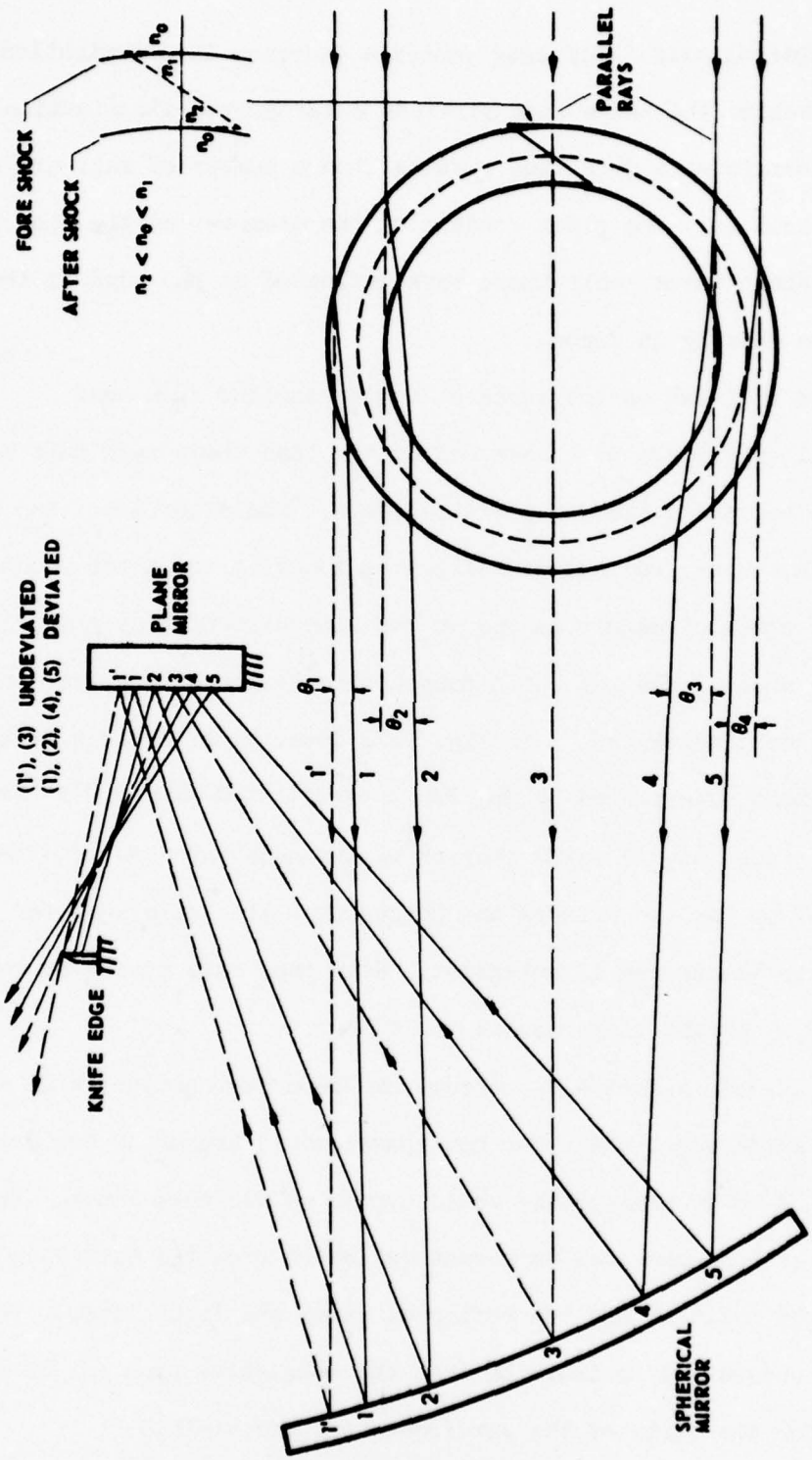

FIGURE 2.10
REFRACTION OF PARALLEL LIGHT BY A SPHERICAL N WAVE

ARL - UT
AS-76-813
DRK - DR
9 - 13 - 76

below the optical axis. Blocking causes a decrease in illumination of the screen behind the knife edge provided a background illumination is present. Therefore, a dark line results when a number of rays are so blocked. Since only the plane containing the diameter of the spherical wave is in sharp focus, only those rays deflected at the edge of the wave will be sharply in focus.

Rays incident on the shock at angles smaller than near grazing will experience much less refraction than those rays passing through the top and bottom of the shock wave. The after shock is visible because the gradient of refractive index at the after shock is of the same order of magnitude and in the same direction as the gradient at the fore shock. The ray which passes through the extreme region of the after shock, as ray No. 4 in Fig. 2.10 does, experiences a deviation similar to that experienced by ray No. 1 except that the bending is upward. The ray continues upward (with respect to its undeviated path) after reflecting from the two mirrors and passes over the knife edge to contribute to the screen illumination. When many rays pass over the edge in this way, a bright line results.

If a whole spherical wavefront had been photographed with a horizontal knife edge, the upper hemisphere would appear as two bright lines and the lower hemispheres would appear as two dark lines. The photograph of the spherical wavefront reflected from the baffle indicates that both the incident and the reflected waves are light lines. This can now be understood to indicate that the refractive gradient of density is upward for the parts of the wavefront that are visible.

Any conceptual problems raised by the previous ray description may be resolved by considering the light-sound interaction as a diffraction phenomenon. See Merzkirch (1974).

The next chapter has a complete description of the equipment and the procedures used for this research.

CHAPTER 3

APPARATUS AND EXPERIMENTAL PROCEDURES

Introduction

The purpose of this chapter is to provide a detailed discussion of the equipment used for this research. As stated in chapter 1, only those readers concerned with procedural detail will find this chapter interesting. A discussion of the approach found successful in arranging and aligning the equipment will be included. Experimental procedures and equipment maintenance will also be given.

During the course of this research, an old schlieren system became available, that was built some time between 1940 and 1950 as a prototype for a much larger system that had been installed in a wind tunnel facility in Daingerfield, Texas. The system, as shown schematically in Fig. 3.1 and photographically in Fig. 3.2, is of the 2-mirror folded type.

Description of System

The system as it now stands (some modifications having been made since its arrival) is divided into two subsystems, each on a movable iron frame. The first frame (see Fig. 3.3) contains a field mirror, a front surfaced plane mirror, and the light source assembly. The second frame (see Fig. 3.4) contains a field mirror, a front surfaced plane mirror, the knife edge assembly, a plano convex lens, a bellows with a rigid extension, and a Polaroid film backpack.

Both field mirrors are front surfaced, 6 ft focal length, 12 in. diam spherical mirrors. The spherical mirrors are mounted so that they may be turned through small arcs in the three orthogonal directions. The accuracy of the surface curvature of the mirrors is not known.

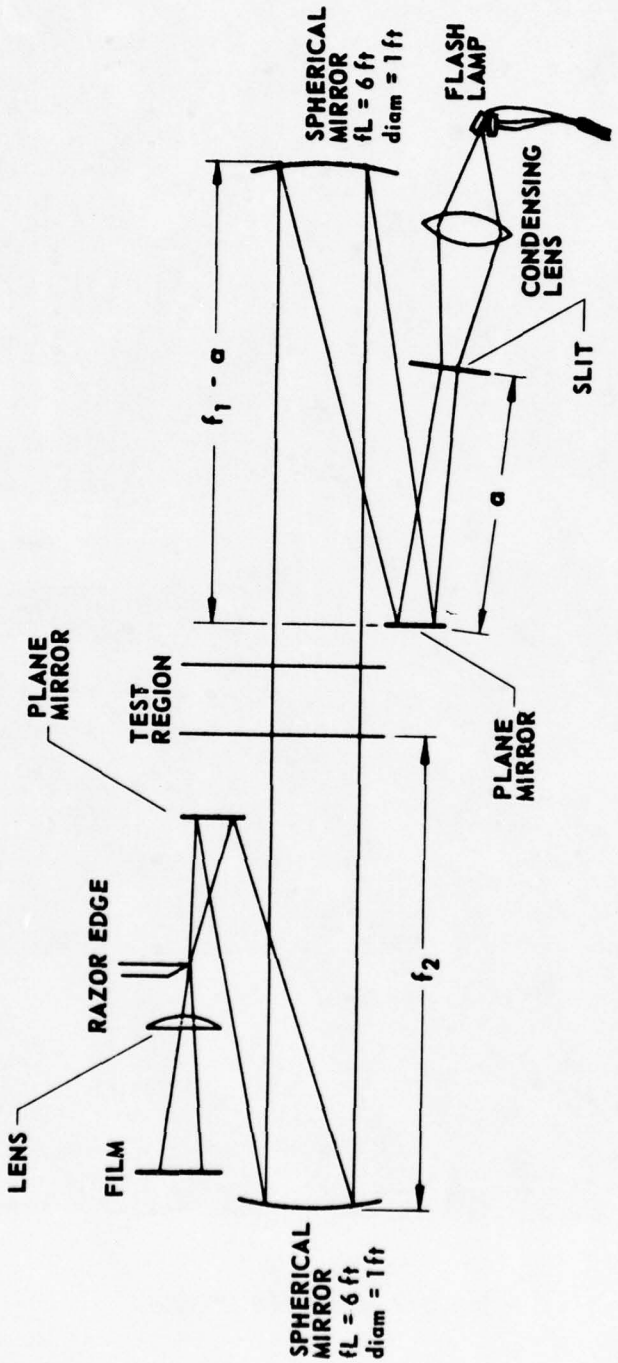

FIGURE 3.1
FOLDED SCHLIEREN SYSTEM

ARL - UT
AS-76-816
DRK - DR
7 - 12 - 76

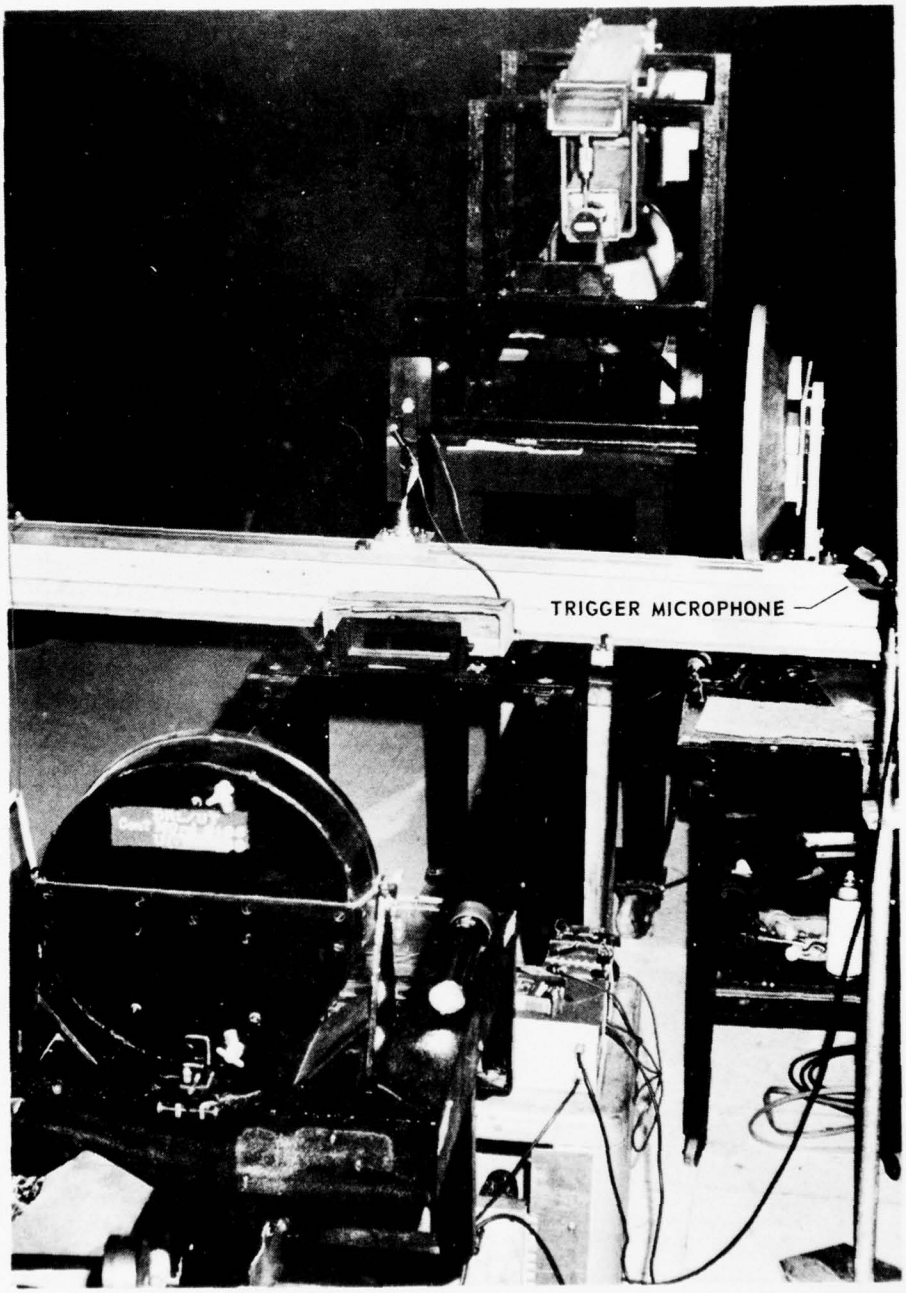

FIGURE 3.2
COMPLETE SCHLIEREN SYSTEM

0867-2

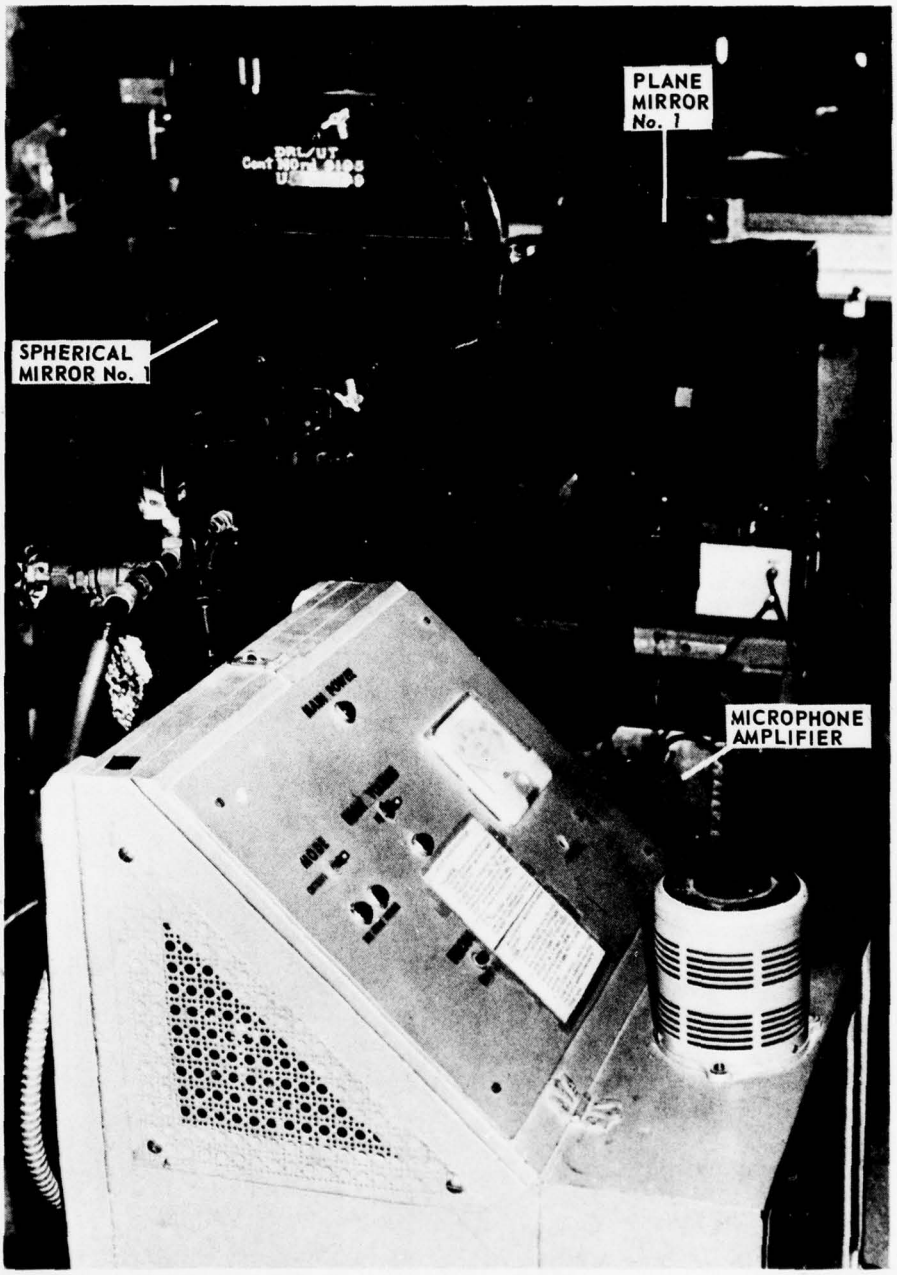

FIGURE 3.3
LIGHT SOURCE FRAME

0867-3

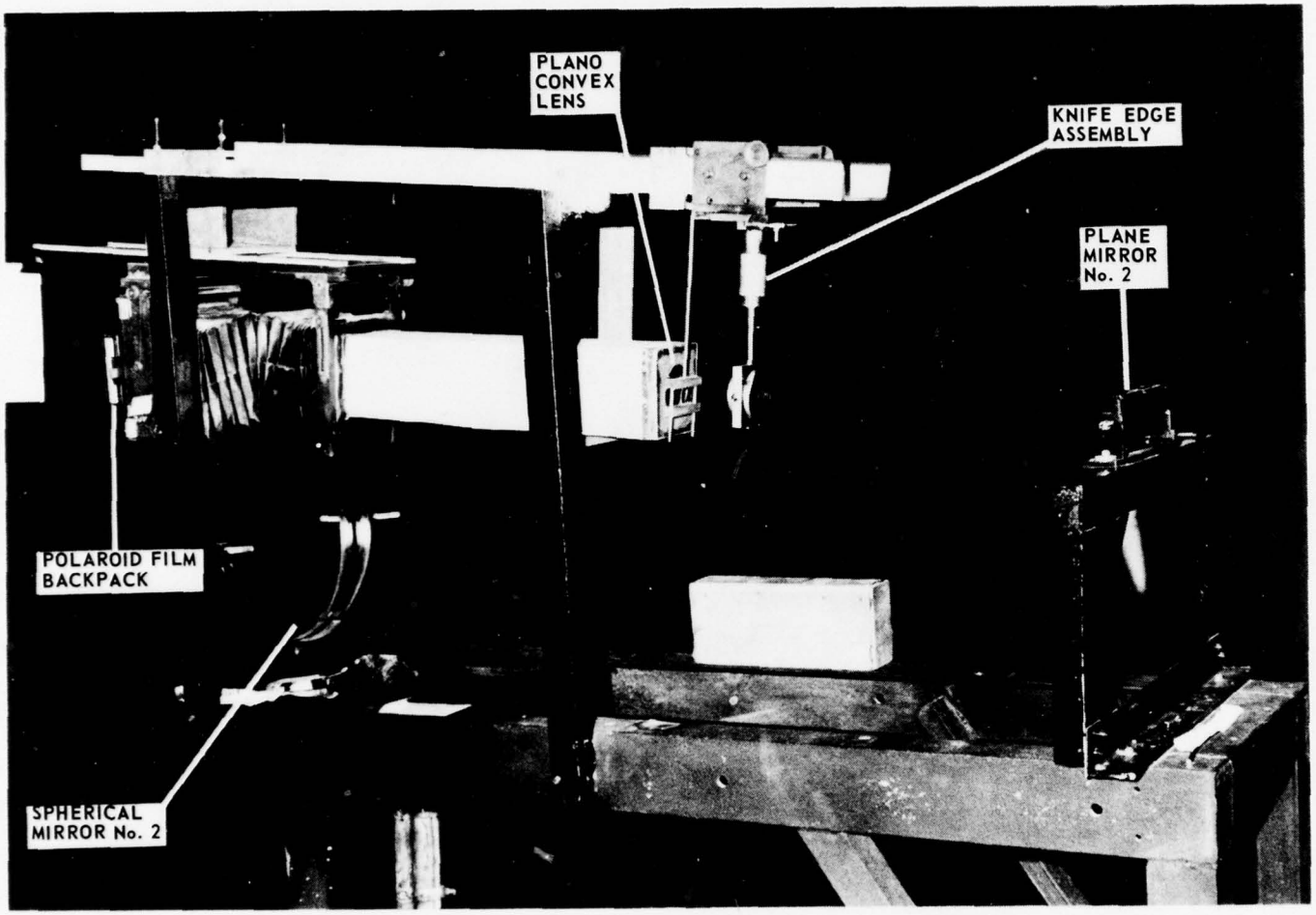

FIGURE 3.4
CAMERA FRAME

The light source assembly (see Fig. 3.5) consists of the source of light (which is either an air cooled General Electric BH6 mercury vapor lamp, Fig. 3.6, used for steady state illumination or a spark flash lamp, Fig. 3.7, used for stroboscopic illumination), a convex condenser lens, and an adjustable slit. The lamp mechanisms can be adjusted in all three orthogonal directions: up and down, backward and forward, and sideways. So that the system can be fed from either a vertical or a horizontal slit source of light, the slit can be rotated and its size varied, although the adjustment is not as precise as one might wish. The slit is part of a separate assembly that is attached to the rest of the light source mechanism with three screws, which allow the slit to be adjusted to positions different from the axis of the rest of the light source assembly. The whole light source assembly can be moved back and forth and sideways and can be pivoted, so that it can be swung through a small horizontal arc. It can also be swung through a large vertical arc to allow an up and down adjustment of the slit.

The knife edge assembly (see Fig. 3.8), located on the second frame, is moved to and fro with a rack and pinion. A second rack and pinion allows it to be moved sideways. The knife edge itself--a razor blade--is mounted on the assembly so that the edge can be rotated about the assembly's optical axis, thus allowing all possible vertical and horizontal orientations.

The plano convex lens with a focal length of 103.1 cm is used to image the disturbance onto the film. The plane mirrors, incorporated to make the system more compact by folding the focal length distance between both the light source slit and the first spherical mirror, and the

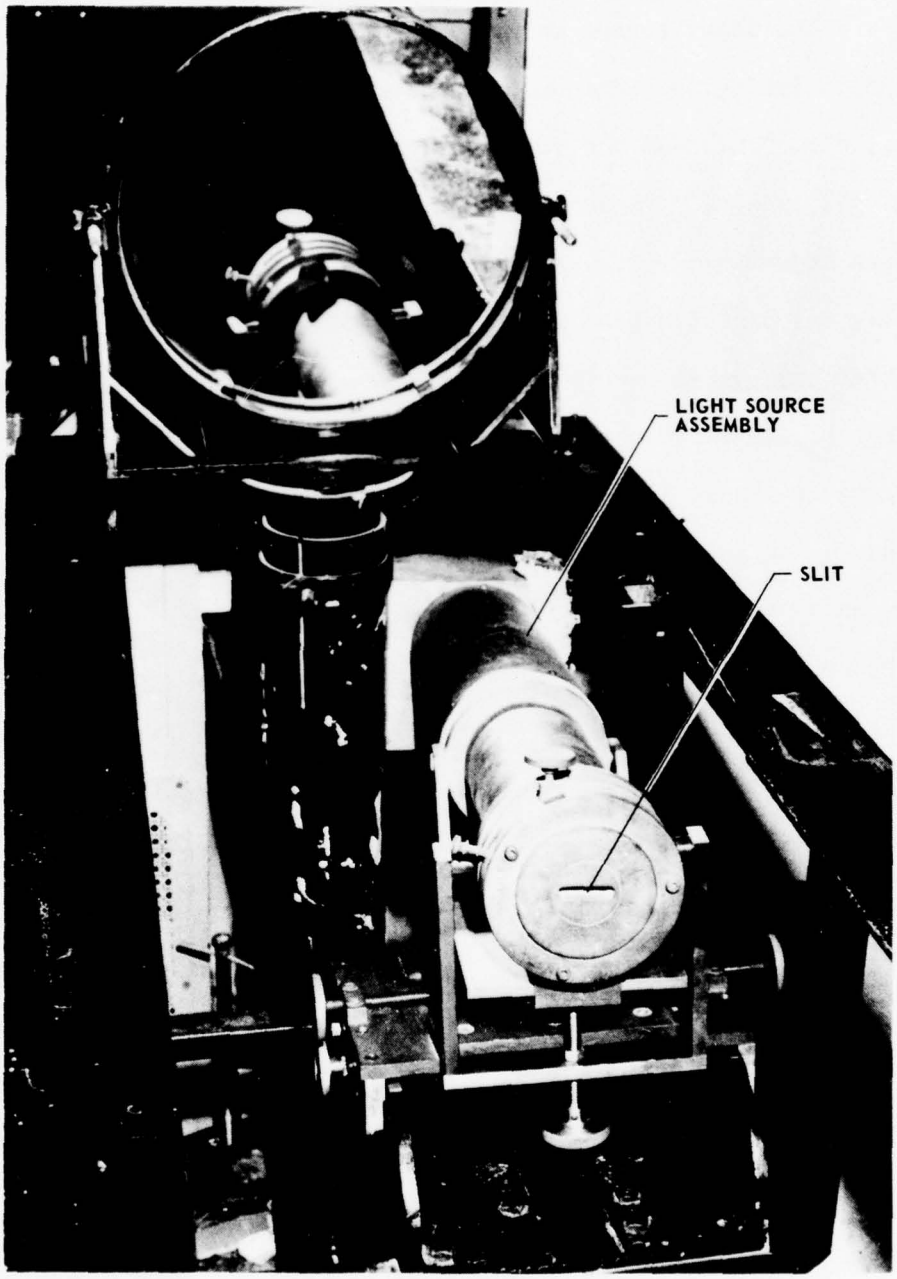

FIGURE 3.5
LIGHT SOURCE ASSEMBLY

0867-5

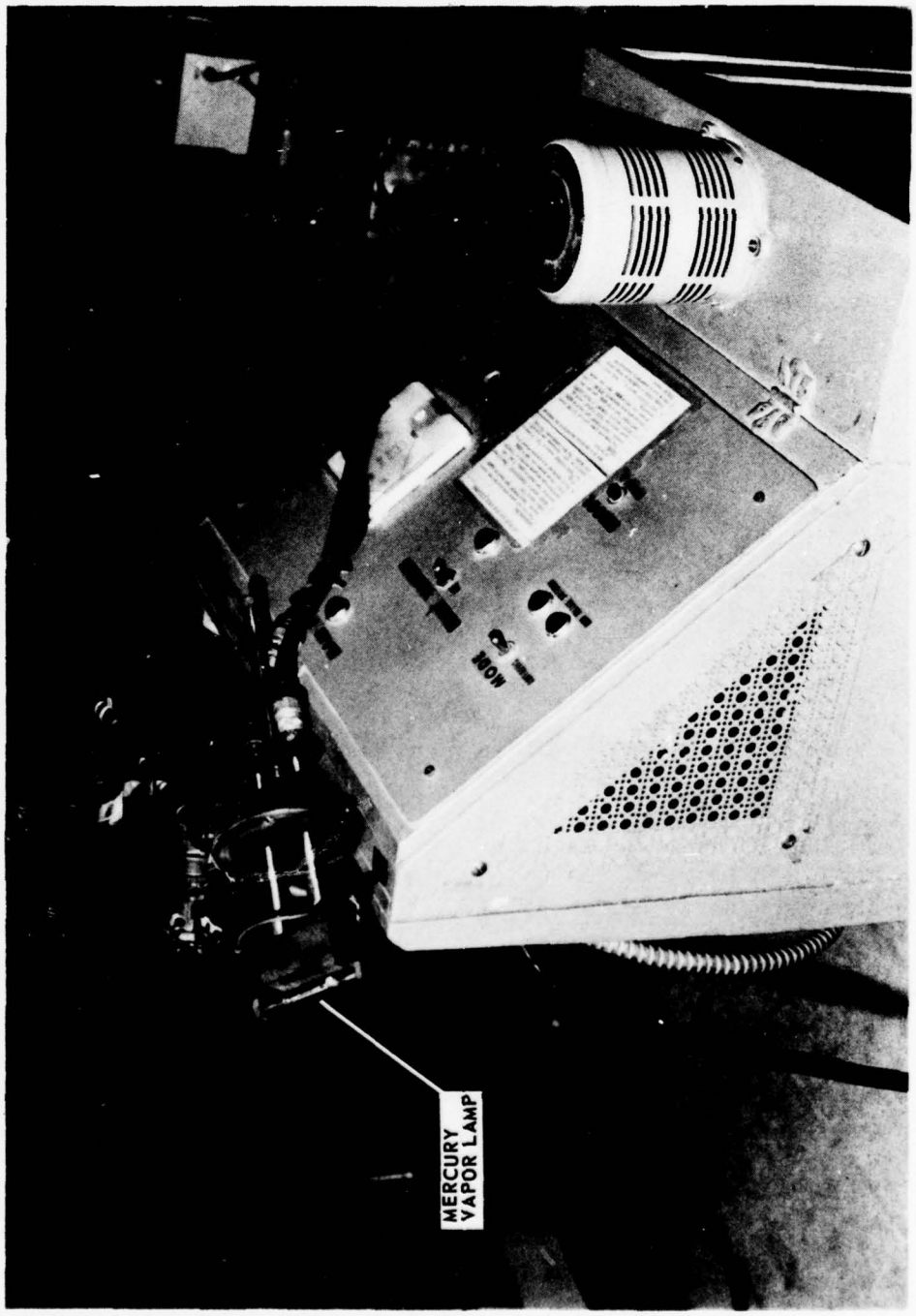

FIGURE 3.6
MERCURY VAPOR LAMP AND POWER SUPPLY

0867-6

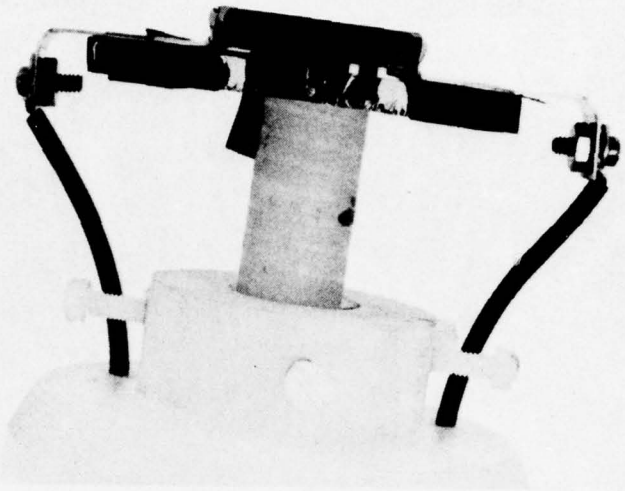

0867-7

(a) EDGE VIEW

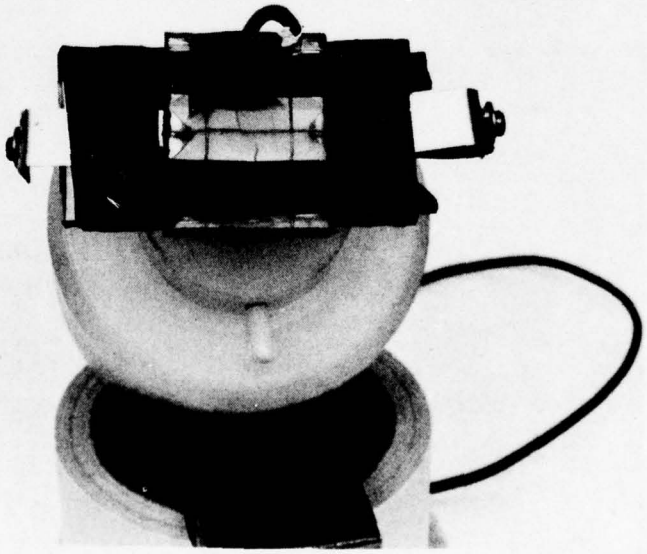

0867-8

(b) TOP VIEW

FIGURE 3.7
SPARK FLASH LAMP

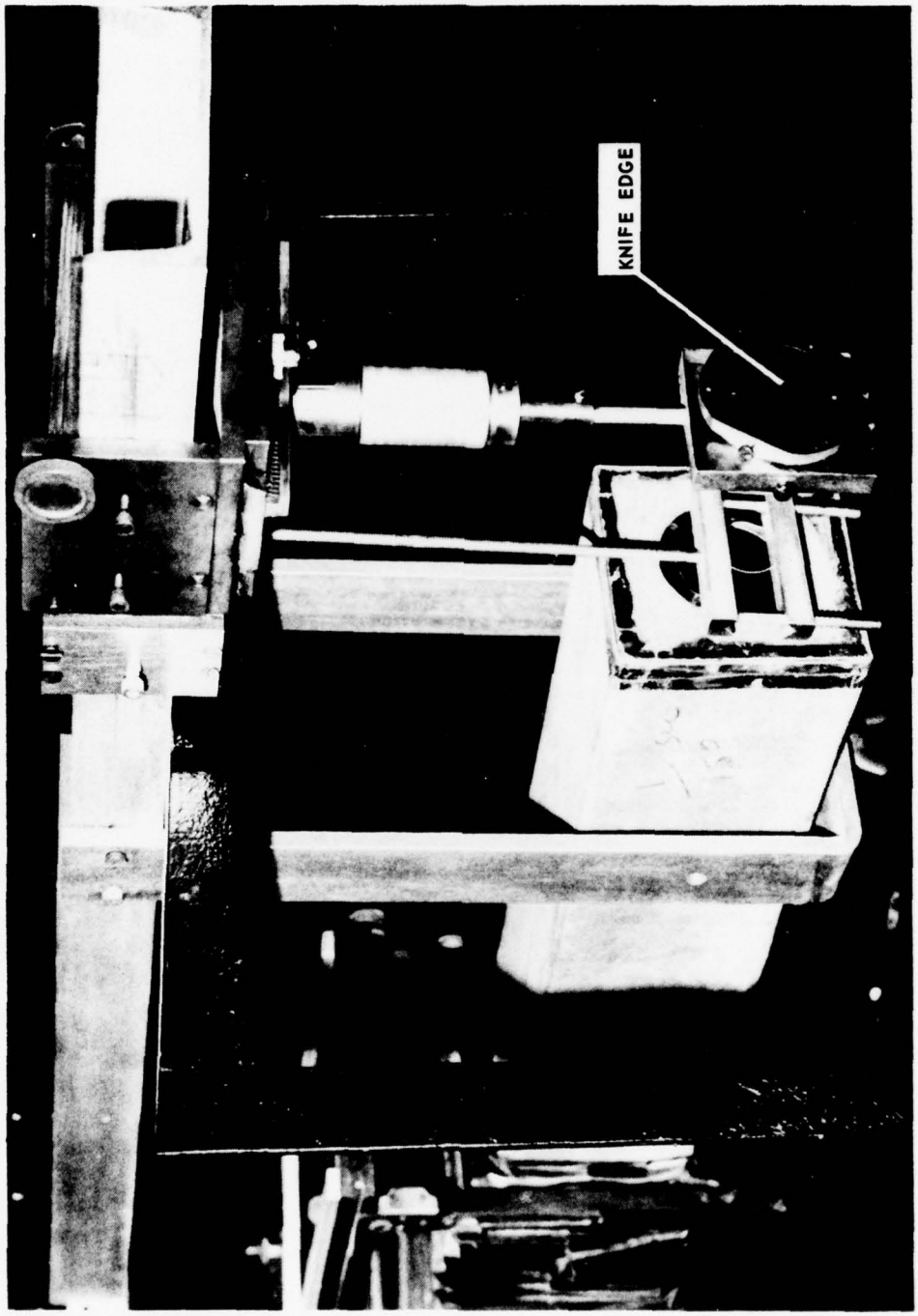

FIGURE 3.8
KNIFE EDGE ASSEMBLY

0867-9

knife edge and the second spherical mirror, can be tilted upward or downward and also moved through a small horizontal arc. (See Fig. 3.9.)

As previously mentioned, the schlieren apparatus underwent several modifications. The most important was the spark flash light source, the construction of which will be discussed later. The light source assembly was made more adjustable by incorporating a rack and pinion to allow to and fro motion to move the slit toward and away from the plane mirror. Up and down motion of the slit on the light source assembly was also incorporated by utilizing a threaded rod and a pivoting action that was already part of the system. The rack and pinion adjustment on the knife edge assembly, which allows the sideways adjustment of the knife edge, and the rotatable section, which holds the razor blade, were also added.

So that photographs could be taken, the Polaroid film backpack and a holder for it were added. (Use of Polaroid film allows quick feedback on the system's operation.) For stability, the camera frame has two braces connecting the column, which supports the spherical mirror, with the wheel base supporting the column. (See Fig. 3.10.) Initially, the braces were only bolted in place where they meet the column such that the stability of the frame was marginal. Welding the braces to the wheel base led to a significant improvement in stability. The wheel bases on both frames had provision for threaded rods to act as feet, most of which had to be fabricated. Use of the threaded rods enabled the frames to be raised or lowered and gave the system more permanence.

Finding a reliable flash light source was an interesting problem. While the BH6 light source has a strobe mode on its power supply, only a manual switch can be used to trigger the strobe light. Both alternative

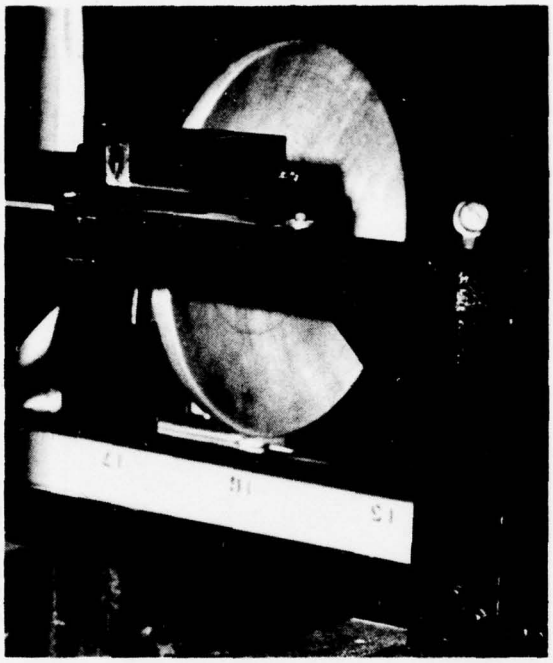

FIGURE 3.9
PLANE MIRROR

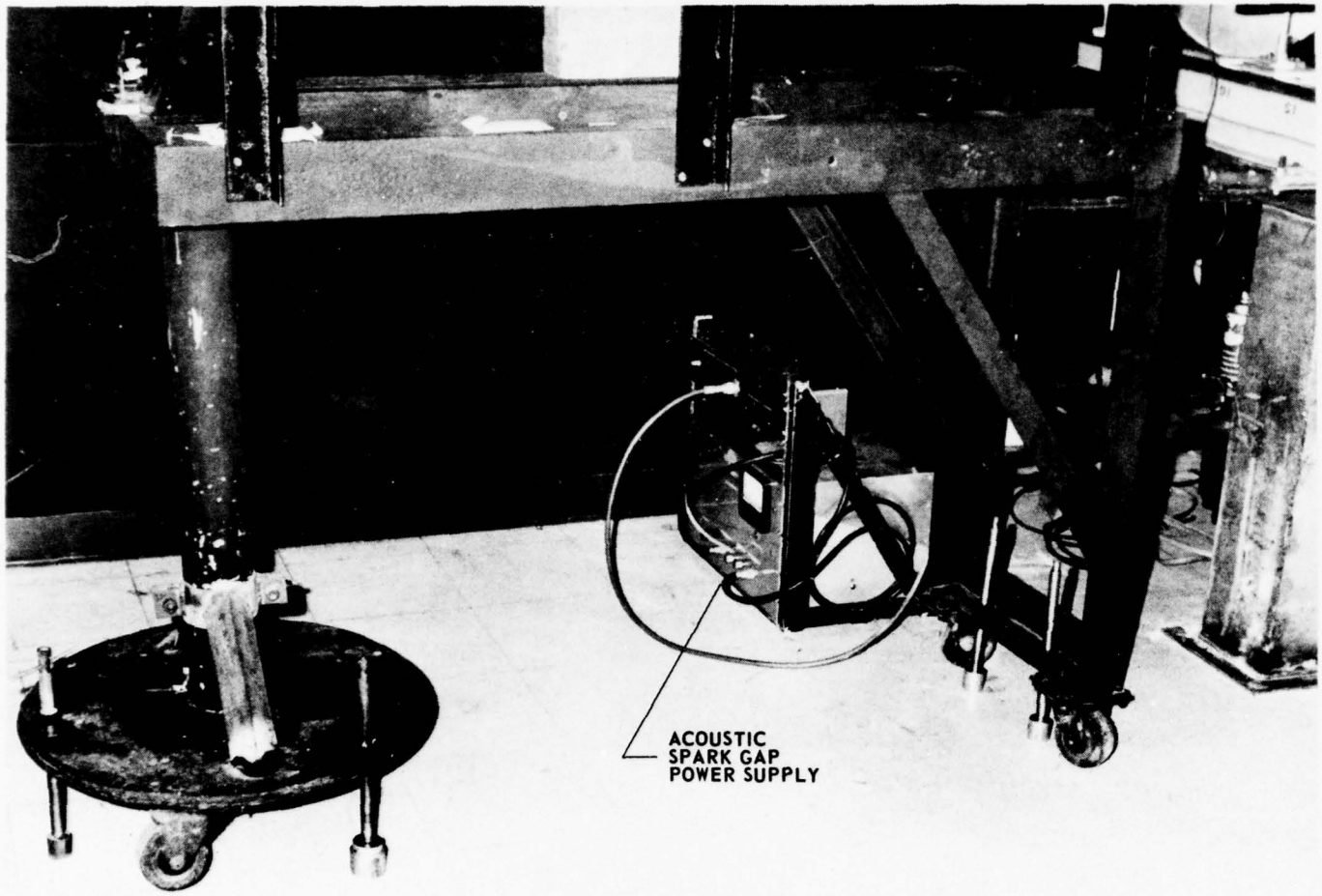

FIGURE 3.10
CAMERA FRAME BASE

0867 - 11

light sources and switching devices that could handle the voltage and current necessary to flash the mercury vapor lamp were investigated. The advantage of using the same lamp for both the steady state alignment and the stroboscopic picture taking is that no realignment is necessary when changing from the steady state to the flash mode. Alternatively, a spark discharge has the advantage that its light lasts for less than 1 μsec. The mercury vapor lamp's duration is about 4 μsec. Since wave motion in air and possibly in water was going to be studied, the two criteria used for choosing the flash source were that it be intense and that it be of as short a duration as possible so that resolution of the wave being studied is high. It was felt that a better flash source in the form of a spark discharge could be built for the same amount of money that would be required to adapt the mercury vapor lamp to a controlled flash source. Use of two separate sources, one for alignment and one for making measurements, does give rise to some alignment problems but the extent of these problems, although not foreseen, did not prove to be insurmountable. A long term solution of the alignment problem is being worked on during the writing of this thesis.

Two different spark discharge light sources have been used. The first one is purportedly the same lamp used in the EE&G Model 549 Microflash light source (see Strong, Scientific American, August 1974). It consists of two wires arranged to provide a 1 in. gap adjacent to a hollow glass rod that was incorporated both to cool the afterglow of the spark discharge and to allow the trigger electrode to be run near the spark gap. (See Fig. 3.11.) A high potential difference below that necessary to break down the air is placed across the gap. When the flash is to occur,

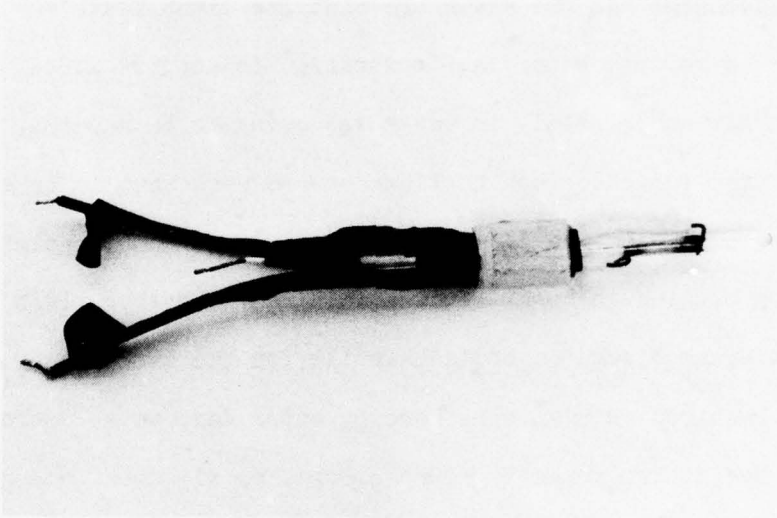

FIGURE 3.11
SPARK FLASH LAMP

a transient pulse field will come from between the trigger electrode and one of the gap electrodes, causing ionization of the air in the gap and a resultant dumping of energy from the storage capacitors into the gap. The outer glass test tube covering (not shown in Fig. 3.11), although useful for reducing the acoustic output of the flash tube, was eventually discarded because the atmosphere inside the flash tube became contaminated with byproducts after each discharge. The contamination gave rise to a corona problem between the gaps which reduced the reliability of the lamp and required that more frequent cleanings be done. After the outer glass covering was discarded, the main problem with the spark light source was the spark jitter. Because the discharge did not occur consistently along the same path, the alignment of the source and thus the illumination of the system became almost a random process. The jitter problem arose mainly because of the flash lamp's geometry; the cylindrical hollow tube could not confine the spark to a line. A partial solution of this problem was to use the light source in a vertical position for a horizontal slit and in a horizontal position for a vertical slit. This crossed arrangement greatly increased the reliability of the light source but decreased both the intensity of the light and the sensitivity of the system because the effective slit length was reduced.

The spark gap lamp shown in Fig. 3.7 is currently in use. It operates essentially the same as the first lamp, but because of its geometry it acts as an effective line source. The lamp consists of two stainless steel electrodes that are tapered on the ends toward the gap. The electrodes are taped onto a rectangular glass plate, which should be made of pyrex or quartz (although neither was at hand when the lamp was

being constructed), and are covered in the gap region by a second glass plate in which wires are imbedded. The second piece of glass was cut from safety glass. The ends of the embedded wires are flush with the edge of the glass, after the glass is cut. One of the wire ends is used as a terminal for the trigger circuit output. The rest of the wire ends were electrically isolated by applying layers of Corona Dope around the edges of the glass. The two pieces of glass form a wedge-shaped cavity for the electrodes to ensure that the light will emerge from the desired direction unobstructed. As with the previous flash lamp, the glass acts as a heat sink to reduce the afterglow of the discharge and thus decrease the duration of the flash. The glass also serves to guide the discharge so that the discharge will act as a controlled line source. The electrodes and glass are held in place with black plastic electrician's tape so that adjustments can be done quickly and the structure can be made fairly sturdy.

The high voltage supply for the flash lamp is shown in Fig. 3.12. The energy for the discharge is stored in the two 0.1 μF capacitors which are components in a voltage doubler. The output potential difference is approximately 18 kV.

To flash the light at an appropriate time, the discharge of the power supply capacitors is controlled by a trigger circuit. The trigger circuit sends a second electric field into the spark gap region when a microphone senses the acoustic signal to be photographed. The trigger circuit consists of an EE&G TR-132C pulse transformer, a 1 μF capacitor, a silicon controlled rectifier (SCR), a 15 MΩ resistor, and a 405 V battery. In operation the charged capacitor is discharged through the pulse transformer when the SCR is gated by a signal applied to it from

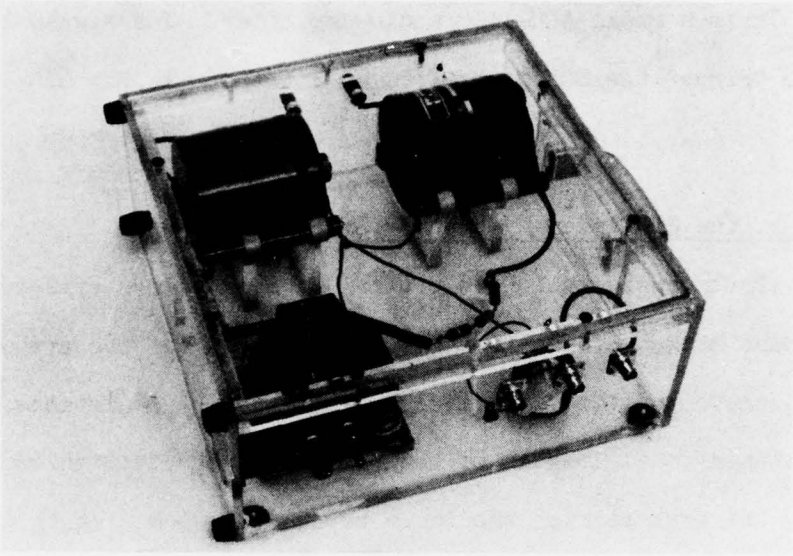

0867 - 13

(a) LIGHT SOURCE POWER SUPPLY

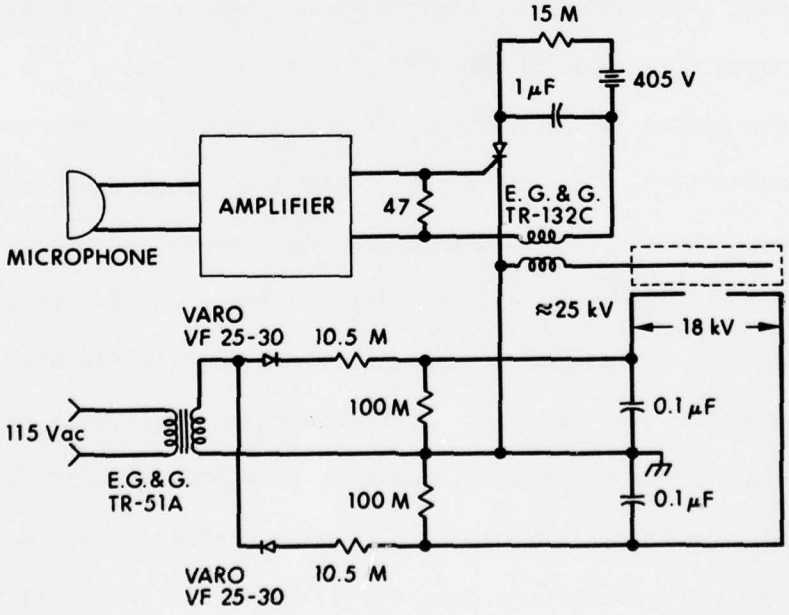

(b) LIGHT SOURCE ELECTRONICS

ARL - UT
AS-76-781
DRK - DR
7 - 7 - 76

FIGURE 3.12

a Stromberg Carlson Model APH-1100 audio amplifier. The signal being amplified to trigger the SCR comes from an Electrovoice No. 630 microphone.

Preparation of the Schlieren System for Experimental Use

The first consideration in setting up a schlieren system is the amount of space needed by and that can be allocated for the system. It is found best to have the two field mirrors separated by a distance greater than the combined focal lengths of both mirrors. In addition to this requirement, the test section should be beyond the focal length of the second field mirror so that the disturbance can be imaged by the mirror into real as opposed to virtual space. For the folded system at hand the disturbance must lie between the two frames so that the illuminating light will be refracted only once by the disturbance.

For the system at hand, the minimum separation between the spherical mirrors is 12 ft. Since the frames are 4 ft long, the minimum distance between the frames (each frame having a spherical mirror at one end) is about 4 ft. With the additional requirement on the distance between the disturbance and the second spherical mirror, 2 ft is the minimum distance needed for the test section. Most references imply that as long as the axis of symmetry of an axially symmetric flow (the form of disturbance of most interest in this study) is at a greater distance from the second field mirror than the mirror's focal length, the refraction will be properly imaged. This seems reasonable because the image of an axially symmetric flow does appear to be a cross section of the disturbance. Varying the distance between the two mirrors and between the disturbance

and the second mirror has been tried. Experimentation seems to indicate that this cross sectional view will be more distinct not only if the axis of the disturbance is beyond the focal length of the second spherical mirror but also if the edge of the disturbance nearest the second mirror is beyond its focal length.

It should be possible to have the test section completely within the focal region of the second spherical mirror. Then if a concave lens is used behind the knife edge, the image of the disturbance will fall on the film. In practice this arrangement usually does not work because the disturbance has a good chance of refracting not only the parallel light but also the light going to the knife edge. The doubly refracted light destroys any correspondence between the disturbance and the image on the screen. Avoidance of double refraction of the light is one of the reasons why the mirrors are to be spaced as prescribed above.

Another consideration concerning the physical location of the schlieren apparatus is the proximity of external air disturbances such as air conditioning ducts, equipment cooling fans, and equipment heat. For a system that is used to study unconfined flows, an area that can be darkened is also very desirable.

Once a location has been chosen, it is best to align the system so that the parallel beam of light will intersect the axis of the disturbance at a right angle. The first steps in alignment therefore are to determine the spatial separation of the two frames and the test section and to approximately align the system perpendicular to the axis of symmetry of the disturbance of interest by sighting along the two frames. The spherical mirrors should be opposite each other and a line drawn from

the center of one mirror to the center of the other mirror should intersect the axis of the disturbance at a right angle. With the system approximately aligned, the screwdown feet should be lowered just enough to keep both frames in place.

Before further alignment is done, the slit assembly should be removed. The edges of the slit should be clean, straight, and parallel. After the edges are cleaned, and perhaps sharpened, the slit is adjusted by setting the approximate anticipated size of the slit (1 mm or a little less should suffice if the experimenter has no experience concerning typical slit size). The slit assembly is then placed about an arm's length away from the eye, between the eye and a more distant, slightly opened door. The room is darkened so that light entering through the slightly opened door from the adjacent corridor will illuminate the slit. By looking through the slit at the door, the observer will see diffraction fringes filling the slit. The fringes should appear parallel and straight. If the fringes adjacent to an edge are not straight, the edge is either dirty or pitted. If the fringes are not parallel, neither are the edges.

After the edges are adjusted to be parallel, the action of the mechanism which controls the slit size should be checked by using both the fringe method and a close visual inspection to see how the parallel nature of the edges is altered due to play in the mechanism as the slit size is adjusted. When checked in this manner, the edges of the existing slit assembly are found to remain more closely parallel when they are brought together than when they are separated. With this information, all later adjustments of slit size were done so that the slit was first made slightly larger than desired and then was brought down to the final size.

Unfortunately, the slit assembly did not maintain a consistent bias in this regard during the course of the experiment.

When the slit assembly is placed back on the light source assembly, it is probably best to align the plane of the slit perpendicular to the axis of the light source assembly even though the slit assembly may eventually be tilted in the final alignment. This alignment of the slit is done so that any further adjustments of the slit assembly will be with respect to a known reference position.

Further alignment will require the use of a continuous light source which, in the present system, is the air cooled mercury vapor lamp. The mercury should be evenly distributed around both electrodes with no mercury in the center of the lamp. Distributing the mercury can be a trying task, especially with a new lamp. It has been found that by holding the lamp lengthwise between the thumb and the forefinger, an appropriate amount of wrist flipping and arm waving will work better than the method suggested by General Electric. Additionally, although no mercury should be in the middle of the tube, application of the high voltage will almost invariably cause some of the mercury to migrate to the middle of the lamp. With the lamp inside the light source assembly, turn on the cooling air and adjust its flow until the pressure gauge on the power supply reads about 50 psi. The power supply should be switched into the continuous mode and then the high voltage should be turned on. If the lamp does not come on within 10 or 15 sec, turn the high voltage off and check the electrode connections to make sure the lamp is securely and electrically connected. Again apply the high voltage. Repeat this process, adding whatever procedures seem necessary to get the lamp operating.

It should be pointed out at this stage that eye protection against the ultraviolet radiation of the mercury vapor lamp should be worn. Regular glass (that is, not plastic) eyeglasses will probably suffice although the eyes will not be completely shielded. Additionally, when one has to look at the light when it is incident upon a highly reflective material, as on the slit, one should wear an intensity reducing filter or else should look at as small an area of the light as is necessary for alignment and then only on a sampled basis at an oblique angle. Ultraviolet radiation has been known to cause cataracts, retinal burns, and even skin cancer if the energy density is great enough and the exposure is prolonged.

After the lamp is operating, the image of the light source is focused onto the slit by moving the light source to and fro until its image on the slit is as small as possible. The other two adjustments on the light source are used to center the source image onto the slit.

With the slit size approximately set, adjust the position of the light source assembly so that 1) the slit is approximately in the focal region of the first spherical mirror, 2) the top edge of the plane mirror frame is just illuminated by the top part of the bright light coming from the slit, 3) the horizontal angular difference between the light incident on the plane mirror and the parallel light beam that should be emerging from the spherical mirror is minimized, and 4) the plane mirror is as evenly illuminated as possible. Adjust the plane mirror so that the first spherical mirror is illuminated in a centered and symmetrical fashion. Then, adjust the first spherical mirror so that the parallel beam of light will illuminate the center of the second spherical mirror. The light emerging from the second spherical mirror will then be converging to a

focus and this converging light should be centered on the second plane mirror. Adjust the plane mirror to send the light through the bellows and onto a piece of paper attached to the wall behind the bellows. (Use of the paper as a screen allows the experimenter to see how adjustments on the second plane mirror or on the knife edge will affect the beam of light incident on the film.) When the illuminated square on the screen is as large as possible, the plane mirror will be adjusted properly vertically. The horizontal adjustment of the plane mirror is determined by observing the top of the lighted region on the screen. Turn the plane mirror about its horizontal pivot until the dark region seen moving about the top of the screen is centered on the screen. Finally, tighten the loose bolt and recheck vertical alignment.

If some uncertainty exists concerning the slit position, the position may be checked by moving the light source assembly to and fro until a diameter of the second spherical mirror is filled with light. Barnes and Bellinger (1945) state that the light should actually diverge slightly from the first spherical mirror when the slit is at the mirror's focus because the light source is extended. If the light source assembly is in a satisfactory position, finer adjustments may now be made.

With the mercury vapor lamp still on, bring the knife edge into the converging light and position it along the light's path so that the smallest slit source image appears on the side of the knife edge. The knife edge is then in the focal region of the second field mirror. However, one should not rely on visual alignment of the edge alone because the focal region is finite in extent, there being aberrations arising from astigmatism and other alignment errors. It is best to observe the screen

on the wall behind the bellows while adjusting the knife edge assembly.

The two adjustments that are critical in the initial placement of the edge are its horizontal and rotational alignments. As an example of what to look for in making such adjustments, consider a horizontal slit and knife edge arrangement. If the edge is between the focused light and the plane mirror and is introduced from below the beam of converging light into the light, the shadow of the edge will appear at the top of the screen (see Fig. 1.1). As the knife edge is moved along the optical path toward, through, and past the focal plane (the vertical position of the edge may need to be adjusted), the shadow will appear to rotate. When the edge is at the focal region, the darkening will appear to come from the side or, if everything is properly adjusted, the screen will darken uniformly. Uniform darkening is the desired effect. On the other hand, if the edge is beyond rather than in front of the focused light, the screen will darken from the bottom as the knife edge is vertically moved into the light. With the edge in such a position that the screen is darkened as uniformly as possible, tighten the screws on the knife edge carrier. Now the optimum rotational position of the knife edge should be ascertained by monitoring the screen while turning the knife edge holder. The image on the screen will be seen to have three distinctive regions, depending upon the angular orientation of the knife edge. When the knife edge is tilted to one side with respect to the slit image, the screen will take on the characteristic violet appearance of the higher spectral lines of the mercury vapor lamp. When the knife edge is tilted to the other side with respect to the slit image, the screen will appear a yellowish green, the color of the lower spectral lines of the

mercury vapor lamp. Between these two positions of the knife edge is a small region in which the screen will appear colorless. When the screen is colorless, the knife edge and slit image are approximately aligned. The final placement of the slit may be obtained by observing the sensitivity of the system to heat flowing from a power resistor placed in the test section and connected to a variac set on a low voltage. Observation of the image of this heat flow will also help give an idea as to the relationship between the vertical position of the knife edge and the system's sensitivity. The color in the rotational edge alignment arises from the chromatic aberration of the condenser and the lack of a filter. A better condenser is certainly desirable, although rotational alignment might then be more difficult. Additionally, if the light flux available from the light source is great enough, a filter may improve the sensitivity or resolution of the system by forcing the diffraction at the knife edge to approach a more monochromatic form. If the screen does not uniformly darken after the knife edge is adjusted, it will be necessary either to readjust the slit assembly so that the light emerging from the slit is better aligned horizontally with the parallel beam of light or to move the camera frame around slightly. These adjustments are done to negate the effect of the horizontal displacement from the system's axis of the light source and other unforseeable aberrations.

Once uniform darkening of the screen is achieved when the knife edge is introduced into the focused light, the frames may be raised to their working height. To minimize the misalignment of and the stress on the frames, the feet should be screwed sequentially one revolution at a time. Since the feet in the part of the frame where the plane mirror

resides have a coarser thread than the feet under the spherical mirrors, they should be turned less often for each complete sequence.

It seems best to raise the light source frame first so that the light beam will be at the desired height. After the camera frame is raised to near the desired height, turn on the continuous light source and monitor the form of the darkening on the wall screen as the frame is raised. Like most of the adjustments mentioned, this is an iterative process in which the knife edge vertical position and the amount of turning of the feet are done interactively.

To take pictures it is necessary to focus the plane of the axis of symmetry onto the film plane. This is done by placing the lens behind the knife edge and putting a sheet of white paper into the film plane inside the backpack. A transparency with various sized lettering (some of it small) is placed in the test region in the object plane. For this research, a bench was installed to hold the various acoustical apparatus in place. The transparency was therefore mounted on the bench within the parallel light beam. With the knife edge clear of the light, the bellows is moved to and fro until the lettering is focused on the paper. The knife edge is then placed into the light so that the screen will be darkened uniformly. When the system is ready for use, it should be fairly easy to see the heat rising from a person's hand.

Photography of sound waves requires the use of the flash light source. As previously mentioned, there is a problem in having the alignment remain the same when the flash source is substituted for the steady state source. Some readjustment, therefore, is usually necessary. Alignment mainly involves ensuring that the light of the flash is focused and

centered on the slit. Although much of the steady state alignment can be done with the room light on (this is not recommended), flash alignment requires both that the eyes be adjusted to the dark and that the source be flashed many times so that each adjustment can be properly evaluated. From the standpoint of extending the flash lamp life, it is best that the flashes do not occur too often. Two or three flashes per minute is a good number to use. Actually the flashing rate cannot get much higher because the time constant for the charging of the capacitor in the trigger circuit is 15 sec. This time constant was chosen to ensure that the light is not prematurely reflashed after a picture is taken. The delay between flashes also allows the spark gap to cool and most of the free ions to recombine.

Each element in the system should be checked to verify that the alignment done with the steady state source is still valid for the flashed light source. Finally, the illumination on the screen should be set so that the effect of the knife edge is noticeable in uniformly darkening the screen. The best position of the edge will then have to be determined by experimentation with film.

Maintenance

The major maintenance problem is the flash lamp. As has already been stated, the breakdown of the air to form the arc causes chemical changes in the gap. As a result of the discharge byproducts, which reside mostly on the glass, a small surface current or corona develops. This corona will increase in magnitude after each discharge until so much of the charge that would have gone to the capacitors flows through the gap

that the discharge will not occur. The spark gap's lifetime between cleanings can be characterized by three stages.

The early age gap usually has little or no sign of corona with the high voltage supply on. The gap will not reliably discharge every time a trigger field is applied.

After about five or ten discharges, the gap is in what might be called its middle age. When the spark gap is closely examined, a periodic low intensity flashing light and accompanying clicking noise will be perceived. The gap is most reliable in this stage and usually seems to work best when the 18 kV is kept across the gap for the full picture taking session as opposed to removing the high voltage during periods of inactivity within a session. Middle age will last for between 25 and 50 firings.

As the spark gap is used further, the surface current on the glass increases to the point where flashing the lamp becomes unpredictable. The symptoms of this old age are the continuous radiation of light and a hissing noise from the gap. When this stage is reached, it is best to finish the film being used and then clean the light source.

The lamp is cleaned by first removing the tape holding down the top glass on the side of the lamp away from the trigger terminal. The top glass is then carefully lifted by its free end. It is beneficial to use a razor blade to cut across both pieces of glass at various positions along the discharge path. This helps reduce the surface current by removing (at least for awhile) the path of the charge flow. The two pieces of glass are then wiped with a cotton swab which has acetone on it. The acetone is also applied with strokes that are perpendicular to the discharge path so

that any impurities left when the acetone dries will not be continuous across the gap. The top glass is then replaced over the gap with the tape applied so that the two pieces of glass will touch on the side of the lamp opposite to the orifice where the light emerges. Either or both pieces of glass may have to be replaced occasionally when the cleaning becomes ineffective. The gap size should also be occasionally checked, especially if after it is cleaned, the gap either never leaves early age or else seems to start in old age when the high voltage is applied.

The Acoustic Apparatus

The acoustic apparatus, some of which is shown in Fig. 3.13, can be placed into two categories: sound source and test items. The sound source consists of a variable width spark gap with tungsten electrodes, a Spellman PN-30 high voltage power supply, two 0.02 μF capacitors, and a 108 MΩ resistor. The test items include the following:

1. a 20 in. x 15 1/2 in. aluminum baffle plate, 1/8 in. thick, having a 6 in. diam aperture in its center,
2. a parallel plane duct model made with plexiglass 1/8 in. x 1 ft x 1 ft,
3. a metal 18 in. diam, 8 in. focal length spherical microwave dish,
4. a metal 15 1/2 in. diam, 9 in. focal length parabolic dish, and
5. a glass 16 in. diam rear surfaced mirror with a 17 in. focal length.

Not all of the test items were used for this research.

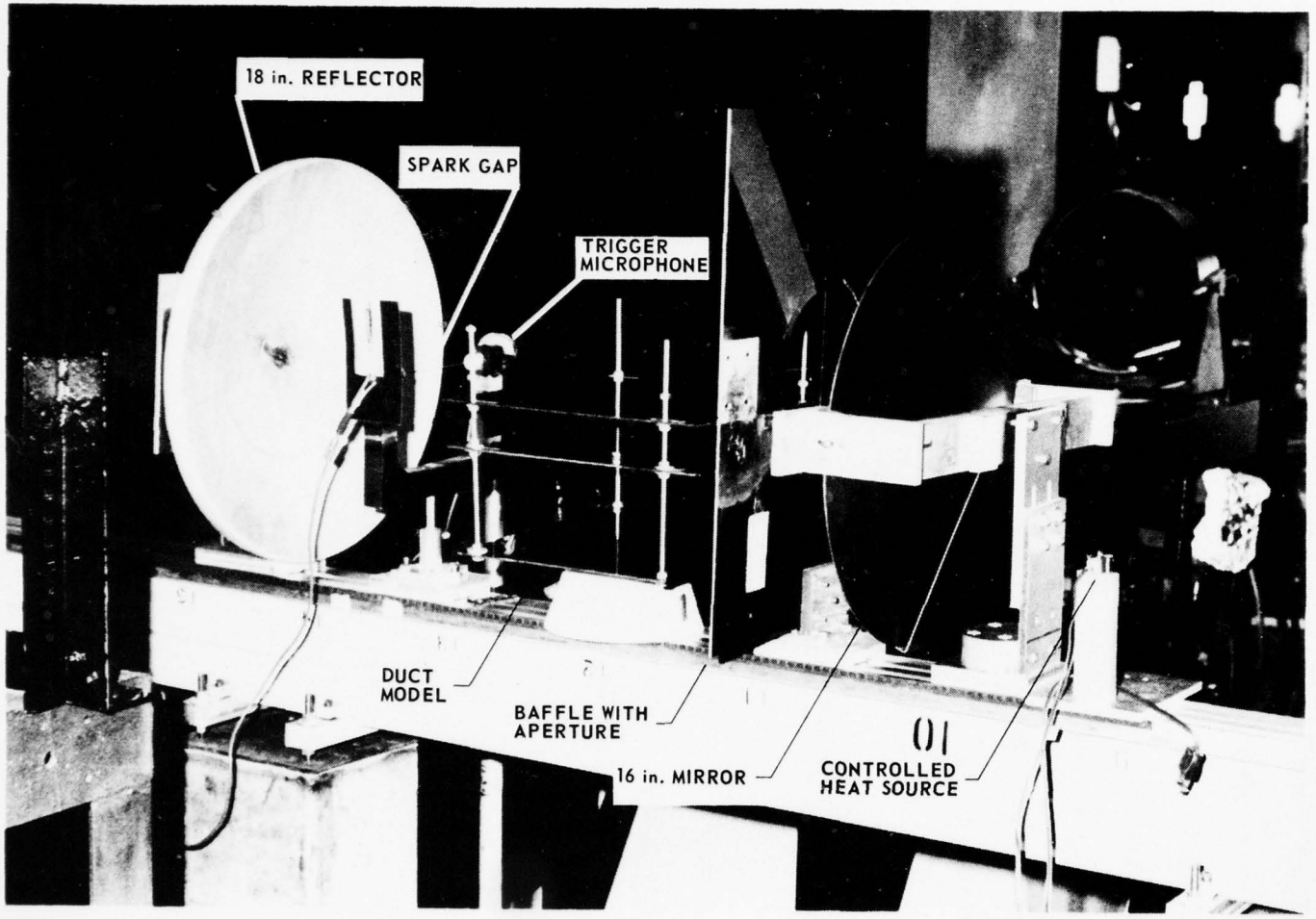

0867-14

FIGURE 3.13
ACOUSTIC APPARATUS

AD-A040 010 TEXAS UNIV AT AUSTIN APPLIED RESEARCH LABS F/G 14/5
DEVELOPMENT AND USE OF A SCHLIEREN SYSTEM FOR SOUND PULSE STUDI--ETC(U)
AUG 76 D R KLEEMAN F44620-76-C-0040
UNCLASSIFIED ARL-TR-76-43 AFOSR-TR-77-0679 NL

2 OF 2
AD A040010

END

DATE FILMED
6-77

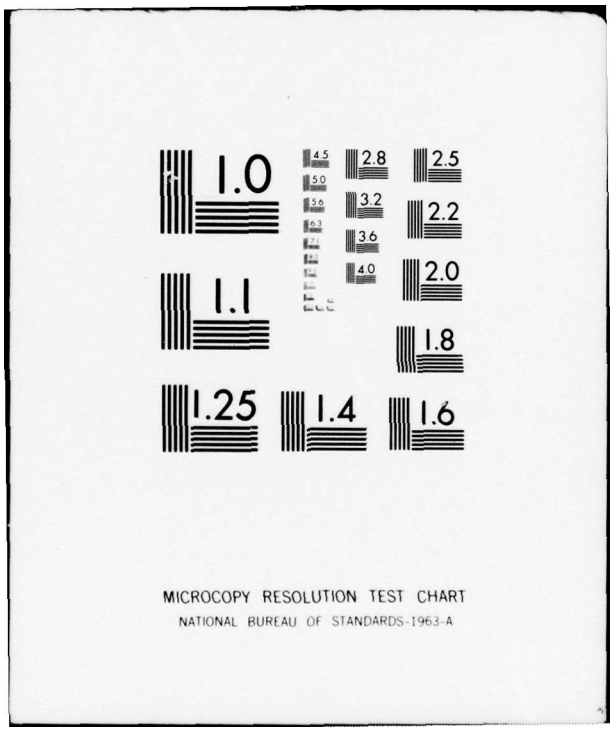
1.0
1.1
1.25
1.4
1.6
1.8
2.0
2.2
2.5
2.8
3.2
3.6
4.0
4.5
5.0
5.6
6.3
MICROCOPY RESOLUTION TEST CHART
NATIONAL BUREAU OF STANDARDS-1963-A

The acoustical apparatus used for a particular sequence of pictures is mounted on an 8 ft optical bench designed by Mark Anderson (1974). (See Fig. 3.14.) The bench is held above the floor by two 8 in. x 8 in. x 32 3/4 in. pillars made of 3/16 in. thick iron. The pillars are bolted securely to the floor. The sound source power supply is located near the end of the work bench where the spark gap is normally used. The two capacitors are placed near the gap to reduce the inherent inductance of the line connecting the capacitors to the gap. The resistor forces the capacitors to charge at a rate slow enough so that they are not impulsively stressed while charging and also so that the experimenter may have time to think between discharges. The time constant of the charging circuit is about 4 sec.

A typical experimental procedure is to first arrange the acoustical equipment so that the acoustic wave of interest passes through the light beam of the schlieren system. Then measure the total distance the wave coming from the spark gap has to travel to reach the desired position and place the trigger microphone the same distance away from the spark gap. The path from the spark gap to the microphone should be free of obstructions. It is also best, especially when the distance becomes larger than about 14 in., for the microphone to be as close to the perpendicular of the spark gap axis as possible so that the acoustic energy is great enough at the microphone to trigger the light source. Of course, the acoustic spark gap size is also a factor in this consideration. With the schlieren system aligned and the acoustic apparatus and trigger microphone in place, connect the trigger battery and turn on the high voltage supply for the light source. This supply should be left on for the

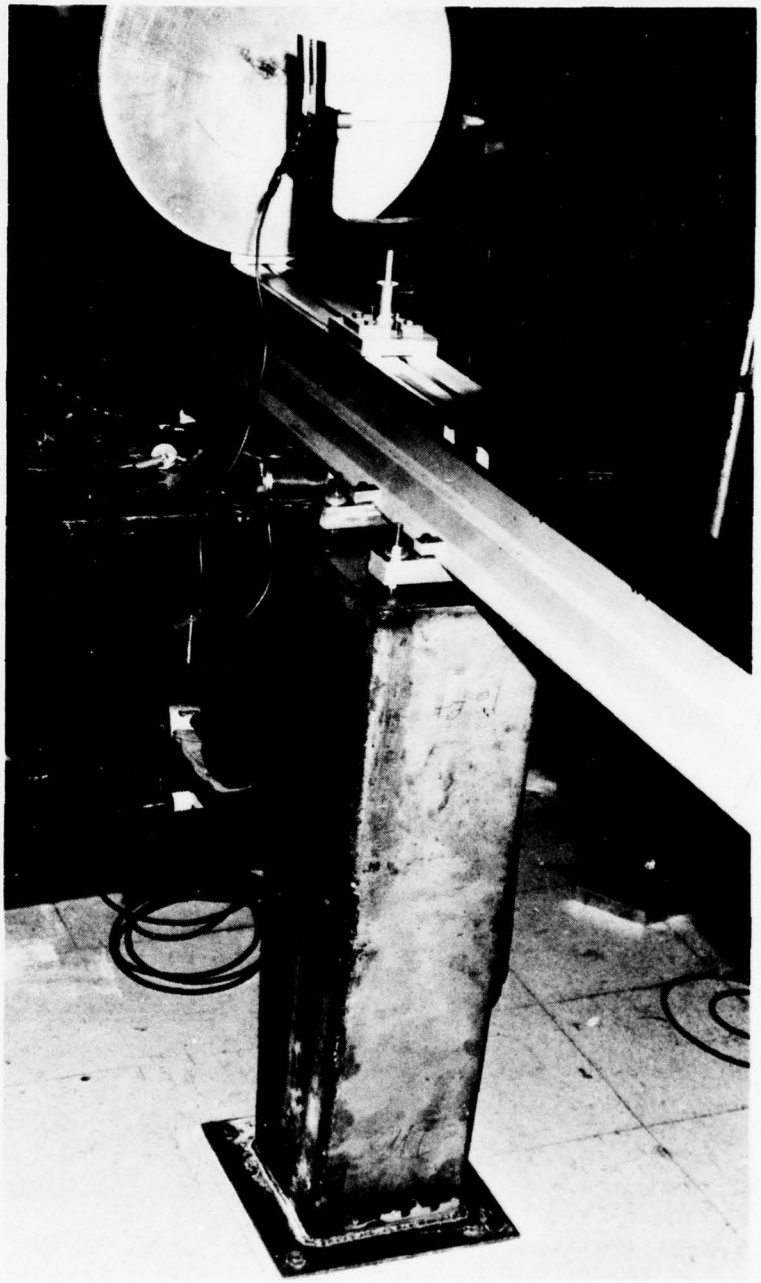

FIGURE 3.14
ACOUSTICAL BENCH AND SUPPORTING PILLAR

0867-15

remainder of the picture taking sequence. If it is desired to make the light source insensitive to acoustic triggering signals, disconnect the trigger battery. The high voltage for the sound spark gap should be turned up to just below the voltage necessary to break down the air in the spark gap when the capacitors are fully charged. This level will have to be empirically determined for each gap size. It is best to do a great deal of this work with the room lights off. The light from the corridor will suffice for most work requiring light, once the eyes have become accustomed to the dark. After the high voltage is applied, the door should be closed so that the room is dark. After waiting two time constants or more for the capacitors near the sound spark gap to charge, the experimenter carefully removes the light cover on the Polaroid film backpack and proceeds to turn the high voltage knob up so that the sound spark will occur in 10 sec or less. After the discharge, the high voltage is removed from the gap and the film cover is replaced.

When it is necessary to place the trigger microphone within 10 in. of the sound spark gap, it is best to cover the microphone with aluminum foil. The foil is connected to the optical bench or some other large metallic body so that the electromagnetic pulse from the spark discharge will not enter the microphone cable and trigger the light source.

Data taken with the system used for this research is given and explained in the next chapter.

CHAPTER 4

TWO APPLICATIONS OF SCHLIEREN PHOTOGRAPHY

Introduction

Information concerning the theory and implementation of schlieren photography has been given in the previous chapters. Two specific acoustical experiments, which serve both to demonstrate the utility of the method and to give additional information that may prove useful in interpreting the phenomena studied, are given in this chapter.

The first phenomenon studied is the propagation of a pulse in a duct formed by two parallel planes. The second study is of the focusing of a spherical wave by a spherical reflector. In both cases the acoustic signal is an N wave generated by an electric spark. Nonlinear effects resulting from the high intensity of the N wave are not expected to cause unusual behavior in the duct case because the propagation distance is relatively short and because the energy density of the wave continually decreases as the pulse travels since the pulse is spherically spreading. The focusing study, on the other hand, involves a converging N wave. The energy density thus increases and, in the limit of geometrical acoustics, the overpressure is infinite at the focus. Nonlinear effects are expected to be important in such a situation. Theoretical predictions based on ray theory were developed for both experiments in order to aid in interpretation of the photographed phenomena.

Acoustic Pulse Propagation in a Duct

Wave propagation in a duct is more often than not approached from the sinusoidal steady state point of view. The higher order modes are

considered to consist of a set of plane waves that make certain angles with respect to the duct walls as the wave is guided down the duct by reflections. Even in the case where pulse propagation in the duct is considered, no attempt is usually made to predict how the guided waves will emerge from the duct. The present study shows quite vividly both the propagation in and radiation from a duct of an acoustic pulse sent out by a point source.

The theoretical model of pulse propagation in the duct is based on the method of images. Each new reflected wave generated in the course of the propagation of the spherically expanding pulse down the duct can be thought of as arising from a virtual source. Graphically the duct to be modeled is scaled down and the position of the spark source relative to the duct is marked. It is not necessary for the spark gap to be inside the duct in order for the method of images to be used.

Two duct models were used in this study. The duct shown in Fig. 4.1 was described in the last part of Chapter 3. The second duct, which is not shown, is 1.5 in. in height and 8.5 in. long by 9 in. wide. Both ducts were built by securing four threaded rods to one plate which serves as the base of the model. The two plates, which act as the duct, are then positioned on the four rods. Fig. 4.1 shows the experimental arrangement used to take all the duct model pictures for this thesis. (The spherical reflector seen in the photograph is used in the focusing pictures. It plays no role in the duct experiment because of its distance from the spark source.)

A comparison of the theoretically predicted wave field with a photograph for the case where the unreflected wave is just emerging from

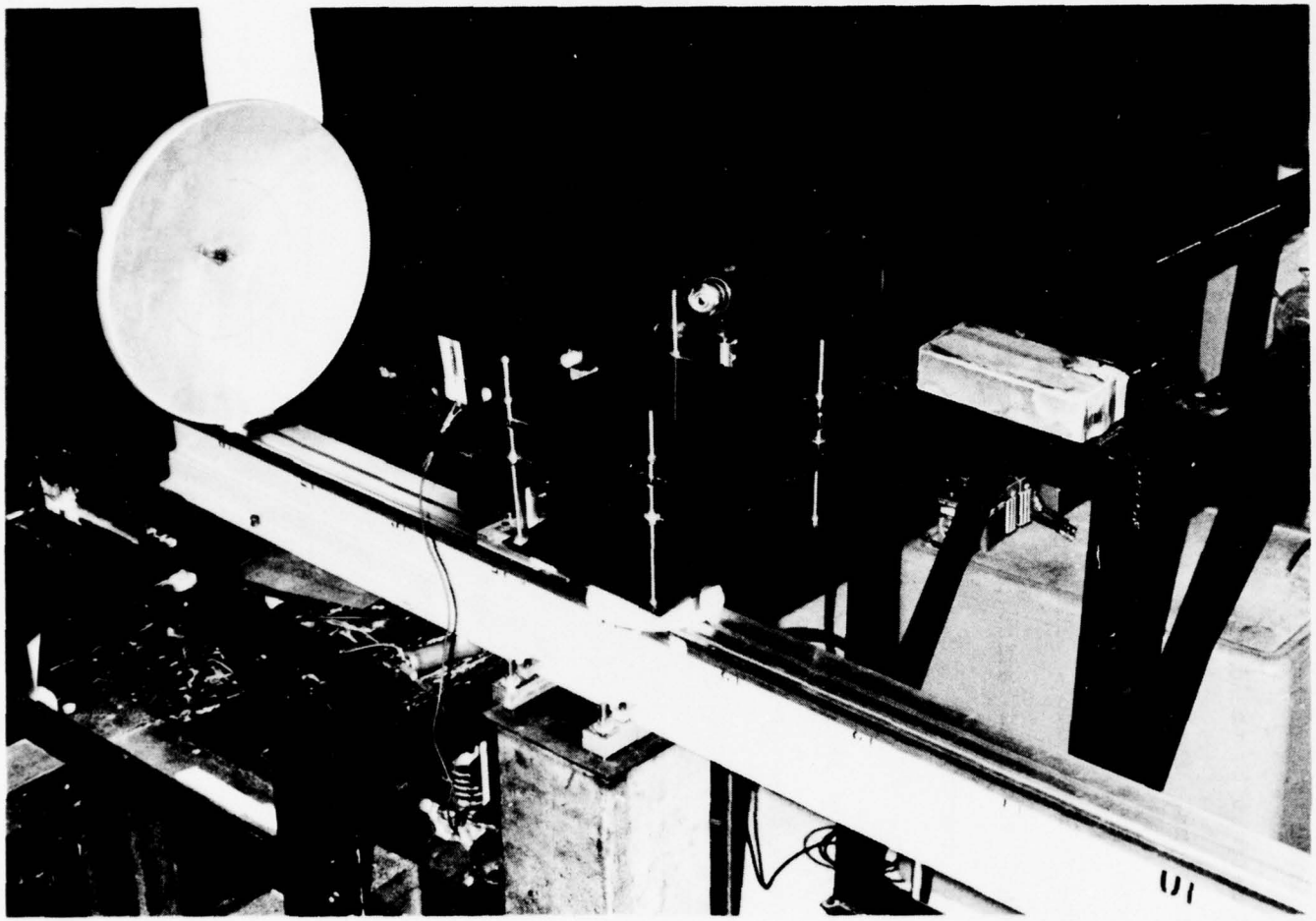

0867-16

FIGURE 4.1
EXPERIMENTAL ARRANGEMENT FOR PROPAGATION IN A DUCT

the duct is shown in Fig. 4.2. The similarity is quite obvious. The photograph indicates that the waves with downward convex curvature have a density gradient component which shifts the light rays that pass through these waves up and over the knife edge. The waves with upward convex curvature refract the light rays incident upon these waves downward to be blocked by the knife edge. The simple theoretical prediction used here, however, does not include diffraction. Each time a wave from the actual source or one of the images emerges from the end of the duct, diffraction wil occur. In the figure the initiation of a diffracted wave is seen at the top plate, where the unreflected wave has just emerged. (The plates were not quite aligned.) Notice how the distance between reflection junctions increases as the spark source is approached. This effect is indicative of the spherical spreading of the wave even though the wave is confined. Part of the sound pulse that did not enter the duct is seen to have reflected back and forth between the lower duct plate and the base plate. It should be noted that the after shock is not visible in these pictures.

Figure 4.3 shows the field in and beyond the duct at a later time. The diffracted waves resulting from the emergence of the first few duct waves are quite pronounced. As later parts of the wave train emerge from the duct, the diffracted signals become undetectable because the energy density of the emerging waves is low. Similarity is again quite strong between the geometrical prediction and the photograph. The only observable discrepancy between the drawing and the photograph is that the wave train in the photograph appears to be slightly ahead of the drawn figure. There are two probable sources for this discrepancy. One is the experimental error resulting from the delay between the incidence of the acoustic

+ VIRTUAL SOURCE

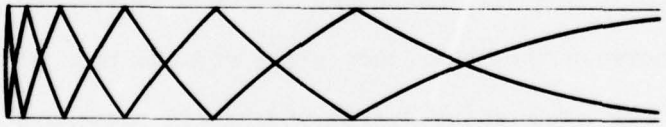

REAL SOURCE

FIGURE 4.2
PULSE JUST EMERGING FROM A DUCT

ARL - UT
AS-76-818
DRK - DR
7 - 13 - 76

+ VIRTUAL SOURCE

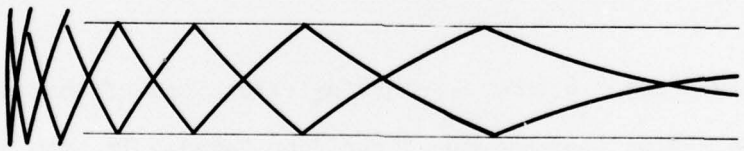

REAL SOURCE

FIGURE 4.3
PULSE RADIATING INTO FREE SPACE
FROM A DUCT

ARL - UT
AS-76-819
DRK - DR
7 - 13 - 76

pressure on the trigger microphone and the flashing of the light source. The second source of the discrepancy may be the difference in the actual speed of sound of the pulse compared with the assumed linear wave speed used in the construction of the figure.

Two phenomena are of interest in Fig. 4.4. In this case the 1/2 in. spark gap was placed vertically off center at the beginning of the duct, which in this case had a height of 1.75 in. The first phenomenon is the alternation of the vertical position of the wave crossings inside the duct. The pattern is asymmetric because of the unbalanced nature of the reflections. The second phenomenon, which can actually be seen to a limited extent in Fig. 4.3, is the separation of the incident and reflected waves when they emerge from the duct. They separate because as they leave the duct their propagation vectors are pointing in different directions.

Figures 4.5 and 4.6 show interesting extensions of the theoretical model beyond the region where pictures could be taken. In both figures the duct is modeled the same as in Fig. 4.2 except that the vertically centered spark gap is placed at the end of the duct. Thirteen reflections are shown in Fig. 4.5; no account is taken of the actual diminution of the wave amplitude as the wave spreads. The image sources of the theoretical model of the duct can, without regard for the diminishing nature of a real pulse, extend to plus and minus infinity. Since the wave diminishes in amplitude even when reflecting between the duct walls, no trace of the pulse will be seen in a schlieren photograph of the duct after the initial pulse has propagated a certain distance. To account for the negligible wave amplitude in the duct after the pulse has propagated for some time,

FIGURE 4.4
SEPARATION OF PULSE REFLECTIONS
UPON LEAVING A DUCT

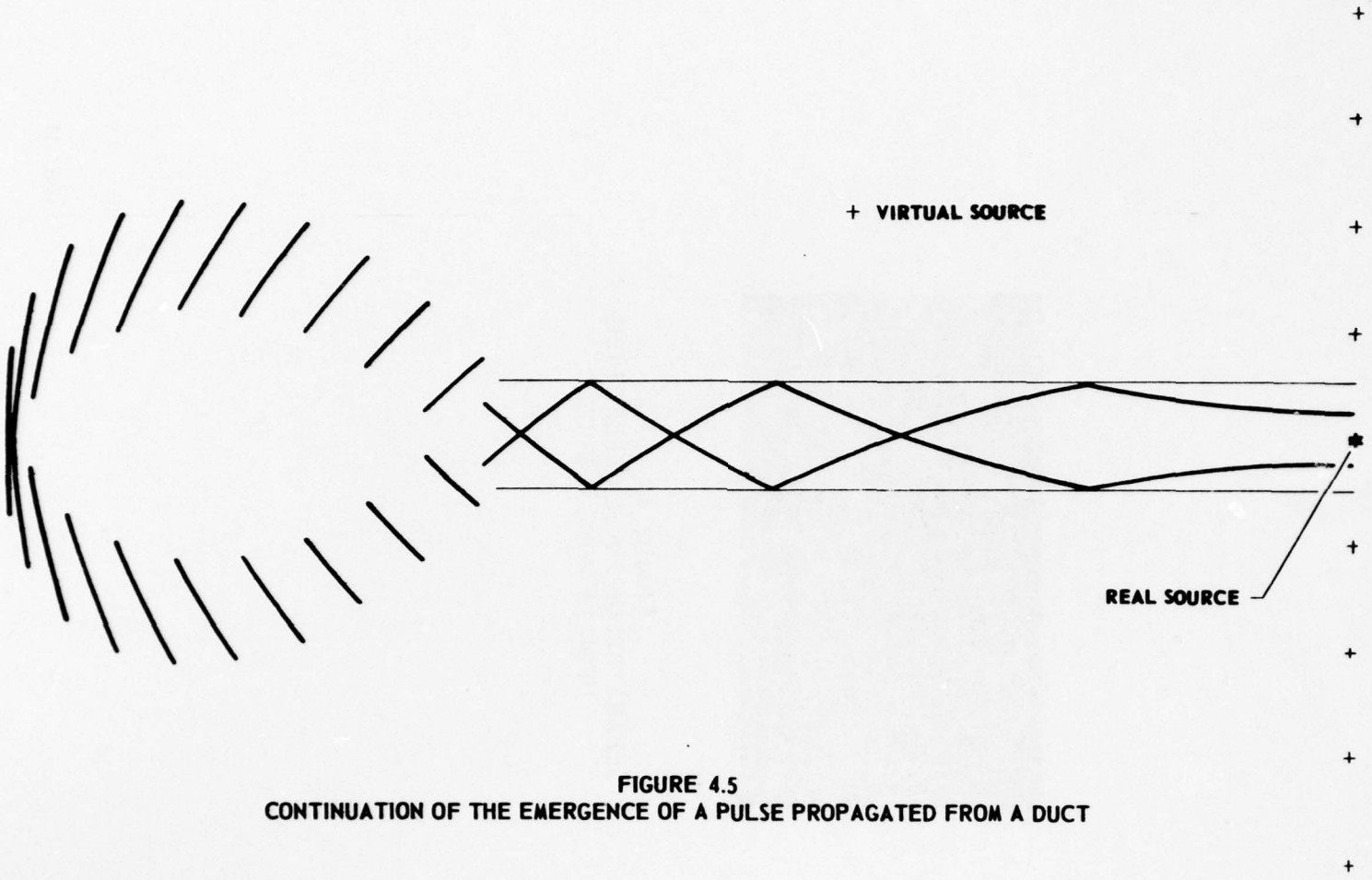

FIGURE 4.5
CONTINUATION OF THE EMERGENCE OF A PULSE PROPAGATED FROM A DUCT

ARL - UT
AS-76-821
DRK - DR
7 - 13 - 76

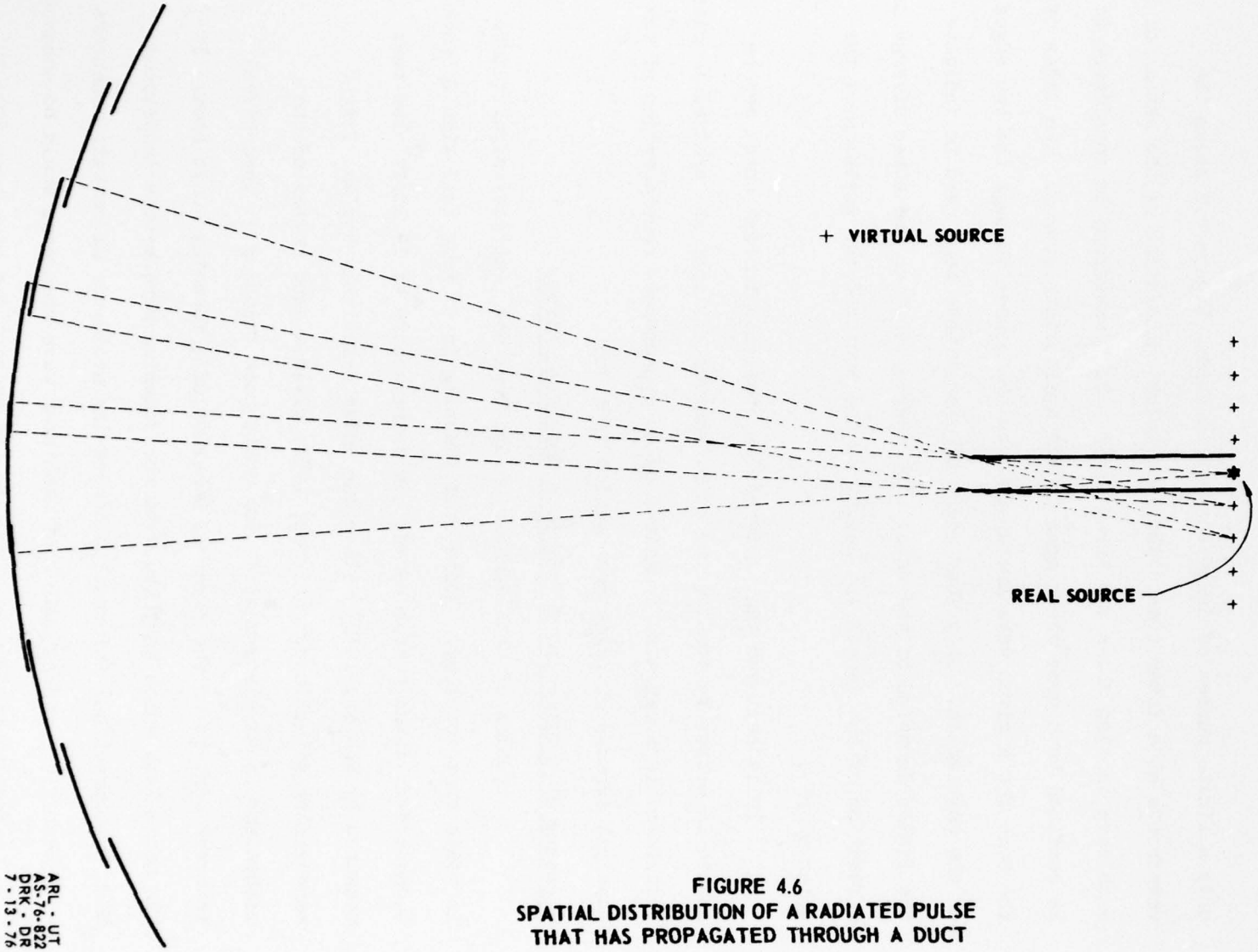

FIGURE 4.6
SPATIAL DISTRIBUTION OF A RADIATED PULSE
THAT HAS PROPAGATED THROUGH A DUCT

only a finite number of image sources is used. Figure 4.6 shows the wavefronts at a later time. The geometrical prediction of the extent of each wave is also shown for three waves. Each wavefront is considered to be confined to a cone whose apex is the appropriate source. The sides of the cone for a given wave are drawn from the source through the two edges of the duct mouth. Only four pairs of images have been used to indicate the finite duration of the wave. The degree to which the cones diverge is a function of the length and height of the duct and the position of the point source.

It is believed that information analogous to that which can be gained in optics by considering point sources of light and spatial Fourier transformations can also be gained by an appropriate consideration of the physical aspects of pulse propagation in a duct.

Focusing of a Spherical N Wave by a Spherical Mirror

A problem of considerable theoretical and practical significance is sonic boom focusing. Sonic boom focusing is of practical significance because very large overpressures (an overpressure of 14 lb/ft^2 has been measured by Wanner, 1970) will occur under relatively typical flight maneuvering situations. (Pierce, 1971, gives a good review of the mechanisms usually responsible for sonic boom focusing.) Theoretical interest centers on the physical behavior of a focusing sonic boom. If the mechanisms which contribute to the focusing were better understood, then both practical information concerning avoidance of certain maneuvers and theoretical understanding of nonlinear wave phenomena would be enhanced.

Studies similar in nature to the present one have been done by Beasley, Brooks, and Barger (1969), and Sturtevant (1974). In both the

above studies, a plane wave was reflected from a parabolic mirror (both two- and three-dimensional) and the resulting focusing wave photographed. Beasley et al. did their study in free space, i.e., not in a shock tube, and used a schlieren system to photograph the wave. Their results indicate behavior as predicted by linear considerations. Sturtevant used a shadowgraph system to view focusing inside a shock tube. The results of his studies indicated that the linear theory of focusing is not adequate for high amplitude sound. Sturtevant suggests a model which essentially bridges linear theory with the theory of Whitham (1957). Whitham states that if the wave is of high enough amplitude, the part of the wave near the focus will speed up because of nonlinear effects. The rays will then be bent in such a way as to prevent focusing from occurring.

The present measurements are somewhat complementary to those reported by Cornet (1972). Cornet made microphone measurements of the focusing of an N wave by a spherical mirror. Most of his measurements were taken along the acoustic axis of the mirror. He observed that the reflected N wave reverses its phase, i.e., becomes an upside-down N, when it passes through the focus. Furthermore, the diffracted wave, which comes primarily from the rim of the mirror, starts out as an upside-down N and lags the reflected wave (on the axis). After focus, the diffracted wave is an ordinary N (right side up) and leads the reflected wave. The diffracted wave is of the same magnitude as the reflected wave on the mirror axis but is appreciably less in magnitude off the mirror axis. The major difference between Cornet's arrangement and the one used for this study is that he placed the spark gap inside the mirror's center of curvature and thus focused the sound beyond the center of curvature whereas in the present

work the spark source is placed outside the center of curvature so that the photographed sound is brought to a focus inside the radius of curvature. Another difference is that Cornet used an optical mirror whereas a metal microwave dish was used in the present study.

To aid in interpreting the schlieren photographs, a computer program to calculate ray paths was developed largely through the efforts of Bill Willshire on a Hewlett Packard 9810A programmable calculator. The program enables the user to draw the wavefront emitted by a point source before and after reflection from a spherical mirror. The algorithm for the program is based on linear geometrical acoustics. For a given incident ray the reflected ray is constructed as follows. Consider the tangent to the mirror surface at the point of incidence of a ray from a source. Let the tangent (see Fig. 4.7) be translated to the mirror's center of curvature. Specular reflection demands that the distance from the center of curvature along the translated tangent to the incident ray must equal the distance in the opposite direction to the reflected ray. The program thus calculates the tangent at the point of incidence of a given ray on the mirror surface and draws a similarly directed line through the center of curvature of the mirror. The distance from the center of curvature to the incident ray is calculated and the same distance is marked off on the opposite side of the center of curvature from the incident ray. The reflected ray is then simply a line drawn from the point of incidence on the mirror surface through the point just marked off from the center of curvature. Actually, for comparison to schlieren pictures, we are interested in wavefronts, not rays. The wavefront may be drawn without any rays. It is simply the locus of points equidistant from the source along the various rays. A representative computer plot is

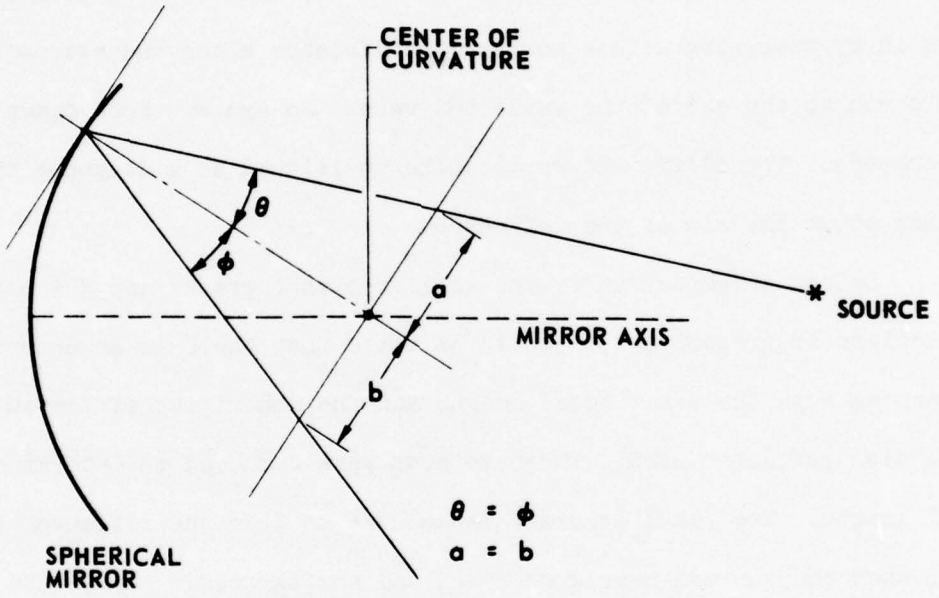

FIGURE 4.7
GEOMETRICAL DETERMINATION OF A REFLECTED RAY FOR A GIVEN SOURCE POSITION AND AN INCIDENT RAY ON A MIRROR SURFACE

ARL - UT
AS-76-829
DRK - DR
7 - 14 - 76

shown in Fig. 4.8. The N wave is shown diverging from focus after having been reflected from the mirror. To include the fore and after shock of an N wave, two separate wavefronts were drawn on a single plot with the spacing between the shocks consistent with that seen on the photographs. The diffracted waves, which are not included in the computer program, were drawn in by measuring with a compass the distance along the extreme ray from a rim to the end of the reflected wave. An arc was then drawn with the compass. The diffracted wave can be envisioned as a doughnut that expands about the rim of the reflector.

Before a comparison of the schlieren photographs and the computer predictions is presented, it should be noted that there is an uncertainty concerning both the exact focal length and the sphericity of the 18 in. metal dish reflector used. Three methods were employed to determine the focal length. The least accurate method was to take the reflector out on a day when the sun was nearly overhead and the sky was clear and to focus the sunlight onto a small piece of white paper. The focal region appeared to be between 7.5 in. and 8 in. The second method involved the suspension of a weight (a threaded rod) by a wire above the center of the reflector. The height of the pivot point for pendulum action of the weight was varied until the weight appeared to coincide with the surface. The center of curvature appeared to be 17.25 in. (f=8.63 in.) although it seemed to vary depending on the plane taken through the reflector axis. In other words, the reflector seemed to be slightly cylindrical. The third method involved placing the spark source at various distances from the reflector in the approximate focal region. Schlieren pictures were taken of the reflected waves. Ideally a plane wave should result when a point source is at the

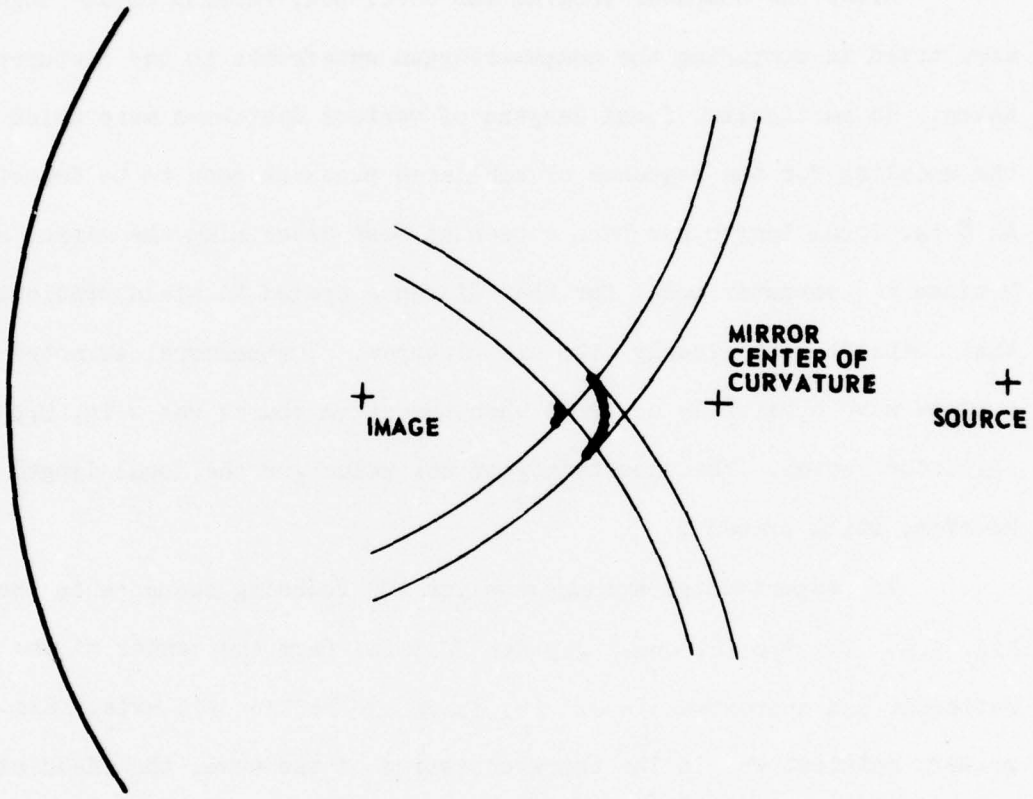

FIGURE 4.8
GEOMETRICAL MODEL OF A REFLECTED SPHERICAL N WAVE
FROM A SPHERICAL MIRROR

ARL - UT
AS-76-828
DRK - DR
7 - 14 - 76

focal point of a spherical mirror although the wave will not be perfectly plane because of spherical aberration. The most nearly plane wave seemed to occur for a focal length of 8 in.

After the computer program was developed, various focal lengths were tried in comparing the computer-drawn wavefronts to the pictures taken. In particular, focal lengths of various distances were tried in the modeling for the sequence of schlieren pictures soon to be described. An 8 in. focal length has been chosen as best describing the mirror mainly because the computer model for that distance seemed to yield predictions that coincide most closely with the pictures. Furthermore, as noted above, a plane wave apparently occurred when the spark source was 8 in. from the reflector center. The uncertainty of the value for the focal length is, however, still present.

The experimental arrangement for the focusing sequence is shown in Fig. 4.9. The 3/8 in. spark gap was 22.5 in. from the center of the reflector and approximately 0.5 in. above the reflector's axis. Since the primary interest was in the characteristics of the wave, the field of view of the schlieren system is limited to magnify the image of the region under study. This magnification is accomplished by using (behind the knife edge) a lens with a focal length longer than is necessary to image all the light passing over the knife edge onto the 4 in. x 5 in. Polaroid film.

A side-by-side comparison of the wavefronts predicted using geometrical theory and those recorded in the schlieren photographs is shown in Fig. 4.10. It should be noted that the center of the wave is high on the photograph. This positioning of the image on the film was done on the assumption that the wave behavior is symmetrical about the propagation

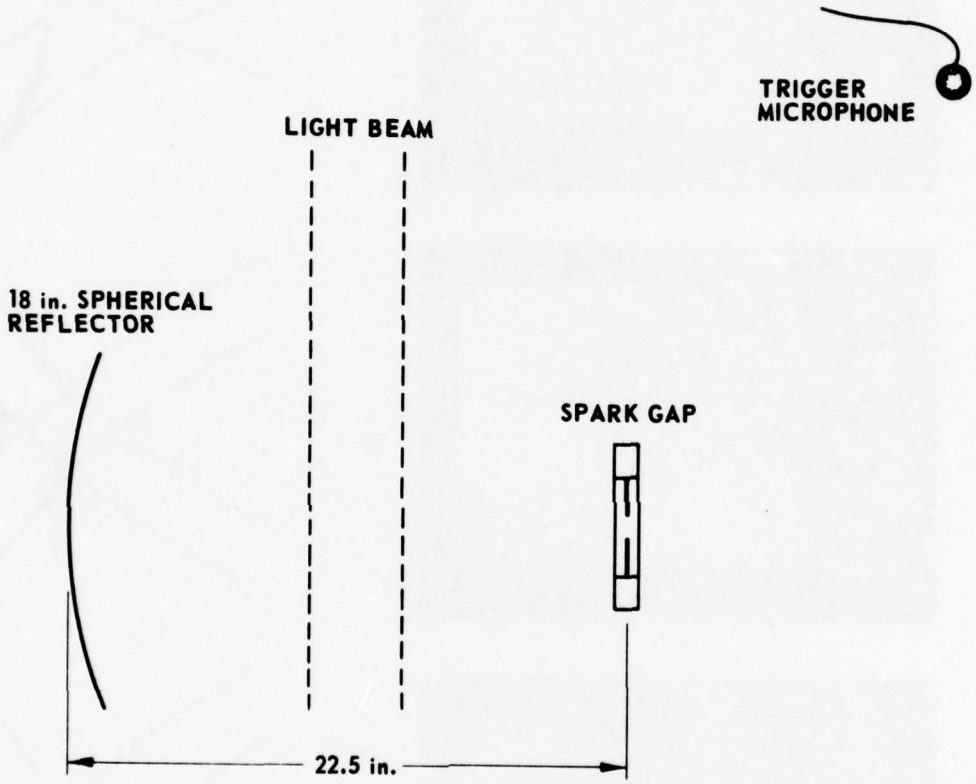

FIGURE 4.9
EXPERIMENTAL ARRANGEMENT FOR N WAVE FOCUSING PROBLEM

ARL - UT
AS-76-825
DRK - DR
7 - 14 - 76

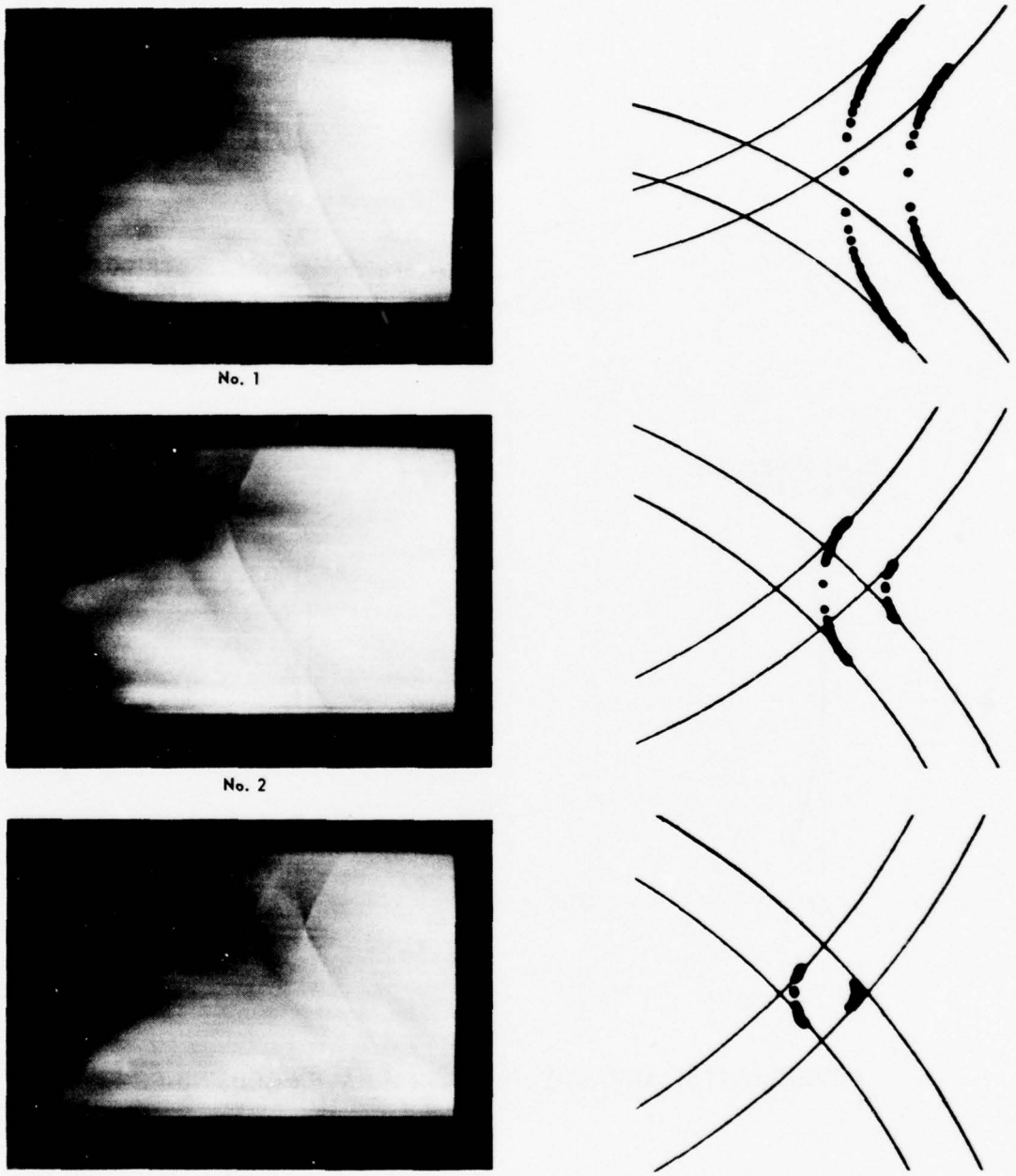

FIGURE 4.10
FOCUSING OF SPHERICAL N WAVES

ARL - UT
AS-76-824(a)
DRK - DR
7 - 13 - 76

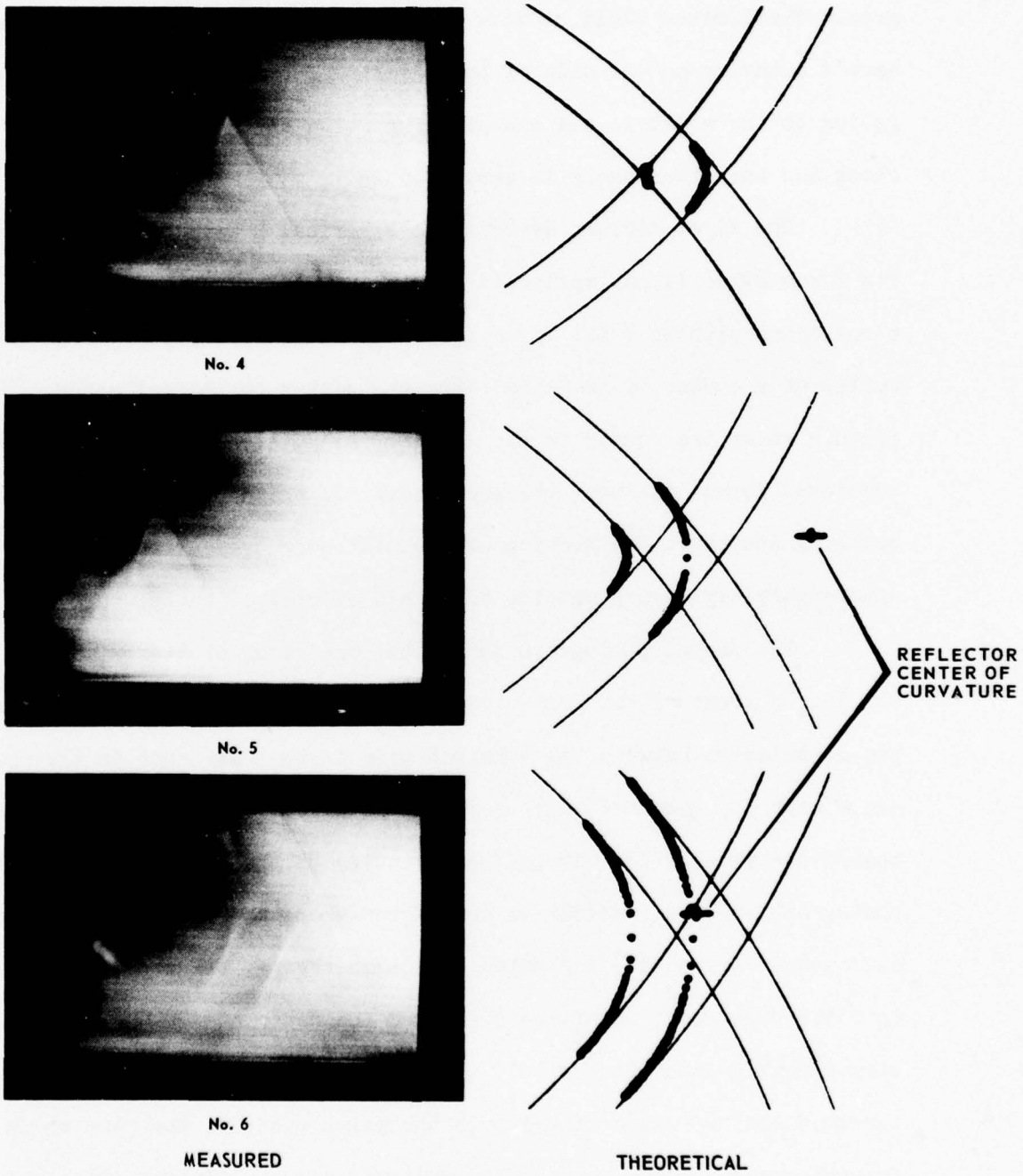

FIGURE 4.10 (CONT.)
FOCUSING OF SPHERICAL N WAVES

ARL - UT
AS-76-824(b)
DRK - DR
7 - 13 - 76

axis. The limited field of view is then used to more closely examine the wave's behavior on one side of the axis. Moreover, the waves are propagating to the right in all six pictures. The distance between the fore shock and the after shock is about 0.5 in.

The first picture depicts the spherical N wave converging toward its focus after it has reflected off the mirror. The paraxial focus for a reflector with an 8 in. focal length and a source 22.5 in. from the reflector's center is 12.41 in. from the center of the reflector. The picture shows the center of the wave approximately 2.9 in. before the predicted focus. Neither the photograph nor the computer drawing shows anything unusual. The meeting of the diffracted wave with the reflected wave apparently occurs outside the field of view of the picture.

The second photograph shows the fore shock at approximately 0.9 in. in front of the predicted focus. Of interest in this picture is the correlation between the straightening of the wavefront in the photograph with the geometrically predicted advance of the diffracted waves toward the axis of the wave. The beginning of the straightening in the photograph appears to occur in the region where the reflected wave and the diffracted wave meet. According to linear theory, the straightening results from the superposition of the reflected and diffracted waves. The straightening should occur only at the inflection point, where the curvatures of the two waves cancel. In the third picture, the fore shock is approximately 0.1 in. beyond the predicted focus. Although signs of wavefront crossing, in which a single wave gives rise to two waves, can be seen in the second photograph, the small bright region emerging from behind the head of the wave in photograph No. 3 definitely indicates a density

gradient in the same general direction as the top half of the head of the wave. Focusing has occurred according to the geometrical prediction and the wave is seen to be essentially straight along either side of the axis of propagation with a slight curvature of the wave occurring near the axis of propagation.

Photograph No. 4 has the head of the wave approximately 0.6 in. beyond the predicted focus. The extension of the wave beyond the crossing has increased in length. Rather than being merely a continuation of the diffracted wave, the extension seems to bend forward. On the geometrically predicted construction the extension, which is a part of the diverging reflected wave, bends backward. The after shock is seen to behave in more or less the same fashion as the fore shock with a delay appropriate for the spacing of the shocks.

Perhaps the most interesting picture is No. 5. At the bottom of the diamond shaped wave crossings is an apparent slope discontinuity which has no counterpart in the drawing. What is indicated by the geometrical theory is that the reflected wavefront intersects the crossed diffracted waves. The geometrically predicted emergence of the reflected wave is not quite seen in the photograph.

Picture No. 6 clearly shows the emergence of the reflected wave as predicted geometrically. The photographic density of the meeting of the emerging wave and the diffracted wave should be noted. A similar density increase can be seen on the front diffracted wave. Thus there is an indication of the presence of the diverging reflected wavefront.

A picture showing the emergence of the head of the reflected wave was not taken because the wave had diverged too much to get a reasonable

picture for this source-to-mirror configuration. It is believed that both the head and the tail of the reflected wave have been seen to emerge from the crossed waves for a different configuration. If the reflected wave after focusing is an upside-down N wave, it would be unstable. (See Cornet, 1972.) This instability or "easing" of the reflected wave may cause the upside-down N to degenerate to a single wavefront before the wave emerges from the crossed diffracted wave.

According to Cornet's measurements, the first pressure gradient detected by a microphone on the axis of the wave propagation will be positive for any position of the microphone. His off-axis measurements similarly predict a positive pressure gradient for any position of the microphone, although the gradient is greatly reduced after the focal region is reached. This reduction results from the diffracted wave, which is strongest on the axis, being presumably the first wave the microphone detects when the microphone is beyond the focal region of the mirror. In the schlieren photographs the light and dark lines remain in the same relationship for the front of the wave in all six pictures. This relationship indicates that the density and pressure gradients in the wavefront do not change when the predicted focus is passed by the wave. This indication then seems to corroborate Cornet's microphone measurements. The discrepancy between the temporal measurements and the present spatial measurements is that the off-axis part of the wave is seen in the photograph to be not much less (by comparing the degree of brightness or darkness along a line) than it is on-axis, especially after the crossed waves have developed. (Cornet measured a greatly reduced amplitude for the diffracted wave off-axis.) The discrepancy becomes greater when it is considered that, according to

Cornet's measurements, the upside-down N reflected wave (off-axis after focus) should show a much stronger deflection of the light in the opposite direction from what it is seen to be. That is, the strong upside-down N wave should be seen as a disturbance on the photograph with the light and dark lines exchanged with respect to their distribution for the reflected N wave before focus. Little more can be said about this discrepancy at this time.

An experiment which could possibly assist in distinguishing the diffracted wave in the focusing situation entails the reflection of the spherical wave from an 18 in. diam flat disk. In theory, the diffraction should be the same if the rims are similar for a flat disk or a concave dish. The strength of the diffracted wave for the focusing situation should then be observable because the sound reflected from the disk would be spherically diverging and should contribute little to the disturbance in the region of interest.

It was noted earlier in the chapter that both Beasley et al. and Sturtevant used parabolic reflectors. One of the motivations for devising the wavefront computer program was to ascertain the effects that the spherical aberration had on the wavefront. The effect seen from the computer drawing is small compared to the effects actually seen in the photograph. It should also be remarked that a well-confined, focused wave was produced during the course of this research. A parabolic mirror was used to produce a plane wave, which was then focused by the 18 in. reflector. The pictures that were taken are highly interesting but they do not seem to be as perplexing as the case shown above.

The comparison between the linear prediction and the data is seen to be rather good as far as geometry of the wave is concerned. The crossed waves, which arise in the photographs after the linear focal region is passed, seem to correspond with the prediction that the diffracted wave from the rim of the reflector should overtake the reflected wave and lead the reflected wave after focus. Questions concerning the curvature, amplitude, and phase distributions of the total acoustic field remain to be answered with greater certainty. Further work which will correlate microphone measurements with the schlieren pictures is desirable.

CHAPTER 5

SUMMARY

This report presented background material necessary to enable the building of a schlieren system. The background material included a review of the possible equipment configurations along with the relative merits of each configuration by discussing the pertinent aberrations inherent in the system elements. It was concluded that, in general, a 2-element parallel light beam system using either lenses or concave mirrors provides the greatest amount of information about an acoustical disturbance if the axis of the disturbance crosses the parallel light beam at 90°. Mirrors were seen to be the most practical field elements when a large field of view was desired. After the requirements of the elements of the system were considered, a brief introduction to a physical optics characterization of a schlieren system was given. A summary of design considerations drawn from the physical optics analysis was then stated. Spherical mirrors with f/numbers between f/6 and f/12 were considered to be of most use in constructing a parallel beam schlieren system.

Schlieren photography was shown to be an experimental technique that enhances the information one may measure in acoustical studies. The schlieren method yields spatial information which is supplementary to the temporal information normally obtained by use of microphones. Essentially the schlieren technique can indicate at once the spatial information about an acoustic field which could otherwise be obtained only by using many microphones. The information yielded from using many microphones is not

actually equivalent to that obtained by the schlieren method because the microphones disturb the field being measured whereas schlieren photographs do not.

Interpretation of the photographs taken by the schlieren method was considered. It was shown that the deviation of a ray of light by a refractive index gradient normal to the ray increases or decreases the film illumination depending upon whether the ray passes over or is blocked by the knife edge. The angular shift of the bent rays was shown to be in the same direction at the knife edge as it was after the rays passed through the disturbance. Thus, in the case where light passes through a region in which the refractive gradient component normal to the rays is downward, the rays will be bent downward and, in the case of a knife edge blocking from above the light source image, will pass over the knife edge and produce an image of higher illumination than the background illumination on the film.

Procedures pertinent to the arranging and adjusting of a 2-mirror schlieren system which has two 1 ft, f/6 spherical mirrors were then given. The construction and maintenance of the flash light source was also described. After the acoustic apparatus was described, the experimental procedure found useful in this research was given.

The results of applying the schlieren system to two specific acoustic situations were then given. The first problem was propagation of an acoustic pulse in a parallel plane duct. The photographs indicated a redirection by the duct of a sector of the spherically expanding acoustic pulse. By use of evidence of the independent propagation of the reflected waves after the waves leave the duct, a geometrical prediction of the

spatial distribution was made of the pulse after leaving the duct. The second problem was the reflection and focusing of a spherical N wave from a spherical reflector. Spatial pictures were taken of the focusing wave to determine how the wave's behavior corresponds with the current theories concerning focused N waves. Comparison between the photographs of the phenomena and the predictions of linear wave propagation were made. Correspondence was high between the predicted and actual wave shapes, but specific conclusions concerning the phenomena could not be made.

The application of the schlieren technique to the two acoustic wave propagation problems quite vividly showed the utility of the method in allowing the experimenter to get a cross sectional view of complex wave behavior that might never be deduced from microphone measurements.

BIBLIOGRAPHY

Anderson, M. O. (1974). "The Propagation of a Spherical N Wave in an Absorbing Medium and Its Diffraction By a Circular Aperture," Applied Research Laboratories Technical Report No. 74-25 (ARL-TR-74-25), Applied Research Laboratories, The University of Texas at Austin, p. 31.

Barnes, N. F., and S. F. Bellinger (1945). "Schlieren and Shadowgraph Equipment for Air Flow Analysis," J. Opt. Soc. Am. 35, 497-509.

Beasley, W. D., J. D. Brooks, and R. L. Barger (1969). "A Laboratory Investigation of N Wave Focusing," NASA Technical Note TND-5306, Langlely Research Center, Hampton, Virginia.

Bergmann, L. (1949). Ultrasonics and Their Scientific and Technical Applications, 3rd ed., Translated by Christa A. Painter, U.S. Navy Electronics Laboratory (NAVSHIPS 900, 167).

Blackstock, D. T. (1972). "Nonlinear Acoustics (Theoretical)," in Amer. Inst. Phys. Handbook, D. E. Gray, ed. (McGraw-Hill Book Co., Inc., New York), 3rd ed., ch. 3n, pp. 3-183 - 3-205.

Born, M., and E. Wolf (1970). Principles of Optics, 4th ed. (Pergamon Press, London).

Brown, E. B. (1965). Modern Optics (Reinhold Publishing Corporation, New York).

* Burton, R. A. (1951). "The Application of Schlieren Photography in Fluid Flow and Heat Transfer Analysis," Master's Thesis presented to The University of Texas at Austin, Austin, Texas.

Clark, J. A. (1975). "Detection of a New Acousto-Optic Effect," Physics Letters 54A, 81-82.

Conrady, A. E. (1943). Applied Optics and Optical Design, Part 1 (Oxford University Press, London).

Cornet, E. P. (1972). "Focusing of an N Wave by a Spherical Mirror," Applied Research Laboratories Technical Report No. 72-40 (ARL-TR-72-40), Applied Research Laboratories, The University of Texas at Austin, Austin, Texas.

Davis, A. H., and G. W. C. Kaye (1927). The Acoustics of Buildings (Bell, London).

Dvorak, V. (1880). "Über eine neue einfache art der Schlierenbeobachtung," Wiedemann's Ann. d. Phys. u. Chem. 9, 502-511.

Foley, A. L., and J. H. Haseman (1905). "Diffraction Fringes from Electric Discharges and from Fluid Streams," Physical Review 20, 399.

Foley, A. L., and W. H. Souder (1912). "A New Method of Photographing Sound Waves," Physical Review 35, 373-386.

Foucault, L. (1859). Ann. Obs. Imp. Paris 5, 197.

Gladstone and Dale (1863). "Researches on the Refraction, Dispersion, and Sensitiveness of Liquids," Philos. Trans. 153, 317.

Goodman, J. W. (1968). Introduction To Fourier Optics (McGraw-Hill Book Co., Inc., San Francisco), p. 26.

Hardy, A. C., and F. H. Perrin (1932). The Principles of Optics (McGraw-Hill Book Co., Inc., New York), pp. 367-368, 80-120.

Hayt, W. H., and J. E. Kemmerly (1971). Engineering Circuit Analysis, 2nd ed. (McGraw-Hill Co., Inc., New York).

Hilton, W. F. (1951). High Speed Aerodynamics (Longmans, Green and Co., New York), pp. 464-465.

* Holder, D. W., and R. J. North (1956). "Optical Methods for Examining the Flow in High Speed Wind Tunnels," Report of the N.A.T.O. Advisory Group for Aeronautical Research and Development, Part 1.

Holder, D. W., and R. J. North (1963). Schlieren Methods (Her Majesty's Stationery Office, London), pp. 26-27.

Howarth, L., ed. (1953). Modern Developments in Fluid Dynamics-High Speed Flow, Vol. 2 (Oxford University Press, London), ch. 11, pp. 583-585.

Jenkins, F. A., and H. E. White (1950). Fundamentals of Optics, 2nd ed. (McGraw-Hill Book Co., Inc., New York) pp. 156-157.

Keller, J. B. (1962). "Geometrical Theory of Diffraction," J. Opt. Soc. Am. 52, pp. 116-130.

* Kinsler, L. E., and A. R. Frey (1962). Fundamentals of Acoustics (John Wiley and Sons, Inc., New York).

Kock, W. E. (1971). Seeing Sound (John Wiley and Sons, Inc., New York), pp. 7-33.

* Ladenburg, R. W., ed. (1954). Physical Measurements in Gas Dynamics and Combustion (Princeton University Press, Princeton, N.J.).

* Landau, L. D., and E. M. Lifshitz (1959). Fluid Mechanics (Pergamon Press, London).

Linfoot, E. H. (1955). Recent Advances In Optics (Oxford University Press, London).

Mach, E. (1876). "Ueber die Momentan-Beleuchtung bei Beobachtung der Lichtwellenschlieren," Poggendorf's Ann. d. Phys. u. Chem. 159, 330-331.

* Mach, L. (1892). "Ueber einen Interferenzrefraktor," Zeitschr. f. Instrkde 12, 89-93.

Merzkirch, Wolfgang (1974). Flow Visualization (Academic Press, New York), pp. 75-76.

Miller, D. E. (1937). Sound Waves--Their Shape and Speed (The Macmillan Co., New York).

* Rossi, B. (1957). Optics (Addison-Wesley Publishing Co., Inc., Reading, Mass.).

Sanai, M., T. Y. Toong, and A. D. Pierce (1976). "Ballistic Range Experiments on Superbooms Generated by Refraction," J. Acoust. Soc. Am. 59, 513-519.

Shafer, H. J. (1949). "Physical Optic Analysis of Image Quality in Schlieren Photography," J. Soc. Motion Picture Engineers 53, 524-544.

Southhall, J. P. E. (1936). Mirrors, Prisms, and Lenses, 3rd ed. (The Macmillian Co., New York).

Strong, C. L. (1974). "An Air Flash Lamp Advances Color Schlieren Photography," Scientific American 231, 104-109.

Sturtevant, B., and V. A. Kulkarny (1974). "Dynamics of Weak Shock Waves at a Focus," Proceedings of Second Interagency Symposium on University Research in Transportation Noise, Vol. 1, Raleigh, North Carolina, sponsored by U.S. Department of Transportation.

* Tolstoy, I. (1973). Wave Propagation (McGraw-Hill Book Co., Inc., New York).

Toepler, A. (1866). "Ueber die Methode der Schlierenbeobachtung als mikroskopi-sches Hülfsmittel, nebst Bemerkungen zur Theorie der schiefen Beleuchtung," Poggendorf's Ann. d. Phys. u. Chem. 127, 556-580.

* Volluz, R. J. (1961). "Handbook of Supersonic Aerodynamics - Section 20 - Wind Tunnel Instrumentation and Operation," NAVORD Report 1488 (Vol. 6).

Wanner, J. E. L., J. Valee, C. Vivier, and E. Thery (1970). "Theoretical and Experimental Studies of the Focus of Sonic Booms," Proceedings of the Second Sonic Boom Symposium, Houston, Texas, sponsored by The Acoustical Society of America.

Whitham, G. B. (1957). "A New Approach to Problems of Shock Dynamics, Part 1, Two Dimensional Problems," J. Fluid Mech. 2, 145-171.

Wood, R. W. (1899). "Photography of Sound-Waves by the 'Schlieren Methode,'" Phil. Mag. 48, 218-227.

Wood, R. W. (1934). Physical Optics (The Macmillan Co., New York) pp. 93-97.

Wright, W. M. (1971). "Studies of N Waves From Weak Sparks In Air"--Final Report, Office of Naval Research Technical Report No. NR-384-321, Kalamazoo College, Kalamazoo, Michigan.

*Found useful but not specifically referenced.

August 1976

DISTRIBUTION LIST FOR
ARL-TR-76-43
UNDER CONTRACTS F44620-71-C-0015 AND F44620-76-C-0040
AND CONTRACTS N00014-70-70-A-0166, TASK 0021 AND N00014-75-C-0867
UNCLASSIFIED

AFOSR/NA (16)
Bldg 410
Attn: L/C L. W. Ormand
Bolling AFB, DC 20332

USAFA (Library) (1)
USAFA, CO 80840

AFIT Library (AU) (1)
AFIT, Area B, Bldg 640
Wright-Patterson AFB, OH 45433

NASA Langley Research Center (1)
Attn: Library
Hampton, VA 23365

AFAPL (1)
Attn: Paul Shahady
Wright-Patterson AFB, OH 45433

Director (3)
Defense Advanced Research Projects Agency
Attn: Technical Library
1400 Wilson Blvd.
Arlington, VA 22209

Office of Naval Research (3)
Physics Program Office (Code 421)
800 North Quincy Street
Arlington, VA 22217

Office of Naval Research (1)
Assistant Chief for Technology
(Code 200)
800 North Quincy Street
Arlington, VA 22217

Naval Research Laboratory (3)
Department of the Navy
Attn: Technical Library
Washington, DC 20375

Office of the Director of (3)
Defense, Research and Engineering
Information Office Library Branch
The Pentagon
Washington, DC 20301

U. S. Army Research Office (2)
Box CM, Duke Station
Durham, NC 27706

Director (1)
National Bureau of Standards
Attn: Technical Library
Washington, DC 20234

Commanding Officer (3)
Office of Naval Research
Branch Office
536 South Clark Street
Chicago, IL 60605

San Francisco Area Office (3)
Office of Naval Research
760 Market Street, Room 447
San Francisco, CA 94102

Office of Naval Research (6)
Code 102 1P (ONR/L)
800 North Quincy Street
Arlington, VA 22217

Commanding Officer (3)
Office of Naval Research
Branch Office
1030 East Green Street
Pasadena, CA 91101

Commanding Officer (3)
Office of Naval Research
Branch Office
495 Summer Street
Boston, MA 02210

Distribution List for ARL-TR-76-43 (Cont'd)

Director (1)
US Army Engineering Research
and Development Laboratories
Attn: Technical Documents Center
Fort Belvoir, VA 22060

ODDR&E Advisory Group on (3)
Electron Devices
201 Varick Street
New York, NY 10014

New York Area Office (1)
Office of Naval Research
715 Broadway, 5th Floor
New York, NY 10003

Air Force Weapons Laboratory (1)
Technical Library
Kirtland Air Force Base
Albuquerque, NM 87117

Air Force Avionics Laboratory (1)
Air Force Systems Command
Technical Library
Wright-Patterson Air Force Base
Dayton, OH 45433

Lawrence Livermore Laboratory (1)
Attn: Dr. W. F. Krupke
University of California
P. O. Box 808
Livermore, CA 94550

Harry Diamond Laboratories (1)
Technical Library
Connecticut Ave. at Van Ness, N.W.
Washington, DC 20008

Naval Air Development Center (1)
Attn: Technical Library
Johnsville
Warminster, PA 18974

Naval Weapons Center (1)
Technical Library (Code 753)
China Lake, CA 93555

Naval Training Equipment Center (1)
Technical Library
Orlando, FL 32813

Naval Underwater Systems Center (1)
Technical Library
New London, CT 06320

Commandant of the Marine Corps (1)
Scientific Advisor (Code RD-1)
Washington, DC 20380

Naval Ordnance Station (1)
Technical Library
Indian Head, MD 20640

Naval Postgraduate School (1)
Technical Library (Code 0212)
Monterey, CA 93940

Naval Missile Center (1)
Technical Library (Code 5632.2)
Point Mugu, CA 93010

Naval Ordnance Station (1)
Technical Library
Louisville, KY 40214

Commanding Officer (1)
Ocean Research & Development
Activity
National Space Technology Laboratories
Bay St. Louis, MS 39520

Naval Explosive Ordnance (1)
Disposal Facility
Technical Library
Indian Head, MD 20640

Naval Electronics Laboratory (1)
Center
Technical Library
San Diego, CA 92152

Naval Undersea Center (1)
Technical Library
San Diego, CA 92132

Distribution list for ARL-TR-76-43 (Cont'd)

Naval Surface Weapons Center (1)
Technical Library
Dahlgren, VA 22448

Naval Ship Research and (1)
Development Center
Central Library (Code L42 and L43)
Bethesda, MD 20084

Naval Surface Weapons Center (1)
Technical Library
Silver Spring, MD 20910

Naval Avionics Facility (1)
Technical Library
Indianapolis, IN 46218

Aeronautical Research (1)
Associates of Princeton, Inc.
50 Washington Road
Princeton, NJ 08540

Case Western University (1)
School of Engineering
Attn: Prof. Greber
University Circle
Cleveland, OH 44106

Stanford University (1)
Department of Aeronautics and
Astronautics
Attn: K. Karameheti
Stanford, CA 94305

Near, Inc. (1)
510 Clyde Avenue
Mountain View, CA 94043

University of Southern California (1)
Department of Aerospace Engineering
Attn: Dr. Ho, Chih-Ming
University Park
Los Angeles, CA 90007

David R. Kleeman (5)
IIT Research Institute
ECAC (Electromagnetic Compatibility
Analysis Center)
P. O. Box 1711
Annapolis, MD 21404

Naval Research Laboratory (1)
Underwater Sound Reference Division
Attn: P. H. Rogers
P. O. Box 8337
Orlando, FL 32806

New London Laboratory (1)
Naval Underwater Systems Center
Attn: M. B. Moffett
New London, CT 06320

NASA Langley Research Center (1)
Acoustics and Noise Reduction
Division
Attn: J. M. Seiner, Mail Stop 460
Hampton, VA 23365

Brown University (1)
Department of Physics
Attn: R. T. Beyer
Providence, RI 02912

Georgia Institute of Technology (1)
School of Mechanical Engineering
Attn: A. D. Pierce
Atlanta, GA 30332

Hendrix College (1)
Department of Physics
Attn: R. L. Rolleigh
Conway, AR 72032

Kalamazoo College (1)
Department of Physics
Attn: W. M. Wright
Kalamazoo, MI 49008

The Pennsylvania State University (1)
Institute for Science and
Engineering
Applied Research Laboratory
Attn: F. H. Fenlon
P. O. Box 30
State College, PA 16801

Raytheon Company (1)
Attn: Jim Lockwood
W. Main Road
Portsmouth, RI 02871

Distribution list for ARL-TR-76-43 (Cont'd)

Mark A. Theobald (1)
Bolt Beranek and Newman
1740 Ogden Avenue
Downers Grove, IL 60515

The Dept of Physics and (1)
Astronomy
University of Tennessee
Attn: M. A. Breazeale
Knoxville, TN 37916

Yale University (1)
Mason Laboratory M4
Attn: R. E. Apfel
New Haven, CT 06511

National Oceanic and Atmospheric (1)
Administration
Environmental Research Laboratories
Attn: E. H. Brown
Boulder, CO 80302

Western Electro-Acoustic (1)
Lab., Inc.
Attn: M. E. Schaffer
1711 Sixteenth Street
Santa Monica, CA 90404

Defence Research Establishment (1)
Atlantic
Attn: H. M. Merklinger
P. O. Box 1012
Dartmouth, Nova Scotia
CANADA

Technical University of Denmark (1)
Fluid Mechanics Department
Attn: L. Bjørnø
Building 404
DK-2800 Lyngby
DENMARK

University of Birmingham (1)
Electronic and Electrical
Engineering Department
Attn: H. O. Berktay
P. O. Box 36 B
Birmingham B15 2TT
ENGLAND

University of Toronto
Institute of Aerospace Studies
Attn: H. S. Ribner (1)
I. I. Glass (1)
4925 Dufferin St.
Downsview, Ontario
Toronto CANADA, M3H 5T6

Catholic University of America (1)
Acousto-Optics Laboratory
Attn: J. A. Clark
Washington, D. C. 20064

University of Toronto (1)
Mechanical Engineering Dept
Attn: David S. Scott
Toronto, Ontario
CANADA M5S 1A4

University of Southampton (3)
Institute of Sound and Vibration
Research
Attn: C. L. Morfey
Southampton SO9 5NH
ENGLAND

Physical Acoustics Division, (1)
ARL/UT

David T. Blackstock, ARL/UT (10)

Wesley N. Cobb, ARL/UT (1)

Thomas G. Muir, ARL/UT (1)

Don A. Webster, ARL/UT (1)

William L. Willshire, ARL/UT (1)

ARL Reserve (3)